INVESTIGATING LAMINATED SEDIMENTS OF THE AL-AZRAQ BASIN, JORDAN AND THE IMPLICATIONS FOR PALEOENVIRONMENTAL VARIABILITY

A Thesis
in
Environmental and Urban Geosciences

Presented to the Faculty of the University
of Missouri-Kansas City in partial of fulfillment of
the requirements for the degree

Master of Sciences

By
Jessica Hirsch

Geography, B.S. University of Missouri Kansas City, 2012

Kansas City, Missouri
2021

INVESTIGATING LAMINATED SEDIMENTS OF THE AL-AZRAQ BASIN, JORDAN AND THE IMPLICATIONS FOR PALEOENVIRONMENTAL VARIABILITY

Jessica Hirsch, Candidate for the Master of Science Degree

University of Missouri-Kansas City, 2021

ABSTRACT

This research examines cored sediments recovered from the Al-Azraq basin, Jordan for laminated sediments. Laminated sediments have long been recognized from the Dead Sea basin, and determined to be varved deposits, or seasonal couplets forming annual deposits. A current debate in the literature refutes the varve designation of Dead Sea sediments (Lopez et al. 2016; Ben Dor et al., 2019; Bookman, 2020; Ben Dor et al., 2020). This study focuses on the Al-Azraq sediments in a micro-scale analysis within the context of this current debate, shedding light on the potential for laminated sediments beyond the Dead Sea basin, and the implications for climate variability. The sediments analyzed from the Al-Azraq basin are in close proximity to the Dead Sea, but separated by the Jordan Plateau into an eastern drainage. It is a low lying, endorheic basin draining an area of approximately 12,700 km^2 of the interior desert extending from Syria to Saudi Arabia. The basin formed by the Hamza Graben is a rare deep sediment archive. Multiple environmental proxies including: lithology, smear slides, x-ray fluorescence (XRF), scanning electron microscopy (SEM) ,and energy dispersive X-ray spectroscopy (EDS) investigate the potential for laminated sediments and characterize the paleolake environments. Lithology and smear slides identified the presence of fine laminated sediments and diatoms. Detailed examination of ten sediment sections totaling 5.76 meters identified three sediment sections 2.02 m in length for further analyses. From these sections subsamples with high probability of laminated sediments were sent for XRF examination. XRF results of micro-scale analysis demonstrate changes in depositional

processes, alternating fine laminae of terrestrial material and Ca evaporite, possibly aragonite, and accompanying changes in moisture flux. The data demonstrate visible laminated rhythmites. XRF results identify alternating laminae of Ca and Si, SEM scans identify seasonal diatoms and EDS demonstrates an encrusting evaporite matrix. Results reveal variability in paleoenvironment with differing sedimentation above and below rhythmite sediments.

The undersigned, appointed by the Dean of the College of Arts and Sciences, have examined a thesis titled "*Investigating Laminated Sediments of the Al-Azraq Basin, Jordan and the Implications for Paleoenvironmental Variability*" presented by Jessica Hirsch, Candidate for the Master of Science Degree and certify that it is worthy acceptance.

Caroline Davies

Caroline Davies, Ph.D., Committee Chair
Department of Earth and Environmental Sciences

Wei Ji, Ph.D., Committee Member
Department of Earth and Environmental Sciences

Jimmy Adegoke, Ph.D., Committee Member
Department of Earth and Environmental Sciences

TABLE OF CONTENT

List of Illustrations

Figure Page

List of Tables

Table Page

AKNOWLEDGEMENTS

I dedicate this work to my parents Elizabeth DuMoulin Hirsch M.D. and Joe E. Hirsch, M.D. Without their life long, unconditional support and love I could have not achieved this milestone. They encouraged a lifelong love of learning and exploration. They taught me to have the persistence to complete what I have started, and the satisfaction of a job well done. My greatest regret is that they are not here to share in my accomplishment.

I would also like to thank the faculty and staff of the University of Missouri-Kansas City for all of their assistance and support along my path to a Master's degree. I would also like to thank Dr. Caroline Davies without her unwavering support, mentorship, guidance, and persistence. I would not have been able to reach this milestone. I am truly thankful for her support.

1. INTRODUCTION

Introduction

This study examines cored sediment samples collected from the Al-Azraq Basin, Jordan, for the presence of laminated sediments which are representative of changing paleoenvironments. These changes represent potentially significant shifts in the paleoclimate regime. This research employs methods for identifying seasonal laminated sediments used in previous research. For example at Meerfelder Maar in Eifel, Germany, X-Ray Florescence (XRF) provides micro-stratigraphical data to better illustrate the interannual, seasonal laminations of sediments (Brauer, 2008). To address the presence of laminated sediments in the Al-Azraq Basin, this study initially identified laminated sediment on the basis of the initial core description and smear slides analyses. Both methods rely on visual observation. Further analyses used both XRF and SEM scans in addition to grains size and magnetic susceptibility methods. The XRF and SEM further allowed for the exploration on a microscale of the mineral elements present in the laminated layers to further explore the hypothesis these laminations are rhythmites and of seasonal origin. This would indicate a significant shift in the paleoenvironments in this region.

Research Objective

The objective of this research is to demonstrate cored sediments within the Al-Azraq Basin record laminated sediments, and that these sediments represent several periods of cyclic deposition, potentially seasonal. A robust suite of analytical methods employed address the research objectives of demonstrating laminated sediments and cyclic deposition within the Al-Azraq basin cored sediments. The research investigates the cored sediments and elements and materials found within them through the application of: initial cored description, smear slide observation, grain size analysis, XRF, SEM and magnetic susceptibility. The research investigates species diatoms within the sediments in relation to

the potential of seasonal cyclic deposition in the basin. The research examines the clear departure from in the environments below and above the core samples. Finally, the research explores the implications of environmental changes represented by these sediments in the basin.

Research Questions

This research addresses the following questions: 1) Are there laminated sediments in the AZ2 cored sediments? 2) If laminations are present, what type of laminated sediments occur? and 3) Are the sediments reflective of environmental change? 4) How do the findings relate to regional records of similar sediments?

Research Significance

The presence of laminated sediments in the Al-Azraq Basin would be the only occurrence of laminated sediments on the Jordan Plateau and outside of the Dead Sea Basin. The next nearest occurrence of laminated sediments are in Turkey at Lake Van (Stockhecke et al., 2012). The research questions are particularly relevant to current debate in the region regarding the nature of laminated sediments (Lopez-Merino et. al, 2016; Ben Dor et al., 2019; Bookman, 2020, Ben Dor et al., 2020). The laminated sediments of the Al-Azraq basin contain information with implications for paleoenvironmental variability. These questions are also relevant to present and future regional climate by demonstrating a range of possible environments.

Thesis Organization

This thesis is organized in seven chapters. Chapter Two expands on the definition and types of laminated sediments. It discusses the occurrence of laminated sediments in arid paleolake settings similar to the Al-Azraq Basin. This chapter also addresses in detail the nature of the most relevant laminated sediments from the Dead Sea, Israel and Qarun Lake, Egypt. The chapter expounds on the current debate surrounding the new and reassessments of the Dead

Sea varves. Chapter Three describes the study area on the Jordan Plateau in terms of its geologic setting. More specifically the geologic history of the Al-Azraq basin. Chapter Three also discusses the present climate conditions and sediment history. It presents a review of sediment chronology from the Al-Azraq and surrounding basin sediments. Chapter Four presents the sampling of sediment sections for further micro-facies investigation based on initial core description and smear slides. The initial visual observation identified three sediment sections with observable laminations for further analysis. Discussed are the multiple methods applied to provide a robust interpretation of the origin and nature of these sediments. These analytical methods included: mineral grain size, X-Ray Florescence (XRF), Scanning Electron Microscopy (SEM) and Energy Dispersive Spectroscopy (EDS), and Magnetic Susceptibility (MS). Chapter Five reports the results of the analytical methods for each of the three sediment sections. Chapter Six discusses each of the sediment sections and the evidence for laminated sediments. Also discussed are the implications for paleoenvironmental variability. Chapter Seven presents a consideration of the evidence discussed supporting laminated sediments and the conclusions of the study. This chapter includes implications for future environments within the basin and region.

2. PROJECT BACKGROUND

Introduction

Evidence for global change in paleoenvironment records commonly reflect coarse timescales, thousands to tens of thousands of years. Laminated sediments provide valuable paleoarchives of fine-resolution sediments as short as intra-annual, seasonal layers to daily tidal layers (Mastalerz et al., 1999). Lamina and their components indicate short-term, dynamic environmental conditions and processes. It is widely understood that laminated sediments occur under very specific geological and climatic conditions ranging from glacial to arid settings. Conditions for deposition are a function of hydrometeorological parameters and subsequent preservation include a mix of protected basin setting, meromictic water column, anoxic conditions, low surface disturbance, changes in paleoproductivity, etc. (van Geen at al., 2003; Ojala, et al., 2014). Laminated sediments occur in arid paleolakes such as the Dead Sea, Israel (Ben Dor, 2019); Lake Van, Turkey (Ojala et al., 2012; Stockhecke et al., 2012), and Qaran Lake in Faiyum Oasis, Egypt (Marks et al., 2017).

Laminated Sediments

Laminated sediments are very small scale, fine sediment layered horizons occurring in depositional settings and sedimentary rocks. They are very thin to ultra-thin depositional layers differing in color or composition, and ranging in size from centimeters to millimeters in thickness (Kemp 1996; Boggs, 2012). There are multiple types of laminated sediments.

Laminae

Laminae can have contrasting colors, composition, texture, structure and/or thickness resulting in distinct changes in depositional pattern. Minerals, macrofossils, or biogenic particles are all potential components that compose laminae. Laminae reflect changes in environment or climate conditions.

Rhythmites

Rhythmites are laminated sediments demonstrating obvious repeating patterns representing repeating and cyclic deposition. The repeating pattern is often alternating sediment types such as shale and limestone cyclothems in the Carboniferous strata of the Midwest (Archer, 1999; Joeckel and Fielding, 2018).

Organic rhythmites are commonly found in vegetated and temperate regions. Spring nutrients promote algal blooms such as diatoms. Silica cell walls encase diatoms and their remains preserve in the sediment after completing their life cycle. This makes diatoms an excellent proxy for past environmental conditions. As a result of the life cycle of the diatoms endogenic rhythmites form the lightly colored summer layer seen in some sections of the drives. (Zolitschka, 2007).

Varves

The term varve, first used by DeGeer (1912), describes a seasonal lamination of coarse (summer) and fine (winter) material deposited in glacial lakes. The original Swedish word varves just means a cyclic event or form regardless of periodicity (Middleton, 2003). The now widely accepted definition for a varve is as follows by Hambrey (2011) "*Annually laminated deposits or varves are rhythmites with annual periodicity: annual layers of sediment or sedimentary rock are laid down through seasonal variations that result from precipitation, temperature, which influences precipitation rates and debris loads in runoff.*" Varves are distinguished from rhythmic sediments because they are demonstrated to be annual or subannual deposits (Zolitschka et al., 2015).

Varves are described as having two or more seasonal laminae. A single laminae layer or pair does not necessarily reflect a true calendar year but more a pattern of regularly fluctuating and cyclic climate. To be truly called a varved, a laminae must demonstrate

annual or subannual layering. This can be determined by radiometric age determination or other source of seasonal indicator (Zolitschka et al., 2015).

Varves in lacustrine environments are often composed of repeating or rhythmite components. These layers often reflect long periods of stable, seasonal lake productivity and are a mixture including: plant remains, carbonates, clastic, diatoms and soft organic tissues Anderson, Dean, 1988). These can produce a layer indicative of the season and climate at the time of their deposition (Stockhecke et al., 2012). These layers can also contain mineral grain sizes indicative of different processes. A coarse layer or layer of silts can represent spring or summer runoff of terrestrial minerals. Fine or clay layers represent fall or winter deposition of terrestrial elements.

Formation Processes

Laminae form in several ways and settings including glacial, tidal, and lacustrine environments. Formation processes are influenced by geological setting, climate and human impacts. These range in time and process scale from stable (geologic) to highly variable (human impacts) (Figure 2.1.). Allochthonous minerals and organic detritus are washed into the basin from the surrounding watershed, or deposited through atmospheric circulation. Autochthonous generation of materials from biologic productivity, oxidation, or mineral precipitation create sediments in situ to the basin. Once within the basin multiple processes can alter the components further both before and after deposition through mixing, bioturbation, and diagenesis, etc.

Analyzing laminated sediments reveals the hydroclimate conditions at the time of deposition. Information about past environments comes from allochthonous materials from the watershed and atmospheric deposition. Autochthonous materials inform about lake processes within the basin. All sources are mixed within the water column and deposited as a lamina. (Hardy et al., 1996; Ojala and Alenius, 2005; Cockburn and Lamoureux, 2008).

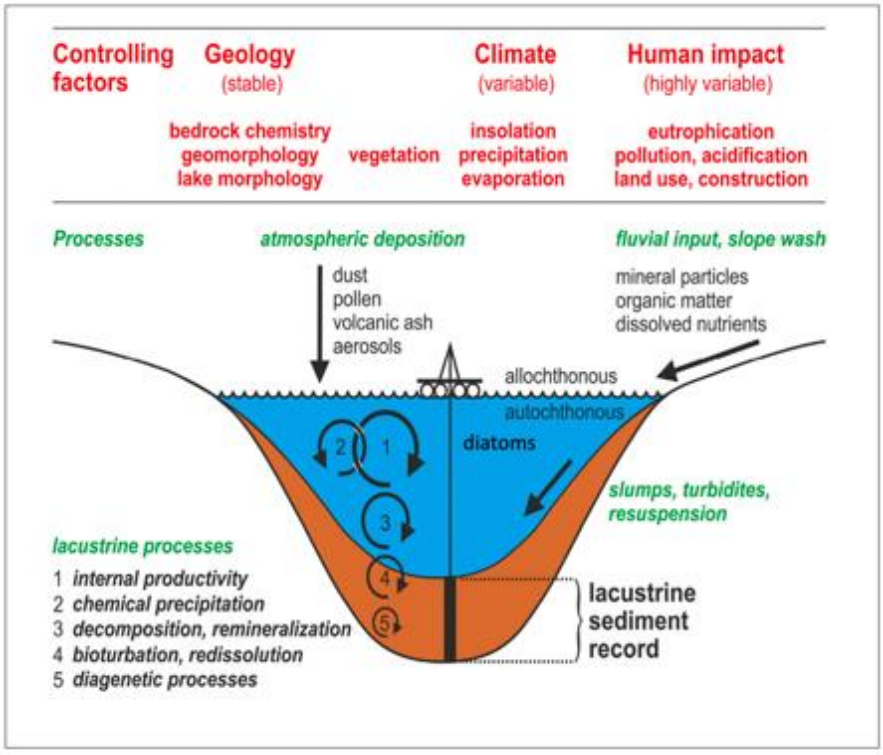

Figure 2.1. Processes of influencing formation of lacustrine sediment records including laminated sediments. These include controlling factors such as bedrock geology, structure, and tectonics; climate and human impacts ranging in scale from stable to highly variable. Modified from Zolitschka and Enters, 2009.

The laminae have contrasting colors, composition, texture, structure and/or thickness. The rhythmic pattern reflects the seasonal hydrological cycle in the environment of laminae deposition. The rhythmic nature of the deposits also represent the events in the environment occurring at the time of deposition such as changes in rainfall, temperature, algal bloom or even a dramatic event in the region such as an earthquake or flood.

Saline lakes form in arid regions where rainfall exceeds evaporation. Laminae of evaporite minerals precipitate as sediments during warmer phases. Evaporate minerals include halite, gypsum, anhydrite, calcite, dolomite, and other carbonates (Reeves, 2008). A high content of dissolved calcium carbonate can lead to the formation of a carbonate layer in the warmest months. The precipitation of the carbonates can be inorganically or biogenically

induced. With the rise of water temperatures or biogenic factors such as photosynthesis, dissolved CO_2 decreases, CO_3 increases and becomes saturated. Laminae can also form during cooler months, when there is little or no fluvial born sediment coming into the basin, clay-size particles settle to the bottom of the lake/basin, along with the remains of the planktonic organisms that flourished during the summer months. As a result, winter sediment is rich in clays. The clays will appear darker due to a small amount of carbon deposited in some. Together these laminae represent and seasonal and potentially subannual deposit reflecting warm and cool periods.

Varve formation

Varves are formed by seasonal variations and recorded in the sedimentary archives variations in hydroclimatic cycle. There are several models of formation processes which can be climate or basin specific. Organic varves form under anoxic conditions which preserve a range of organic source materials such as: pollen, plant debris, algae, humic, and fulvic acids (Sturm, Lotter, 1995; Kirkland, 2003). In one organic model spring and summer laminae are composed of several species of centric diatoms and calcite crystals. The fall season is composed of diatoms, Chrysophyte casts, fine clays and calcite. In this model spring/summer is light in color and winter is dark (Fig. 2.2.).

Clastic varves are formed by seasonal inputs of terrestrial mineral matter during spring flooding. The larger particles are washed in by meltwater and flash flooding events which also contain organic martial (Sturm, Lotter, 1995). There is an upward grading of coarse to fine sediment layers which represent the seasonal changes from the more active spring summer to lower sedimentation in summer. The winter months are very low energy and sedimentation is in situ clays and fine silts (Fig. 2.2.)

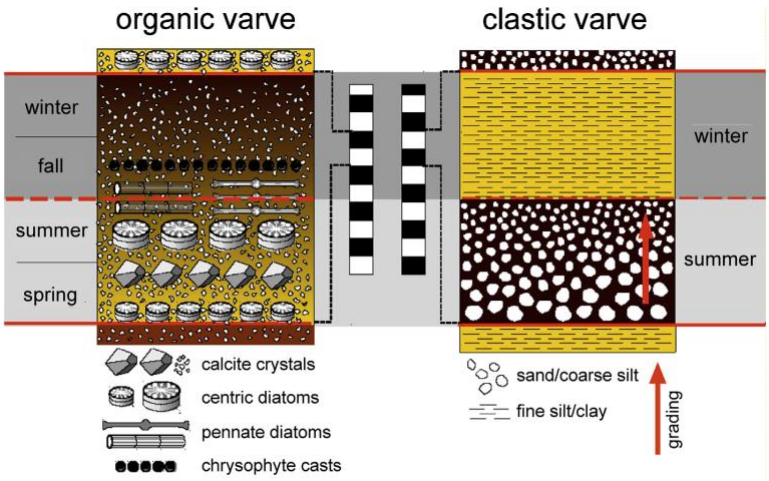

Figure 2.2. Simplified models for depositions of a calcareous and organic (mixed) varve and a clastic variation varve (modified from Sturm and Lotter, 1995).

Laminated Sediments in Arid Paleolakes

Laminated sediments have long been observed in arid to semi-arid environments across the globe. The model of seasonal deposition of these sediments originates in Scandinavian glacial deposits (deGeer, 1912), but an arid lake model of seasonal deposition comes from the famous finely laminated sediments along the Dead Sea's uplifted coastal margins.

Dead Sea Varve Debate

Dead Sea varves first described in the literature by Bloch (1944), developed the concept of seasonal white and dark couplets representing one annual cycle. These sediments became the classic example of varve deposition in arid environments for researchers for decades. A new debate surrounding the annual nature of the Dead Sea varves arises from three recent studies. Following the International Continental Drilling Program's new long core from the Dead Sea, the results published by Ben Dor et al. (2019) state the Dead Sea is the only deep hypersaline lake in the region known to have deposited long sequences of finely laminated, annually deposited sediments of varied compositions, including aragonite, gypsum, halite, and clastic sediments. They develop a new and more refined model of varve

formation identifying three types of laminated sediments: alternating aragonite and detritus (*aad*) laminated detritus (*ld*), and layered halite (*lh*). The *ld* laminated sediments containing pollen, represent flood deposits and are not annual. The *lh,* layered halite, are determined to be annual deposition representing summer precipitation of halite and winter flood materials. The *aad* laminae are also interpreted as annual deposits with the aragonite as summer evaporite deposition and the detrital laminae from winter rainy season (Haliva-Cohen et al., 2012).

The first argument against annual deposition, a very detailed pollen and grain size study by Lopez et al. (2016), demonstrates pollen was transported into the basin from the watershed and from reworked soils. Identified as flashflood events, these are not annual deposition. Detrital and aragonite laminae were shown to both be deposited during the rainy season, and therefore not representative of separate seasonal layers. Additionally aragonite is shown to precipitate in wet as well as dry seasons and therefore not exclusively an indicator of dry season evaporation. They conclude the laminated sediments from the basin marginal deposits of Ze'elim for the Holocene are not annual varves, and call for older laminated sediments to be reevaluated.

In a response to Ben Dor (2019), Bookman (2020) further argues the Dead Sea varves originally based on an observed "whitening" event; these events are rare and therefore not annual. Micro-facies analyses indicate detrital material to be from both single flood episodes and accumulation from an entire rainy season, also indicating these laminae are not annual. Ben Dor et al. (2018) concluded when these detrital episodes were capped with aragonite, whether single or multiple it represents an annual cycle. Bookman cites Lopez et al. (2016) as demonstrating aragonite deposition can be in both dry and wet season. The limitation to aragonite formation is not temperature dependent, but limited by availability of TCO_2. This

also argued against annual sedimentation and calls for reassessment of the varve characterization of Dead Sea laminates.

Qarun Lake, Egypt

An additional recent study of an arid lake with laminated sediments in the Eastern Mediterranean is Qarun Lake. It located in the Faiyum Oasis, west of the Nile River in Egypt and contains a Holocene record of seasonally laminated deposits (Marks et al., 2017). While not nearly as deep or large as the Dead Sea, Qarun lake contains a fine resolution record of hydrologically driven sedimentation. It is also under the influence of the Eastern Mediterranean climate regime fluctuations. The Faiyum depression is one of the most important hydrological basins of the western Sahara, and similar to the Dead Sea is an endorheic, closed basin. It has throughout the Holocene been influenced periodically by inflows of flood waters from the Nile River. In addition to geochemistry, the sediment record is notable for its diatoms assemblage.

3. STUDY AREA

Introduction

The Jordan Plateau is between 35°30'-37°30'E latitude and 29°30'- 32°00'N longitude with the Al-Azraq basin covering an area approximately 708.9 km^2 (Ibrahim, 1996). The Jordan Plateau defines the two major drainages areas in the region, one channels water west into the Dead Sea Valley, a small extension of the East African Rift Valley; and the other flows east into the Al-Azraq basin in the desert interior (Burdon, 1959; and Bender, 1974). Jordan Plateau elevation ranges from 1734 to 500 meters at the Al-Azraq central Qa or mudflat area.

Oriented along the NW-SE axis of the Wadi Sirhan fault, the Al-Azraq basin is an endorheic or hydrologically-closed basin. Today it is a seasonally dry basin. Although the weather on the Jordan Plateau today is arid to semi-arid due to the rain shadow created by the western escarpment, the past environment was moister as demonstrated by the presence of lacustrine deposition within the basin (Davies, 2005; Ahmad and Davies, 2017). The Al-Azraq basin presently receives source water from winter rain and can remain without rain for several years. The Al-Azraq cored sediments are the focus of this research into the presence and characteristics of laminated lacustrine sediments.

The Al-Azraq basin has long been a critical source for water in the region (Ibrahim, 1996). Due to spring waters it has also long been considered an important trade and migration route throughout human history. Archaeological evidence dating back to the paleolithic demonstrates the basin's importance as a regional water source and migration route in the Pleistocene (Khoury, 2003; Davies, 2005). Previous research indicates a lacustrine environment associated with a moderate climate, and periods of high moisture (Davies, 2005; Ahmad and Davies, 2017). The capital city of Amman, the surrounding cities, and refugee

camps are within the Al-Azraq basin drainage and it remains a critical source of water today (Deutsche Welle, 2016; Hegazi, 2016).

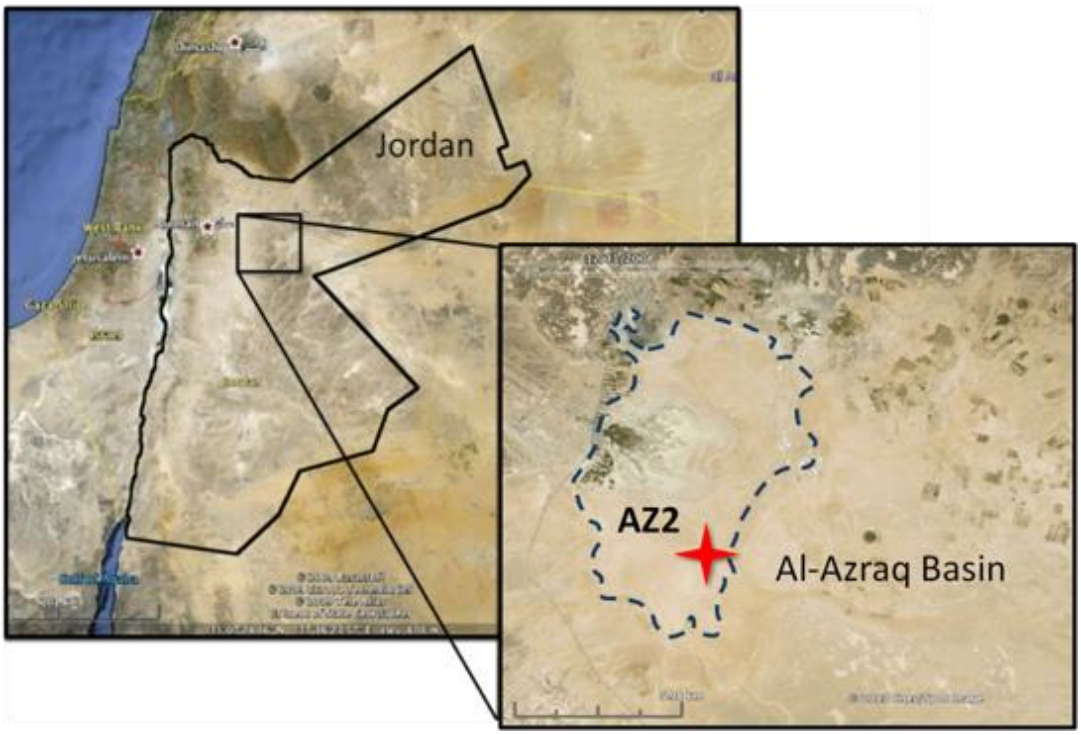

Figure 3.1. Google image of the AL-Azraq Basin, Jordan. Inset shows the location of the AZ2 sediment core drill site on the eastern margin of the basin.

Geologic Setting

The principal geology of the region consists of Cretaceous and Tertiary chalky limestone. To the north and northeast of the basin are Oligocene basalts (Bender, 1974). The Dead Sea Transform is a dominant geotectonic feature in the area. The plate boundary covers an area between the Arabian plate and the Sinai microplate, and is a part of the African plate. These plates are part of the larger Syrian African Rift system covering 6000 km, which runs from central Africa, through the Red Sea, to the Taurus mountains in Turkey (Girdler, 1990; Klinger et al., 2000). There are serval faults in the area that form the Jordan plateau and later the Azraq depression. The Jordan plateau consist of serval fracture zones, the Karak-Feiha Fault which runs to the southeast. The Sirhan Fault extending from the Wadi Sirhan in Saudi Arabia in a NW-SE direction. The Fuluq Fault, the Karak-Feiha Fault and the

Sirhan Fault form the Hamza Graben forming the Al-Azraq basin (Margane et al., 2002; Kaudse, 2014).

The Qa Al-Azraq or central mudflat is bounded by the northern (AL-Bayda Fault) and southern (Ar-Rattam Fault) transform faults intersected by western (Al-Qaislyeh Fault) and eastern (Baqawiyya Fault) parallel faults. This rhomboid area forms a grabben whose downthrust block forms the Azraq depression, which is the deepest area of sediment deposition.

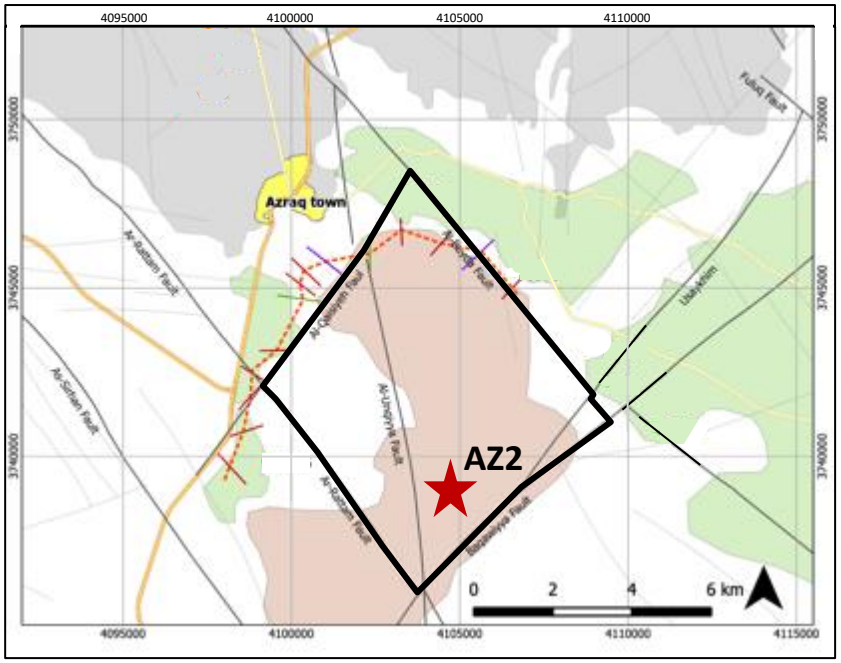

Figure 3.2. Al-Azraq basin illustrating the northern basalt margin (gray), the fault lines forming the basin; the Ar-Rattam Fault (southern) and AL-Bayda Fault (northern) transform faults intersected by Al-Qaislyeh Fault (western) and Baqawiyya Fault (eastern) faults. The coring location of AZ2 is indicated by the red star (modified from Kaudse, 2014).

Al-Azraq Basin and Sediments

The Al-Azraq basin is a closed basin system. These systems are found throughout arid and semi-arid regions of the world, where evaporation can exceeds precipitation (P/E) for periods of the year. Several wadies, tributaries, and a low depression covering a total ca.12,000 km^2 comprise the surface inputs to the Al-Azraq basin. The basin has several

springs fed by groundwater creating the Azraq Oasis. (Nelson, 1973; Garrard, 1998). There are two wetland areas, the wetlands to the north cover approximately 1.8 km^2, and the marshes to the south covering 5.6 km^2 (Nelson, 1973). The basin sediments are known to contain diatomite identified by Ala'li (1993).

The tectonically formed basin allows for a much deeper depression than is typical for playas in the eastern Al-Nafud Desert. The Al-Azraq depression perseveres a long and unique sedimentary archive of paleoenvironments. The sediments are primarily Quaternary age limestone sands, silts, clays, and evaporites.

Climate

Three climate characteristics define the Mediterranean climate regime characterizing the Jordan Plateau. First, the Subtropical High-Pressure belt is responsible for summer high temperatures along with a lack of summer precipitation (Lamb, 1995). Amman has a temperature ranging from 8.5°C in winter to a relatively high 26.5°C in summer. Second, the winter rainfall influenced by fluctuations in the Northern Jet Stream brings moist, cool air carried eastward across the Mediterranean Sea by temperate latitude westerlies brings the winter rains (Lamb, 1995). And third, the western escarpment creates a rain shadow resulting in the semi-arid to arid climate of the eastern desert. As a result, the eastern portion of the Jordanian desert receives less than 50-100 mm of rainfall annually (Rahman et al., 2015) (Fig 3.3). Current precipitation in the Al-Azraq region is low, less than 100 mm annually, but the Jebel Druze, Syria at the northwestern edge of the basin has been known to have as much as 200 mm/yr. (Nelson, 1973; Garrard and Byrd, 1992).

The Al-Azraq interior drainage flows into the basin which is an endorheic or hydrologically closed system. The closed basin provides a critical aquifer for the region. The aquifer has filled over geologic time spans during periods of higher than present precipitation. The basin's main source of water is from winter rainfall and may not receive any measurable

rain for several years (Al Naber, 2016). Presently, the people of the capital Amman, city of Zarqa, and several refugee camps depend on the aquifer and it is the main water supply for a majority of the country (Frances, 2015; Deutsche Welle 2016; Hegazi, 2016).

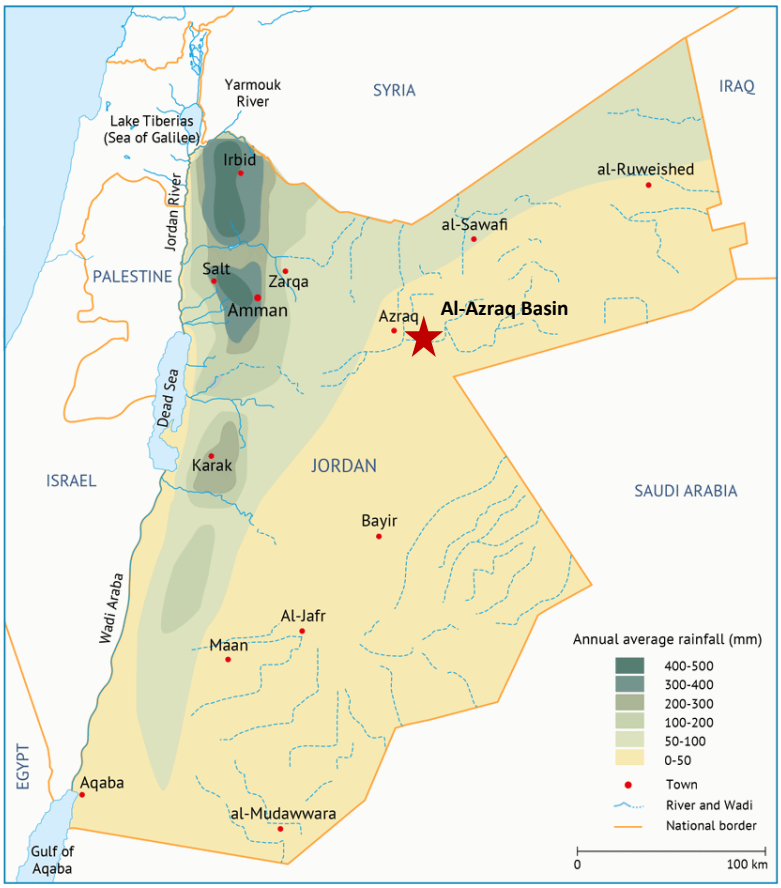

Figure 3.3 Isohyet map of Jordan with annual average rainfall. Modified from Jordanian Metrological Department Data, 2014.

Al-Azraq Basin Chronology

Dating of the Al-Azraq basin cored sediments comes from radiocarbon and infrared stimulated luminescence (IRSL). While radiocarbon and IRSL ages from samples in the upper sediments are not in agreement, they all return Pleistocene ages (Cane, 1972; Davies 2005). The IRSL ages however are internally consistent and reveal very old ages of the upper 11 meters of sediment. Sediments at greater depth are beyond the limits of IRSL.

Additional ages from sediment sections along the eastern basin margins include

radiocarbon ages, from 9,610 ka to 23,980 ka, OSL ages from 2.7 ka to 62 ka, and Uranium-Thorium (U-Th) series ages ranging between 93 ka and 118 from ʻAyn Qasiyya (Jones and Richter, 2011; Cordova et al., 2008; Cordova et al., 2013). U-series age from a deposit at the outer margins near Umari 43 km to the south returned a much older age of 330 ka (Abed et al., 2008). Turner and Makhlouf (2005) also provide an age for exposed lacustrine sediments from Umari dating approximately 600 ka.

Table 3.1 Chronology of the Al-Azraq basin sediments.

Depth	Age	Method	Reference
5 m	11,460 ± 40 B.P.	charcoal	Davies, 2007
6.30 m	40,000 B.P.	charcoal	Cane, 1972
0.20-0.28 m	24.2 ± 2.0 ka	IRSL	Davies, 2005
5.37-5.46 m	163.3 ± 11.7 ka	IRSL	Davies, 2005
11.62 m	> 250 ka	IRSL	Davies, 2005

4. METHODOLOGY

The following describe the methods and procedures followed to prepare samples for multiple proxy analyses used in this study. Sample preparation followed protocols from the Limnological Research Center, Core Facility at the University of Minnesota (Schnurrenberger et al., 2003).

Initial Core Description

Initial core description (IDC) are the observed lithologic characteristics of the cored sediments. After the core is split and the interior surface cleaned, sediment characteristics are described. These include: grain texture, fabric, bedding structure, color (based on the Munsell color chart system), inclusions, and any features or marks. Images are taken of sections following surface cleaning and lithological description. The ICD also notes any known incidents occurring to the core between the points recovery and examination. This is beginning process for all sediment analysis.

Smear Slides

After the routine examination and description of cored sediment, smear slide sampling at regular intervals provides a quick micro view of sediment composition. A smear slide is a small drop on the end of a toothpick of unprocessed sediment mixed with water and covered for visual observation at 10x. This is a quick and efficient method for planning more in-depth, high resolution sampling and processing, which is both time consuming and expensive. Smear slides are a quick method for examining detailed stratigraphic changes, changes in grain size, changes in color, basic mineralogy, and any organic inclusions within the sediments. Fifty samples processed for smear slide examined sediments for potential laminated horizons.

Grain Size

Grain size analysis in paleoenvironmental research indicates relationships between transport energy and grain particle size at the time of deposition (McCave and Syvitski, 1991). Processing sediments for grain size analysis also reveals how much or how little organic matter is present in the sediment. Grain size analysis provides the percentages of clay, silt, and sand by particle diameter in the sediment identifying the characteristics, frequency, and distribution of sample sediments. Grain size also contributes to determining the mineral source of sediments, as well as particle size range- clay, silt, and sand. One hundred and eighty-four sediment samples run on the Coulter Laser Particle Analyzer LS2000 in the Department of Earth and Environmental Sciences at the University of Missouri Kansas City identified particle sizes after dissolution of organics and carbonates. Nine replicates were measured for each sample.

Statistics on grain size data provide a range of metrics for determining energy environment parameters. The median identifies sediment midpoint of the distribution between coarser and finer particles. Mean refers to the arithmetic average grain size. Calculating the standard deviation determines the sorting values of sediments. Kurtosis is the degree of peakedness or flatness related to the probability distribution relative to benchmark normal distribution. Skewness measures the distribution within the tails of a curve and is independent of the sorting of the samples (Folk and Ward, 1957).

The Shepard/Folk are classification systems used to characterize sediment distributions. Folk's (1974) classification system uses the term mud instead of silt and is based on two diagrams. The Folk system has a less detailed separation between clay and silt. The major difference between the Folk (1974)and Shepard (1954) system is the Folk system focuses on the velocity of a current at the time of deposition and the maximum grain size of debris present (Poppe et al., 2013). Shepard's system is more focused on the ratios of clay,

silt, and sand making it a more detailed system in regard to sediment classification. (Poppe et al., 2013). The USGS program SEDCLASS helps to standardize the classification systems and is used in this research (Poppe et al. 2003).

X-Ray Florescence

X-Ray Fluorescence spectroscopy (XRF) is a non-destructive analysis providing qualitative and quantitative data through the emission of secondary X-rays. When a primary X-ray source bombards a sample with high energy X-rays or gamma rays, samples emit secondary X-rays. The emissions or fluorescence characterize specific elements and their concentrations are based on count rates or energy intensities (Fitton, 1997). This provides elemental and geochemical data. (Richter et al. 2006).

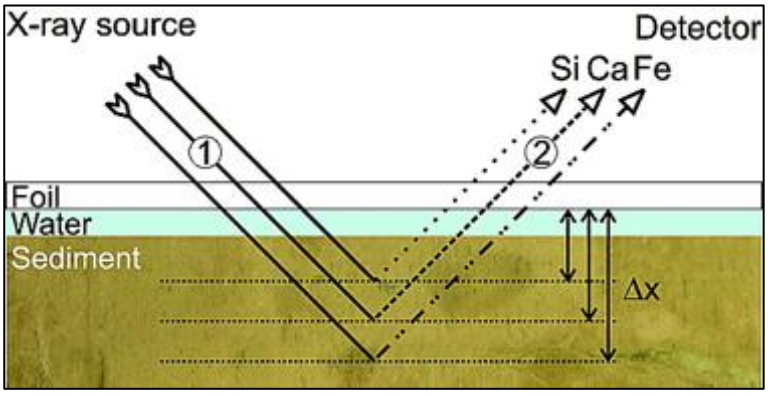

Figure 4.1. X-Ray Fluorescence Analysis schematic. The x-ray beam ionizes elements (1); radiation emits element-specific fluorescence (2), registering on the detector. Heavier elements emit stronger fluorescence energy (Richter et al., 2006).

Scanning core sediments through the XRF beam produces an element map. XRF run at The Scripps Institution of Oceanography analyzed sediment sections every 0.5mm and 1mm, at 10 seconds at 10kv, 20 seconds at 30 kv, and 30 seconds at 50kv, on a total of 176 cm. Cores lightly scraped to expose less oxidized surface layers of sediment were then covered with 4 mm thick SPEX Certi Prep Ultralene VR foil to prevent excess drying or contamination of the sediments during analysis as the XRF sensor moved downcore. Element mapping of laminated sediment generates positive and negative spikes in elements

corresponding to visible changes in light and dark sediments or changes in element concentrations.

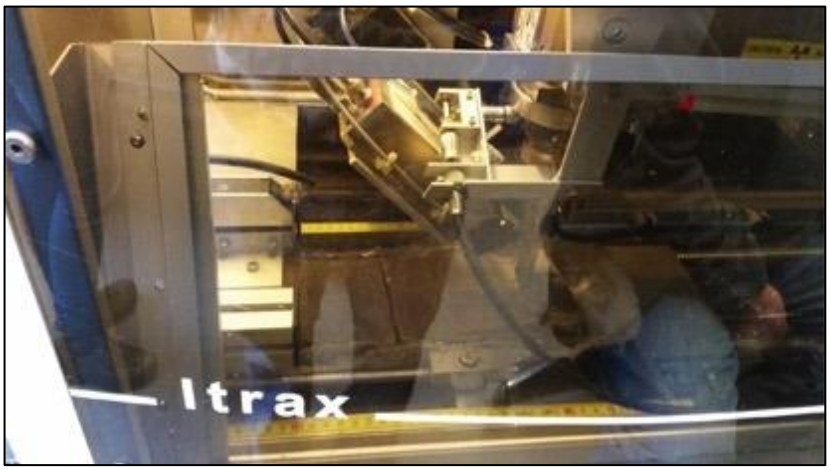

Figure 4.2. Photograph of XRF Itrax scanning sediment Section 3.

Scanning Electron Microscopy and Energy-Dispersive X-Ray Spectroscopy

The scanning electron microscopy (SEM) produces a signal from a high energy beam of electrons focused on a sample which produces an image from the position of the beam and element specific intensity of the detection pattern. When atoms and electrons interact, the signals produced relay information about the sample's surface topography. The Energy-Dispersive X-Ray Spectroscopy (EDS) provides a distribution of elemental composition (McMullan, 2006). SEM together with EDS analysis provide nano-scale information of specific samples and the elemental composition.

Preparation of samples for SEM analysis includes either coating with a thin layer of conducting material, commonly carbon, gold, or some other metal or alloy, or simply run without any coating in low vacuum mode (Goldstein et al., 2003). Coating materials, referred to as sputter coating, such as metals can increase signal-to-noise ratio during imaging due to their high conductivity, thereby producing better quality images. Coating can eliminate electron traps at the surface of non-conductive materials. Twelve AZ2 samples were scanned on Tescan Vega 3 LMU variable pressure SEM equipped with a Bruker Quantax Energy-

Dispersive Spectroscopy (EDS) system and a Tescan color cathodoluminescence detector. A majority of samples had no coatings, a few samples had carbon coatings. As part of the SEM analysis, Energy-dispersive X-Ray Spectroscopy (EDS) were performed on the samples to assist with the analysis of elements in the sample.

Table 4.1. Types of analyses performed on AZ2 cored sediments, instrumentation, laboratory, and number of samples processed.

Analysis	Instrument	Laboratory	# Samples
Core description	-	UMKC	25 meters
Smear slides	-	UMKC	12
Grain Size	Coulter Laser analyzer LS200	UMKC	184
XRF		Woods Hole Oceanographic Institute & Scripps Institute	176 cm (scanned)
SEM/EDS	Tescan Vega 3 SEM/Bruker Quantax EDS	UMKC	12/5
Total Samples			**414**

5. RESULTS

Sample Selection

AZ2 cored sediments extend from 6.5 m to 36 m below the surface. There is a gap between 25 and 35 m where during drilling a 10 m thick bed of white quartz sand cause a blow out of the hole and no sediments were recovered. Initial core description, smear slide and grain size analyses, identified sections of laminated sediments for further analyses.

Initial Core Description

The initial core description (ICD) of the total 36 m of AZ2 sediment core and photographic images revealed a detailed lithology of intricate fine sediment deposition with many subtle changes in texture and coloring. On the basis of this visual inspection, three sections totaling 4.5 m of sediment from the original 36 m exhibited laminated horizons of both fine sediments and alternating colors (Figure 5.1). These sections, referred to here as Section 1 (12.5 m to 13.80 m), Section 2 (14 m to 15.5 m), and Section 3 (20.5 m to 22 m), are the focus of the remainder of this study.

AZ2 sediment lithology 35 is a sandy, silty mix with visible lens of clays, carbonates, and oxidation throughout the core. The core is well laminated in sections. Between 11 m and 20 m there are repeating lens of oxidation along with thin dark and light laminated sediments. There is visible slumping, rounded and embedded clumps of sediment from upper sections. There are also numerous angular slumping of horizons and some vertical faulting. These are all possibly due to tectonic events starting at 14 m. The core has some missing and broken sections, but it is largely intact. The sediments have white spots and horizons are possible carbonate and halite deposits. There is a 10-meter section between 25 m and 35 m of quartz sand bed lost during drilling. Of the 25 m recovered and examined, ten sections were pulled for further analysis and of these, three underwent micro-facies analysis of laminations. These three sections are the focus of this study.

Figure 5.1. AZ2 cored sediments images, lithology, and legend. (a.) 11 m to 22 m exhibited laminated sediments; (b.) Section 1 (14 m to 14.50 m, Section 2 (19.00 m to 19.50 m), Section 3 (20.5 m to 22 m) analyzed for micro-facies.

Section 1

Section 1 extends from 14.00 m to 14.50 m. The lithology of the first 1 cm was very dry friable, with faint white carbonate. Colors are stated according to the Munsell Color Chart designation (2009). 1.5 cm was dark olive-gray clay (7.5Y, 4/3-5/3) color, and 6-8 cm horizon of yellowish and olive gray (7.5Y, 5/2). 10-12 cm sediments were more brittle, hints of lighter gray 5/1 and rust colored horizontal streaks. 12-13 cm were olive yellow (7.5Y, 6/3), still brittle with possible halite. 13-19.74 cm were dark olive (7.5Y, 4/3) and brittle. 19-20 cm was horizon of oxidation. 19.75-21 cm was a yellowish-brown horizontal stripe (10YR, 5/6). 21-37 cm were grayish-yellow brown (10YR, 5/2) with hints of possible halite. 37-39.5cm were grayish-yellow brown (10YR, 6/2) smooth, hard clay and more possible halite. 39.5-41cm very dark grayish-olive stripe (7.5Y, 5/2). 41-44.5 cm were grayish olive with vertical white sediment (7.5Y, 6/2). 44.6-50 cm olive yellow (7.5Y, 6/3) with horizontal halite sediments. The section was 50 cm in length.

Section 2

Section 2 extends from 19.00 m to 19.76 m and overall composed of clay mixed with some silt. The top of the section, from 1 cm to 8.5 cm was friable. Colors were alternating thin layers of black (5Y 2.5/1) and a dark gray (5Y 4/1) horizons. There were also some yellowish red sediments (5YR 4/6) with yellow (10YR 8/6) streaks. There was a small crack running horizontally across the core at 8 cm to 9 cm. From 14.4 cm to 16.5 cm a chunk was missing from middle of core. At 11.5 cm there was a black line (5Y 2.5/1) running half way across the width of the sediments. 12 cm to 14.5 cm another thicker black line (5Y 2.5/1) ran across core and slopping down to 15.5 cm. There was a break in the core at 19 cm. At 22 cm extending to 22.5 cm was a crack slopping to the right. At 24 cm the color to lightens to gray (5Y 4/1). At 32 cm small cracks with reddish/orange colors, suspected to be Fe, ranging from yellowish red (5YR 4/6) to dark grey (5YR 4/1). There was a small chunk missing at 33 cm

just under the possible Fe. Overall, color was mottled, dark gray (5Y 4/1) and black (5Y 2.5/1). More possible Fe at 38 cm. There was a break in the core at 39 cm on the bottom of the broken section there was dark gray (5YR 4/1) mixed with yellow (10YR 8/6). From 33.5 cm down to 42 cm color was yellowish red (5YR 4/6). The color from 43 cm to 48 cm was dark gray (5Y 4/1). At 49cm there was a missing chunk. At 53 cm a small crack. At 55 cm and 56 cm there were black (5Y 2.5/1) horizons, mottled with dark gray (5Y 4/1). At 61 cm to 65 cm the color returned to a solid black (5Y 2.5/1). At 67cm to 76 cm more black (2.5Y 5/1) horizons, with some mottled dark gray (5Y 4/1). The end of the core is uneven and somewhat friable. The sediment section measured 76 cm long.

Section 3

Section 3 extended from 20.50 m to 20.96 m. From 0 to 5 cm was friable with some yellowish red (5YR 4/6) showing in the broken chunks. The overall color of the sediments was a mottled black (5Y 2.5/1) and dark gray (5Y 4/1). The core is mottled from 0 cm to 15.5 cm, at 15.5 cm to 16 cm was streaking of yellowish red (5YR 4/6), then again at 17 cm streaks ran the width of the core. From 17 cm to 20 cm the core was a solid dark gray color (10YR 4/1). At 21 cm was a small break with a yellowish red streak (5YR 4/6). At 22 cm was a small line of yellowish red (5YR 4/6). At 27 cm a small black line (5Y 2.5/1) curved upwards. At 29 cm to 30.5 cm more yellowish red (5YR 4/6). From 40 cm to 4 6cm the sediment was a solid chunk mottled with black (5Y 2.5/1) and dark gray (5Y 4/1). After cleaning, photos, and being exposed to air it appears there is some oxidation at 21.5 cm and 28 cm to 30 cm. The upper section from 0 cm to 21.5 cm has turned a little darker than originally reported in field notes at dark gray (10YR 4/1). The sediment section is 46 cm long.

Smear Slides

In addition to the visual observations in the initial core descriptions, smear slides identified diatoms, minerals, and other materials found in the sediments. It is also a relatively quick way to determine where further sampling should be focused. Twelve smear slides examined samples at the micro level for components of laminated sediments. This investigation revealed fragments and partial valves of two types of diatoms, one centric and one cylindrical. Also observed were algae and quartz sand grains.

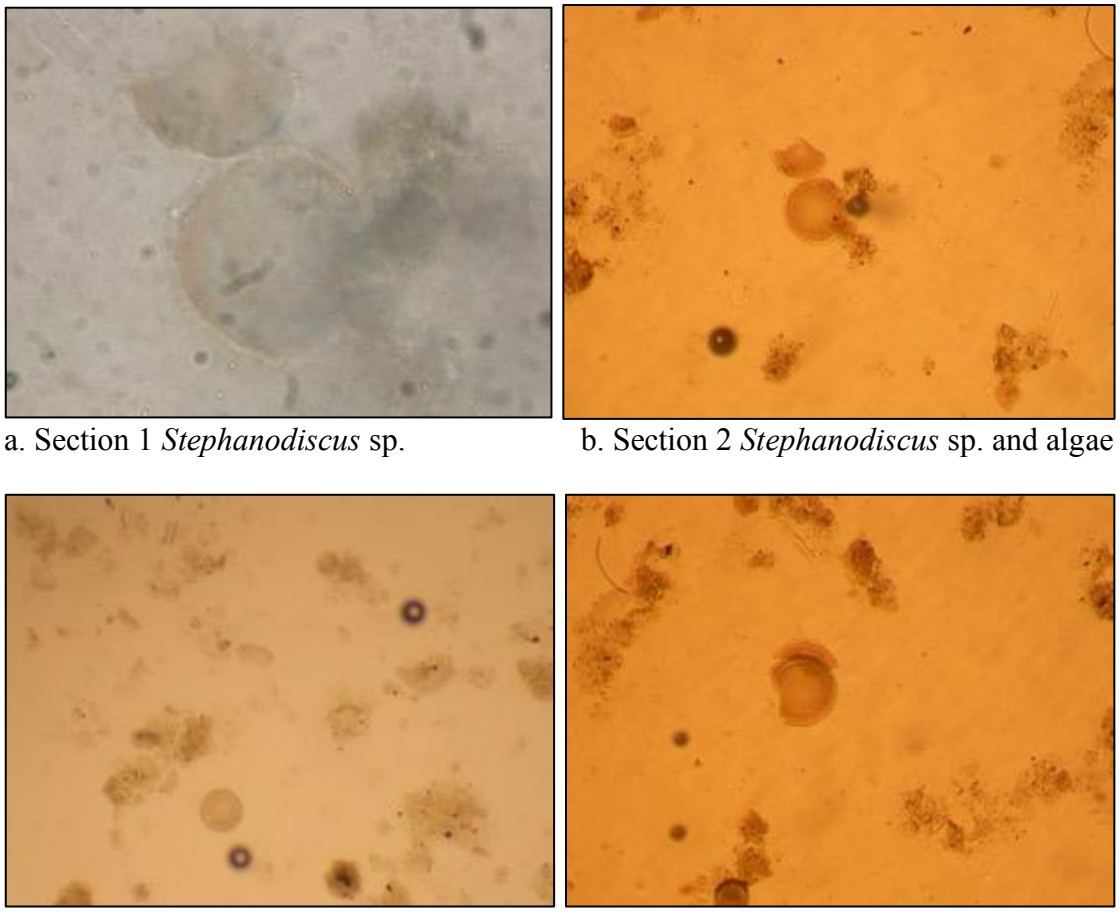

a. Section 1 *Stephanodiscus* sp. b. Section 2 *Stephanodiscus* sp. and algae

c. Section 2 *Stephanodiscus* sp. and algae d. Section 3 *Stephanodiscus* sp.

Figure 5.2. Smear slides images (a., b., c., and d.) from Sections 1, 2, and 3 showing the presence of the centric diatom *Stephanodiscus* sp., random clumps of algal material, and mineral detritus.

Grain Size

Grain size analysis is important for characterizing the energy environments of lacustrine sediments. The total percent clay ranges from a minimum of 11.20% to a maximum of 55.71% throughout the core, averaging 10.26%, with 26.23%. in the uppermost 5 m. The total percent of clay is relatively constant, but total percentages of silt and sand fluctuate. Silt ranges from 25.85% to 85.33% and averaging 63% throughout the core. Between 25.24 m and 25.51 m silt averages 79% and peaks as high as 85.33%. Sand percent ranges from zero at the top of the core to 53.47%. Sand lenses occur at 11.49 m with 50% sand and 23.73 m with 53.47% sand. Lenses of silt, silty-sand, and clayey-silt punctuate the core. Above 25 m grain size distribution fines upwards and correspond to the formation and deepening of the lake. A 10-meter-thick quartz sand bed lies between 35 to 25 m. Below 35 m angular chert gravels were encountered, but not recovered (Figure 5.3).

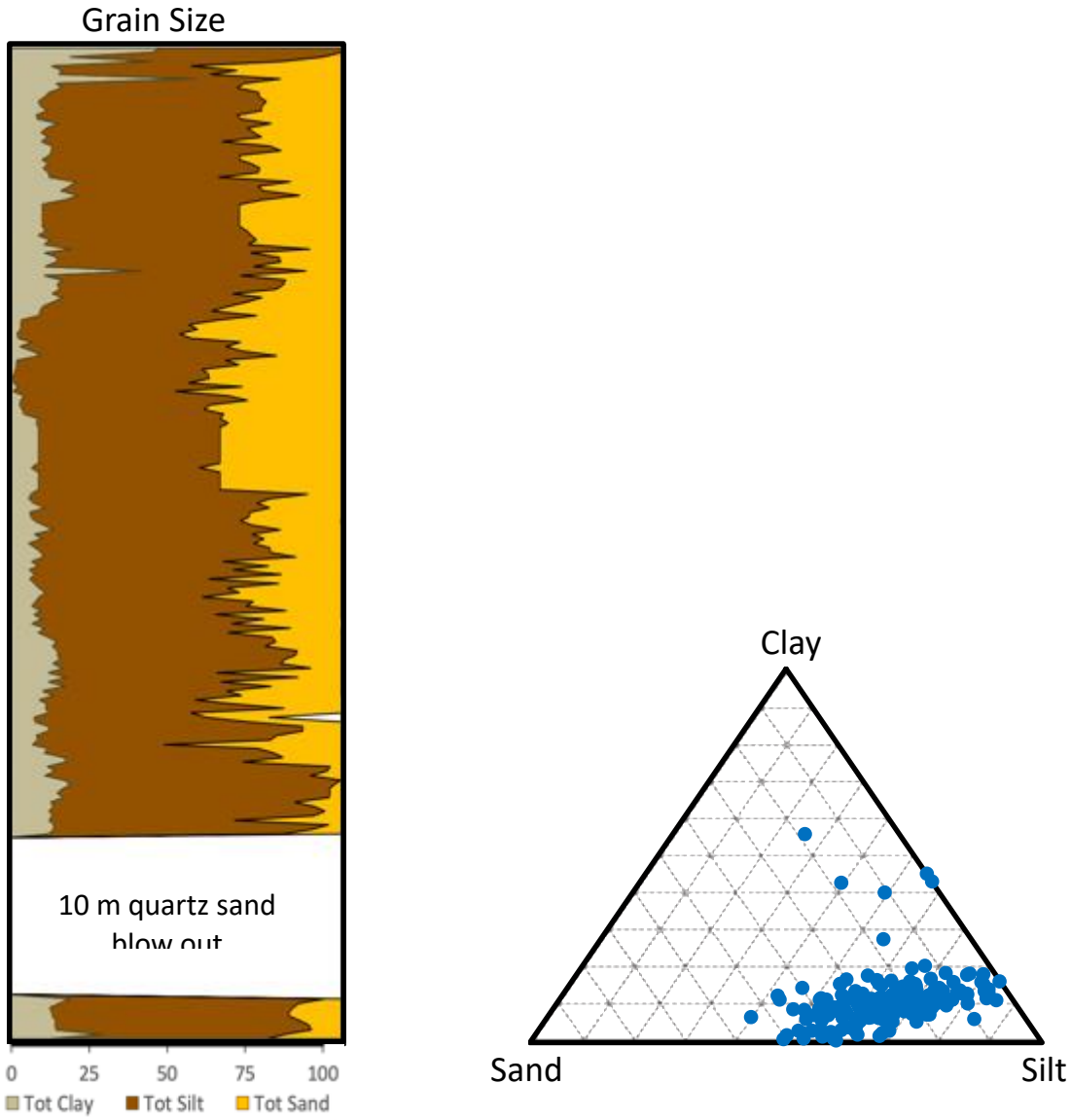

a. b.

Figure 5.3. Graph of cumulative percent grains size distribution of clay, silt and sand (a.); tertiary diagram of percent grain size distribution illustrating Shepard/Folk classification as predominately sand/silt throughout the cored sediments (b.).

Section 1

In Section 1 the grain size shows silt percent to be consistently averaging around 54.82% and sand percent averaging 36.74%. Total clay percent for Section 1 remains low at below 10%. Folk and Shepard classification of the sediment in Section 1 is Sandy Silt.

Section 2

In Section 2 the silt percent fluctuates more between 65 and 74%, with sand fluctuating between 15 and 38%. Total clay percent for Section 2 also remains low below 10% with the except of one reading at 10.37%. Although there are increased fluctuations in silt and sand percentage, the Shepard/Folk designation for this sections remains Sandy Silt. Tan colored and oxidized nodules occur throughout the section.

Section 3

In Section 3 there are far fewer grain size samples at only four. The silt percent ranges from 64 to 72%, and the range of sand percent between 13 and 22%. Clay percent is slightly higher ranging from 11 to 14.41%. This still earns a classification of Shepard/Folk Sandy Silt with the except of 22 m which earns a Shepard designation of Clayey Silt.

X-Ray Florescence

The XRF analysis preformed at Scripps Oceanographic Institute scanned 176 cm of sediment at 0.5 mm intervals and 10 kv. Scans included Section 1 from 14.30-14.46 m, Section 2 from 19.62-19.76 m, and Section 3 from 20.83-20.66 m show fluctuations in major (Al, Ca, Fe, Si) and trace elements (Cl, Cr, K, P, Mn, Ti, S, Sr, Rh) occur throughout the section sediments (Appendix C). Overall the micro-scale mm scanning reveals repeating patterns of fine resolution fluctuations.

Section 1

The XRF data, reported in Area and DArea for each major and trace element, were tested for accuracy of percent fit to model calculations by dividing the DArea model

prediction by the Area of the recorded element scan. Element scans are considered most accurate below 10% and not above 25% (Witter et al., 2018). The XRF pattern of major elements Aluminum (Al) and Calcium (Ca), particularly Ca, fluctuate in very regular, short nearly 5 mm periods, with very low amplitude over the length of the Section 1. Al demonstrates longer-term trends of possibly two oscillating cycles. There are two sharply decreasing excursions at 135 mm,185 mm, and the very bottom in Fe, and Si patterns. Al has the decrease at 185 mm and gradual decrease at the bottom.. Between the downward excursions at 135 mm and 185 mm, both Fe and Si increase in threshold to new highs (Figure 5.4.).

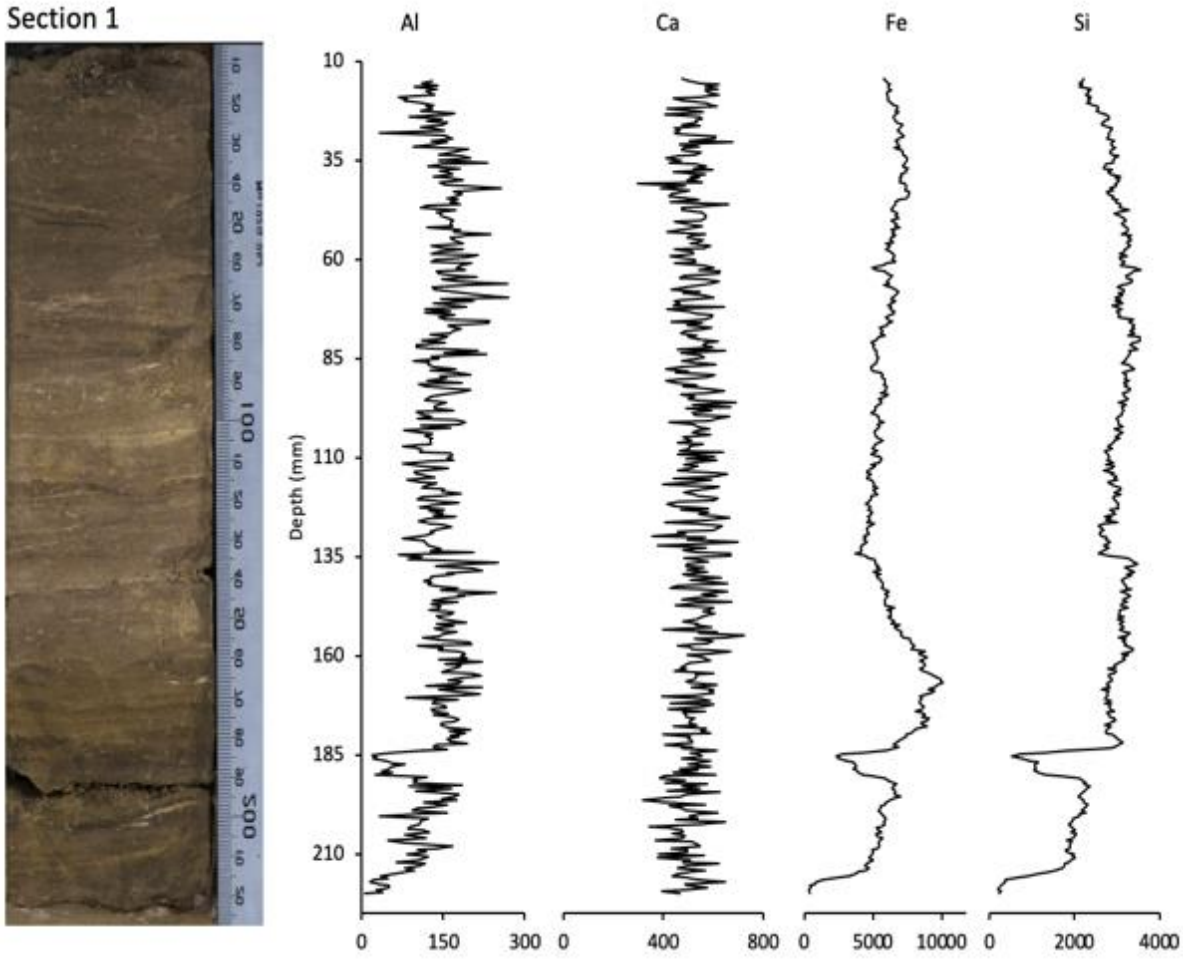

Figure 5.4. XRF graphs of major elements in Section 1. Scale in mm and XRF units measured in Area.

The Section 1 minor elements reflect similar fine mm scale fluctuating patterns seen in the major elements. Strontium (Sr) was recorded only Section 1. Chromium (Cr) very closely mirrors the low amplitude fluctuations of Ca and is in phase. for the entire length of Section 1. Overall patterns are harder to discern with the exception of Cl, K, Sr, and Ti. All decrease at 185 mm. Rh and Mn both increase slightly at 195 mm (Figure 5.5.).

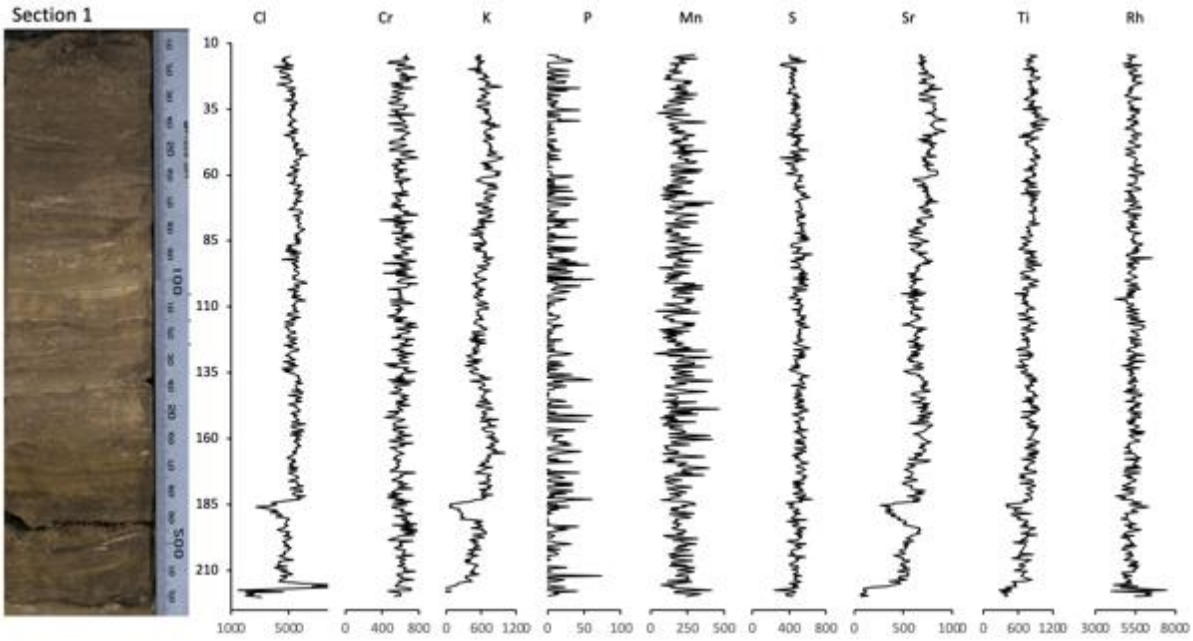

Figure 5.5. XRF graphs of minor elements in Section 1. Scale in mm and XRF units measured in Area.

Section 2

The XRF major elements in Section 2 have a very similar short period, low amplitude pattern as seen in Section 1 major elements for the upper 80 mm. From 80 mm to the bottom the pattern in Ca changes dramatically with two large episodes of increase over 20 mm which each increase the threshold to a new average. Al follows an opposite pattern of decreasing over the same range as the double peaks in Ca. Al is slightly out of phase beginning before 120 mm and extending to 60 mm. Fe and Si also show a similar trend with this long-term cycle in Al, but with less extreme fluctuations over the same range Al (Figure 5.6.).

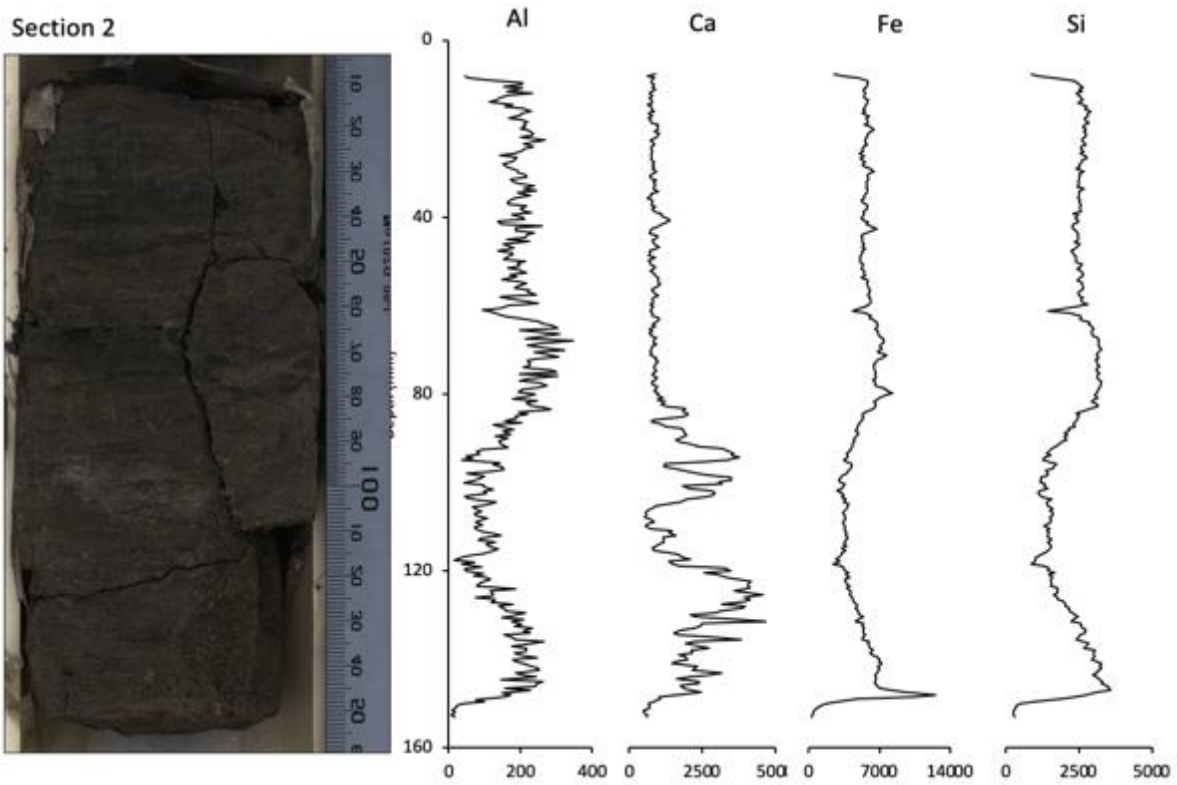

Figure 5.6. XRF graphs of major elements in Section 2. Scale in mm and XRF units measured in Area.

The Section 2 graphs of minor elements illustrate similar low amplitude fluctuations seen in Section 1 in Section 2 elements Cl, Cr, Mn, and P (Figure 5.7.). However, there is significant range in cycle trends in K, S, and Ti. Potassium (K) very closely mirrors the major element pattern of Al, and fluctuations in Ti are similar, but less intense than Al and K. All have cycles spanning approximately 150 mm to 60 mm. Sulfur (S) very closely mirrors the pattern of Ca with two large peaks below 60 mm.

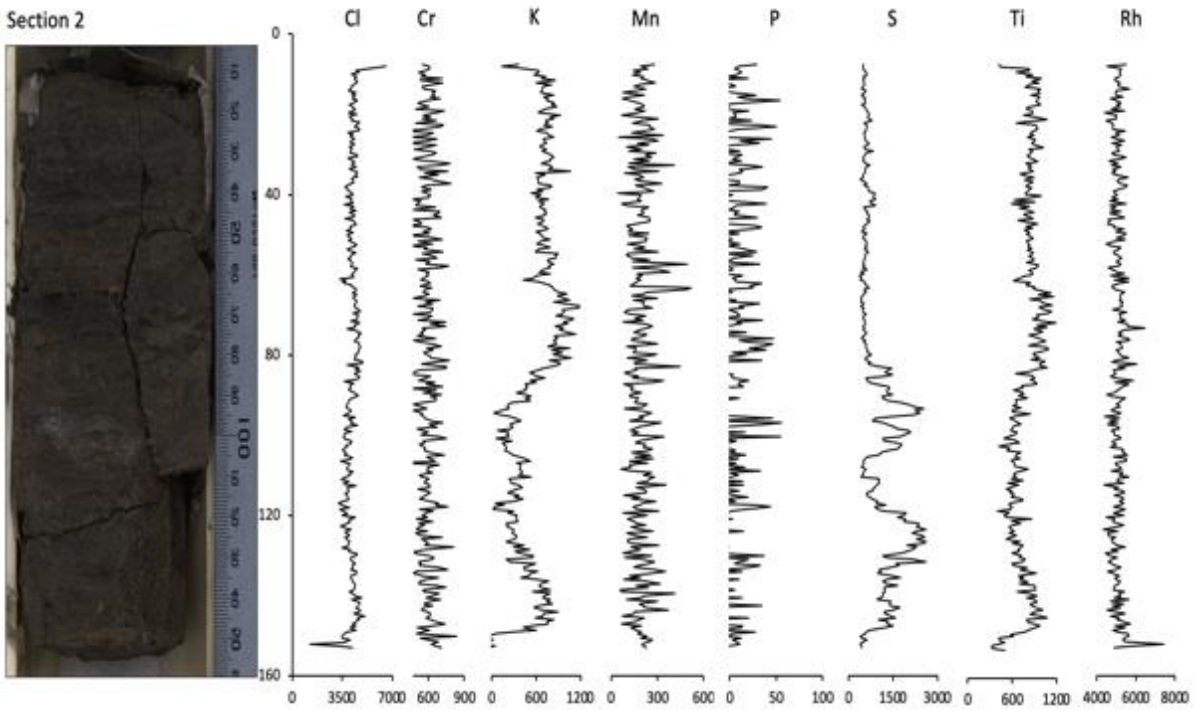

Figure 5.7. XRF graphs of minor elements in Section 2. Scale in mm and XRF units measured in Area.

Section 3

In Section 3 the major element of Ca for the majority of the section fluctuates very tightly around a narrow mean with four significant peaks occurring at: 3.5 mm, 122.5 mm, 148.5mm, and 158.5 mm. These peaks average 2886, with the highest peak extending to 5355 at 122.5 mm. For the remainder of the section Ca averages 74% less at 738. Al also fluctuate around a slightly less narrow mean, but the overall trend increases gradually in a bend from 160 mm to 60 mm. This same gradual increase and decrease is mirrored in Fe and Si, whose fluctuations are very low amplitude with very short periods. Fe and Si both have sharp decreases at 120 mm, concurrent with the very large spike in value in Ca.

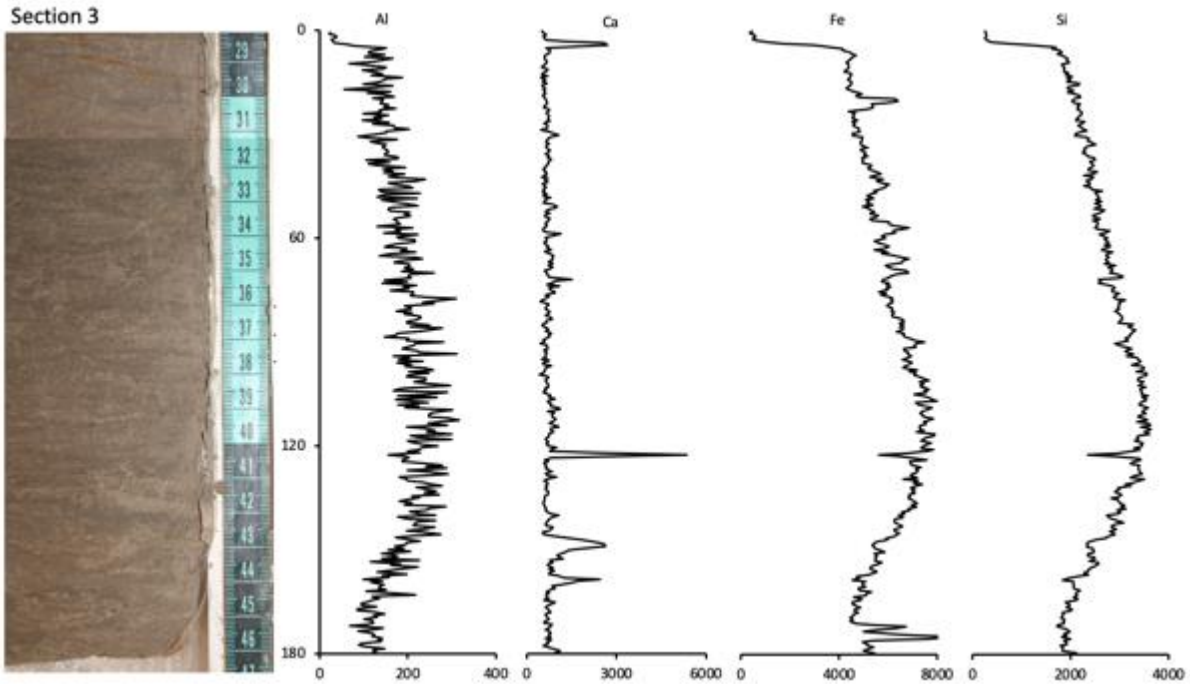

Figure 5.8. XRF graphs of major elements in Section 3. Scale in mm and XRF units measured in Area.

Some Section 3 minor element fluctuations mirror particular major elements. Chlorine (Cl) and sulfur (S) very closely mirror the very low amplitude fluctuations and very narrow mean of Ca, and each have four major peaks in values, including the large spike at 120 mm. Potassium (K) and titanium (Ti) also mirror the gradual increase and decrease of Aluminum (Al), iron (Fe), and silica (Si).

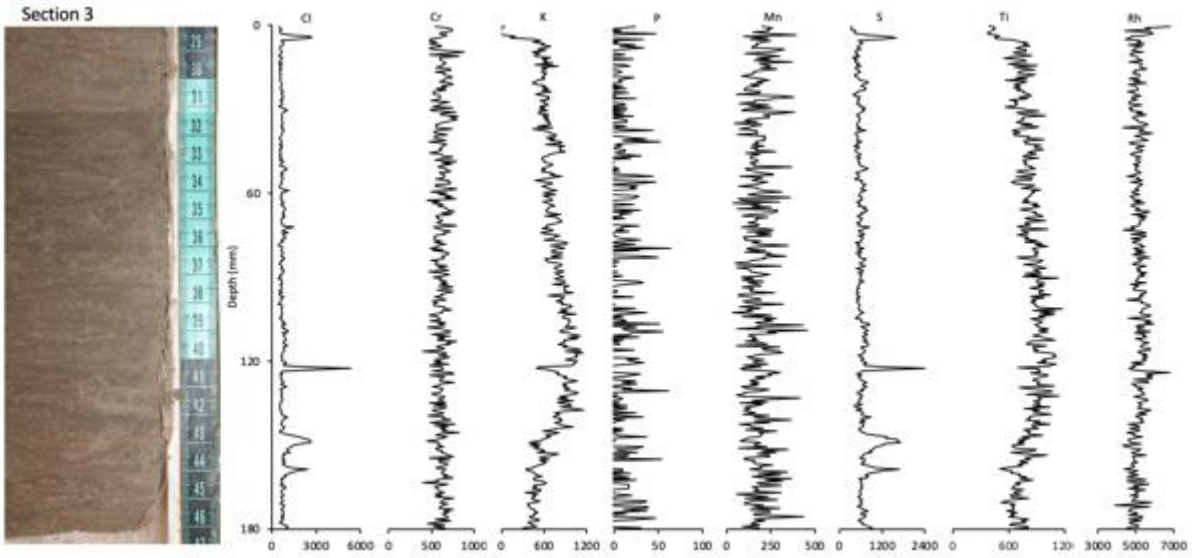

Figure 5.9. XRF graphs of minor elements in Section 3. Scale in mm and XRF units measured in Area.

Scanning Electron Microscopy (SEM)

Scanning Electron Microscopy (SEM) of specific representative samples from the three sections further explored the diatoms first observed in the smear slides and inferred from the higher amounts of silica (Si) detected by the XRF. The nano-scale focus and detail provided by SEM images allowed the identification of two species of centric diatom, one discoid and the other cylindrical. All sediment sections contain a mix of *Stephanodiscus* sp. and *Aulacoseira lirata* (Figure 5.10.). The images revealed diatoms species mixed together, stacked, crushed, and fragmented with a low number of intact frustules. Diatoms frequently observed in SEM images to be embedded or encrusted in a matrix.

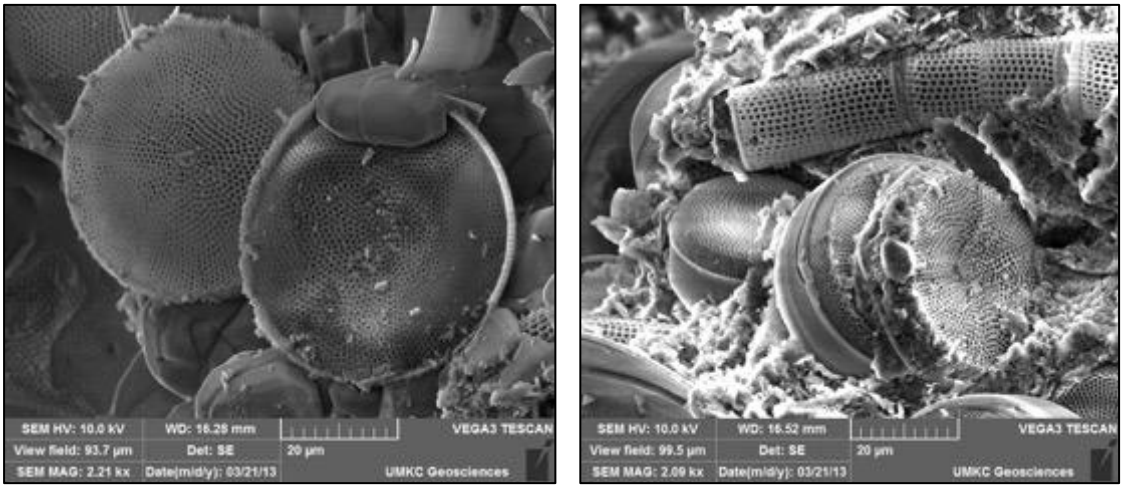

Figure 5.10. SEM images of diatoms from Section 3, identified as *Stephanodiscus sp.* (left) and Section 2, identified as *Aulacoseira lirata* (right).

Energy Dispersive Spectroscopy (EDS)

Energy Dispersive Spectroscopy (EDS) run on the same SEM samples found elevated levels of Al, as high as 30 cps/eV; Si and O at extremely high levels to 70 cps/eV. The EDS also recorded lower levels of Cl, Fe, K, Mg, and Na. EDS determined halite to be in all three sediment sections. Additionally, the EDS confirmed the composition of the diatoms with extremely high Si and O. analysis further identified the composition of the encrusting matrix

as halite (NaCl) and Fe-Mg-Al clays (figure 5.11.). A total of five samples underwent EDS analysis.

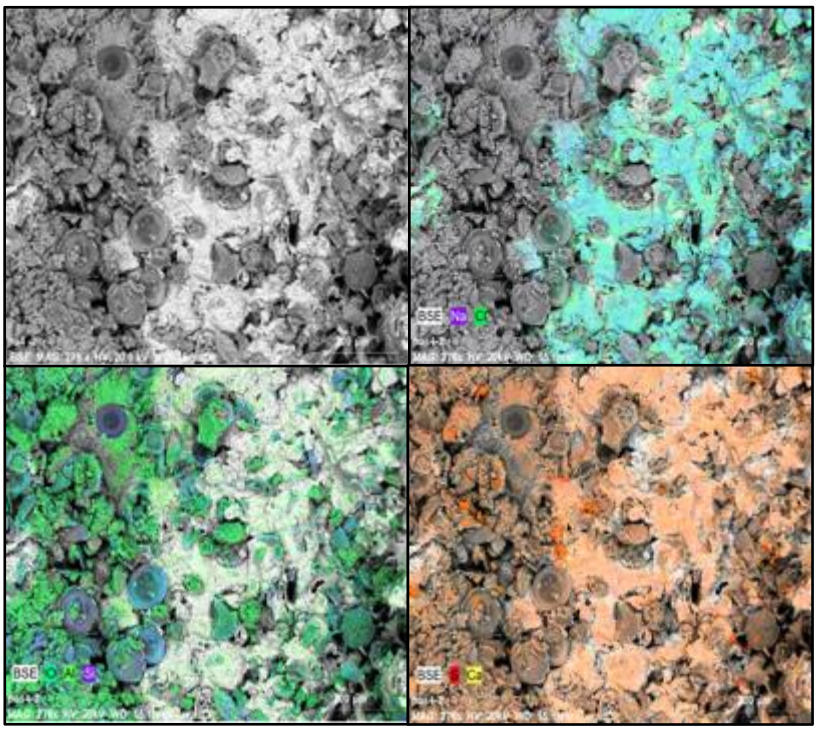

a.

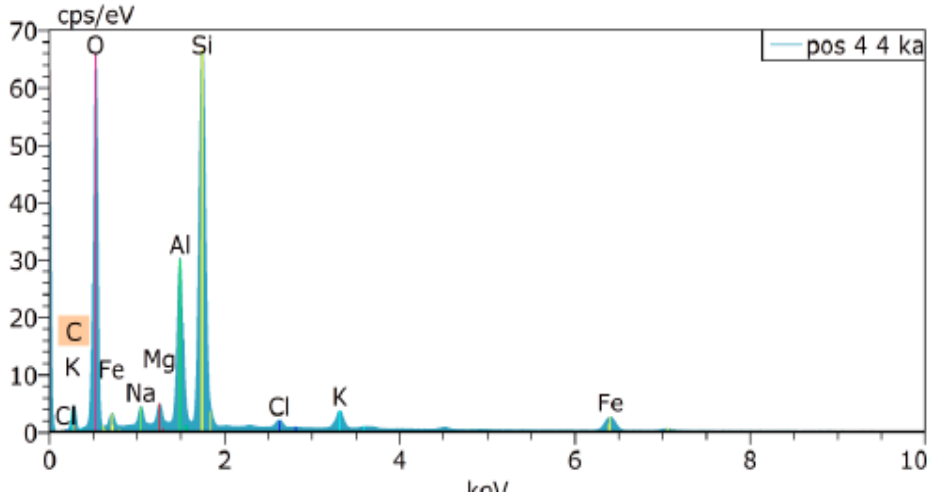

b.

Figure 5.11. SEM image multiple centric diatom frustules embedded in matrix (a. upper left); EDS images (a. upper right, lower left and lower right) of diatom frustules highlighting dominant elements. Image identifying the encrusting matrix as halite (teal color) by the presence of sodium (Na) and chloride (Cl) (a. upper right). Image with green, blue, and purple identifies the diatoms with extremely high (Si, O) in a matrix of Al clays (a. lower left). Image with orange highlights identifies sulfur (S) and calcium (Ca) in matrix of crushed tests, Fe-Mg-Al clay (a. lower right). The EDS diagram further confirms element identification and abundances.

6. DISCUSSION

Introduction

This project investigates the cyclic nature of laminated sediments from the Al-Azraq Basin, Jordan. A 35 m sediment core was described, and analyzed with smear slides and grain size analysis. These initial analyses demonstrated the presence of very thin laminated sediments of alternating layers of light and dark sediment laminae with varying textures. The rhythmites consist of silt, clay, carbonate, clastic minerals, organic detritus, and diatoms. This is consistent with rhythmically laminated sediment (Glenn and Kelts 1991). Three sediment sections were chosen to further investigate the rhythmite layers through micro level geochemical analysis. X-Ray Florescence, performed at the Scripps Institution of Oceanography, scanned these sections at 5 mm intervals. Additionally, SEM and EDS analysis illustrated abundant diatoms which were identified to species.

Section 1

Calcium (Ca) is a proxy for carbonates which often form through evaporation during a dry season. Work published by Lopez et al. (2016), Belmaker (2019), and Bookman (2019) identify the formation of the evaporite carbonate aragonite as not linked exclusively to temperature, but is alkalinity limited. Until the specific source of the calcium in AZ2 sediments is identified through X-Ray Diffraction analysis, more cannot be determined on the seasonality of the Ca. However, the Ca relationship with other elements can provide some insights in to the nature of the laminated deposits. In all three sections Ca returns very fine scale alternating Ca

Silica (Si) is proxy for a mix of terrestrial silica and diatoms which are an *in situ* source of Si (Neuberger 2018). Both represent wet periods. The terrestrial clastic material washes in from the watershed during winter or spring flooding. The flood waters create an influx of fresh water bringing with it terrestrial silicas and organic detritus, and these in turn

supply the diatoms with silica and nutrients. In all three sediment sections Ca and Si alternate in very short and tight periods of low amplitude at the sub-millimeter scale which indicate short and alternating depositional conditions. There are also longer term tends visible in these patterns, as well as abrupt transitions in pattern (Section 2) (Figure 6.1.).

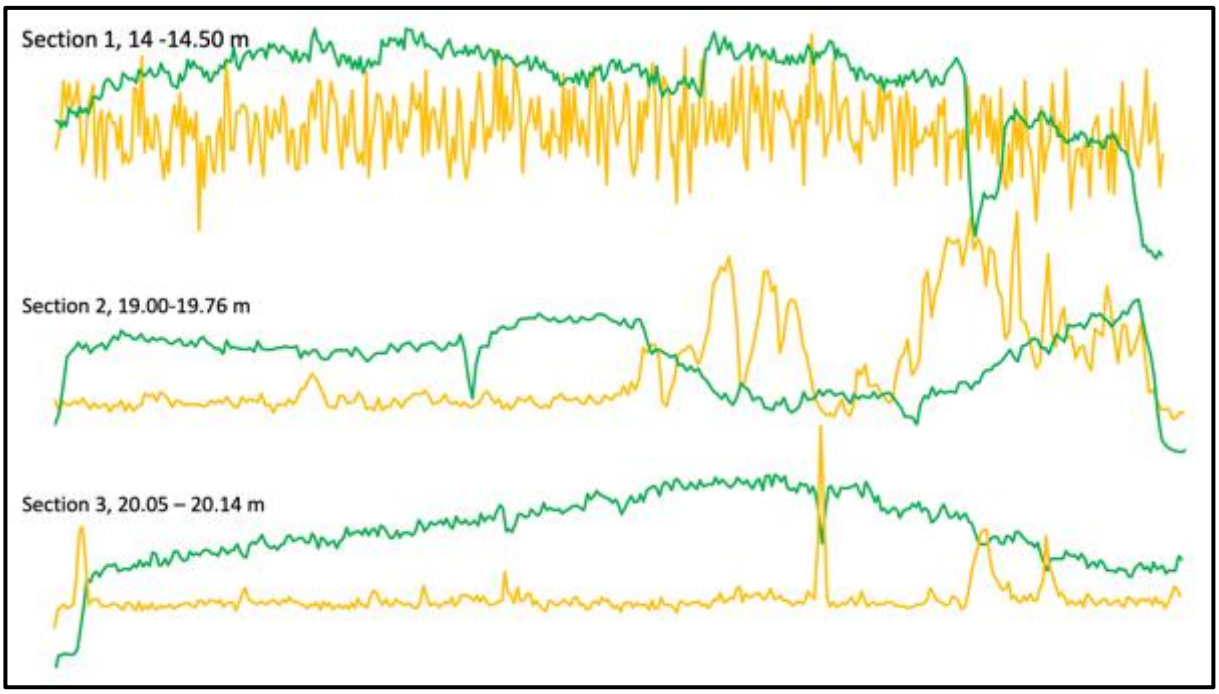

Figure 6.1. Alternating calcium (Ca = yellow) and silica (Si = green) XRF readings from sediment Sections 1, 2, and 3. Vertical scale not shown. The XRF readings are 0.5 mm at 10kV and clearly demonstrate fine resolution, alternating expressions of calcium and silica.

In addition to the simultaneously alternating peaks of Ca and Si seen in Figure 6.1., peaks in Sr/Ca are typical for aragonite layers, however the source of calcium for AZ2 sediments is not yet established for these sections (Figure 6.2.). Peaks in element ratios of Ti/Ca and Ca/(Sr+S) are proxies for increases in terrestrial detrital carbonates and silicas, respectively, washing in from watershed (Neugebauer et al., 2014). Chlorine is a proxy for salts and very positively correlates with the ratio of S/Ca which can indicate gypsum, again the exact type of calcium is not yet determined. There are significant decreases in elements at 185 mm, except the ratio Ca/(Sr+S) which peaks here. This is right before a crack in the core, however, the analyst feels these are real decreases and not a result of the crack in the section

(personal communication). Notable is the consistency of the rapid fluctuations over depth, the narrow range of their amplitude, and the tight correlations, positive and negative, of elements. While several of the element ratios contain Ca, other elements such as Sr, S, Cl, and Mn/Fe also demonstrate similar patterns providing a more robust interpretation. Mn/Fe represent terrestrial deposition and correlates negatively to Ca. High amplitude in Mn can reflect deep water turnover and can therefore be an indicator of water depth (Naeher et al., 2013; Zuo et al., 2020).

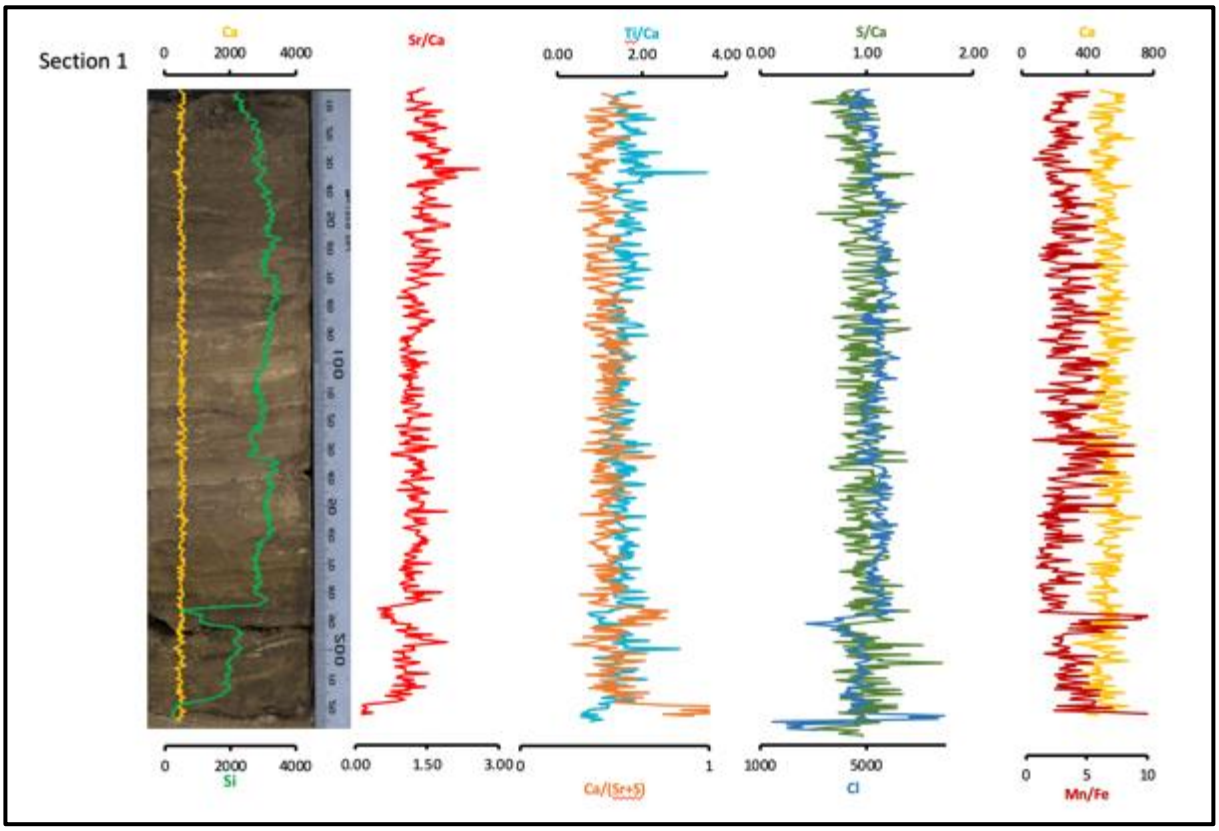

Figure 6.2. Section 1 core photo with XRF elements Ca and Si and rations of Sr/Ca, Ti/Ca, Ca/(Sr+S), S/Ca and Cl, and Mn/FE and Ca. These are proxies for changes in depositional inputs and potential indicators of repeated seasonal cycles.

Section 2

In Section 2 the pattern of simultaneously alternating fluctuations in Ca and Si continues similar to Section 1 for the first 80 mm. The very short period and low amplitude pattern is also similar. Below 80 mm there is a dramatic shift in both period pattern and

amplitude. Silica decreases slowly, stays low then increases slowly. This could represent a decrease in available water from the watershed or a decrease in diatom productive. Both are potentially related. During this period calcium has two dramatic episodes of multiple large spikes separated by a decrease. This is a clear divergence from the previous pattern and indicative of a significant shift in longer term sources of freshwater and higher evaporation. Strontium (Sr) was not recorded for this section, but Ti/Ca is contrasted with sulfur (S). Lake sulfur cycles are complicated with biogenic origins in microbial production, or abiotic influx from watershed erosion. In Section 2 sulfur tracks the terrestrial detrital carbonate influx represented by Ti/Ca moderately well including the shift below 80 mm, mirroring the significant drop in Ti/Ca and gradual increase, with one exception. In the middle of the decline at 107 to 110 mm, Ti/Ca has a significant peak returning to previous high level. This may indicate a strong influx of terrestrial carbon that is not reflected in the Si record. The peaks in sulfur signal may reflect reduced organic sulfides, and a decrease in sulfur signal indicate a decrease in microbial activity concurrent with a decrease in diatoms. Some portion of the sulfur signal most likely also reflects oxidized sulfur species. Further examination of sulfur species by isotope analysis or X-ray absorption near edge structure spectroscopy (XANES) is recommended (Bostick et a., 2005). Chlorine is a proxy for salts and continues to exhibit a very similar pattern to Section 1. It also continues to very positively correlate with the ratio of S/Ca. Chlorine maintains a very consistent patterns throughout Section 2 as does not reflect the major perturbations seen in Ca or S. Lastly the ratio of Mn/Fe continues to correlate negatively to Ca with high amplitude variations. After 80 mm the amplitude of Mn/Fe remains high, but the trend changes following the overall increase in calcium without the decreasing and continuing to correlate negatively. All major and most of the trace elements reflect a very similar pattern to Section1 until 80 mm, then depict a major excursion from this pattern indicating a change in climate impacting the watershed.

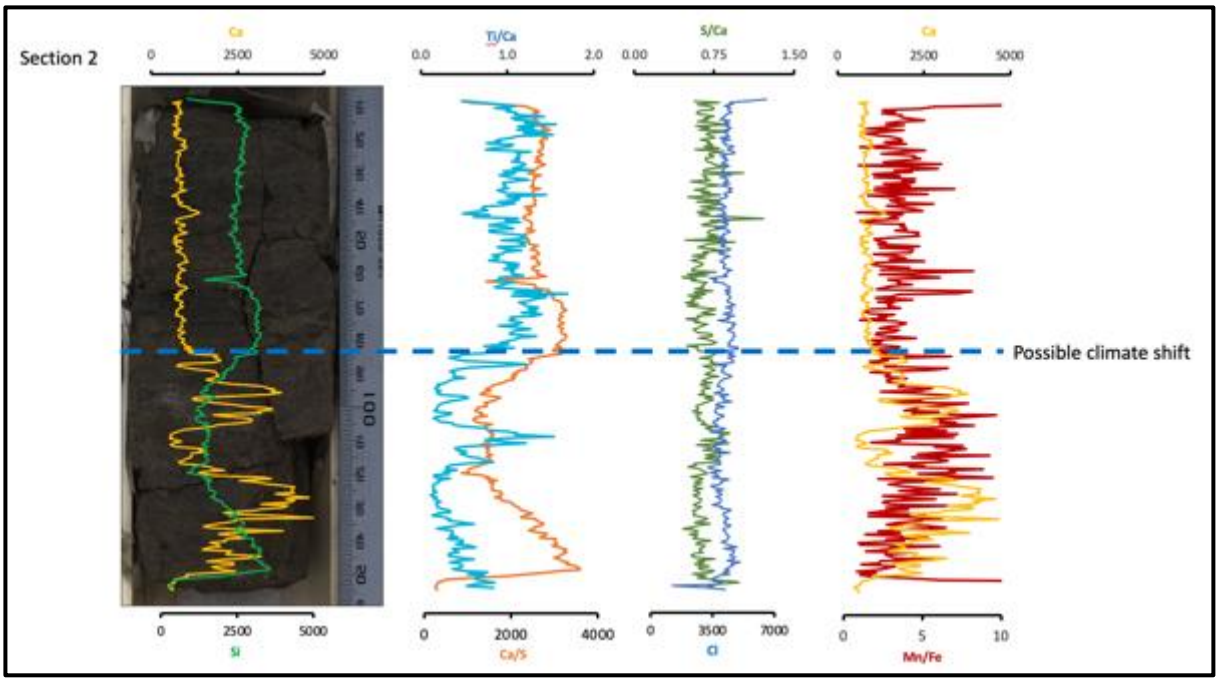

Figure 6.3. Section 2 core photo with XRF elements Ca and Si and rations of Ti/Ca, Ca/S, S/Ca and Cl, and Mn/Fe and Ca. These are proxies for changes in depositional inputs and potential indicators of repeated seasonal cycles. A notable shift in pattern and amplitude just below 80 mm indicates a significant and abrupt change in large scale basin inputs.

Section 3

Section 3 has long continuous visible laminae of alternating light and dark colors. The XRF results are similar to Section 1with simultaneously alternating peaks of Ca and Si throughout. The long term rend of Si increases throughout this section despite its fluctuations and amplitude remaining the same. This may reflect an overall increase in water to the lake. However, Ca has four major spikes. The largest spike occurs at 122 mm and is several orders of magnitude in scale. The other elements independent of Ca also peaking at these same four locations and similar scale are chlorine and sulfur. Iron (Fe) and silica (Si) also decrease significantly at the 122 mm depth, perhaps reflecting a significant short term arid event. The pattern and relationships of Ti/Ca and Ca/S, S/Ca and Cl, and Mn/Fe and Ca remain very similar to Section 1 indicating a stable, but seasonal climate regime dominating sediment deposition in the Al-Azraq lake.

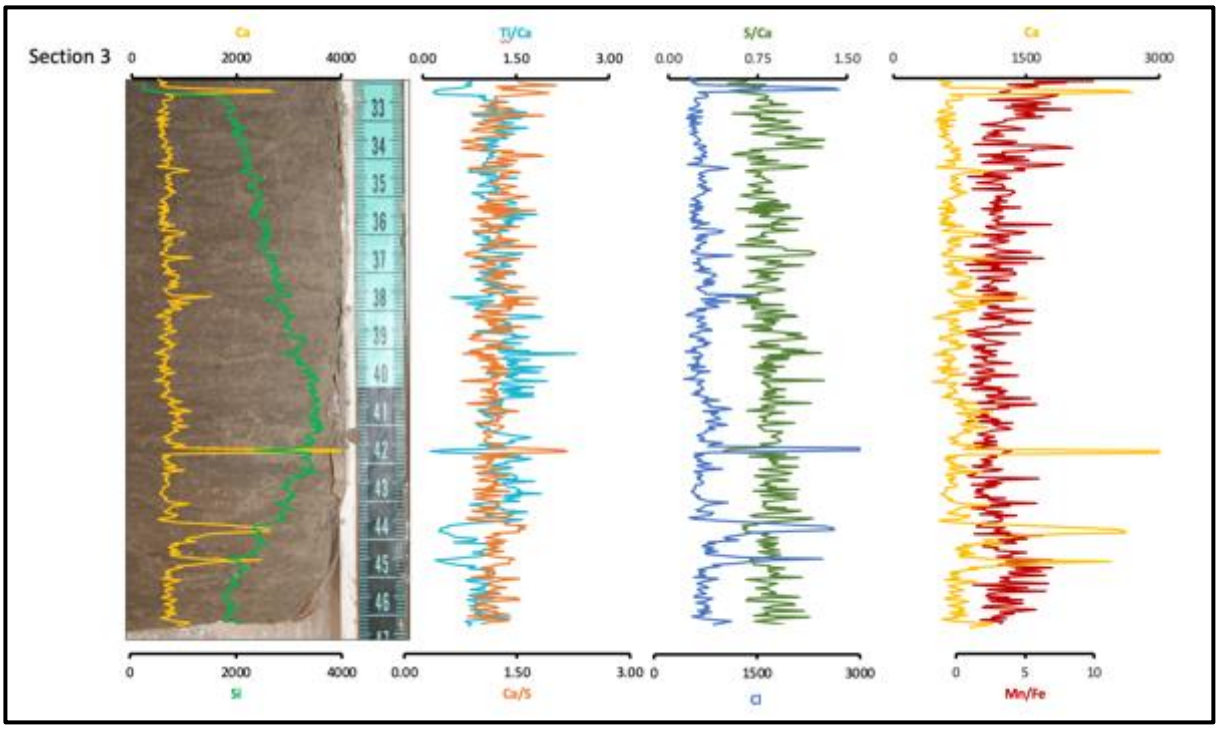

Figure 6.4. Section 3 core photo with XRF elements Ca and Si and ratios of Ti/Ca, Ca/S, S/Ca and Cl, and Mn/Fe and Ca. These are proxies for changes in depositional inputs and potential indicators of repeated seasonal cycles. A notable shift in pattern and amplitude just below 80 mm indicates a significant and abrupt change in large scale basin inputs.

Diatoms

Diatoms (Bacillariophyceae) are unicellular algae with well over a 100,000 species. They are ecologically sensitive, but can live in almost any environment that has or has had water. (Dixit et al., 1992), Their siliceous frustules are species-specific making them excellent proxies of environmental change (Battarbee, 1984). There are many factors affecting diatom preservation including: dissolution, pH, salt concentration, bacterial concentration, population, and water temperature (Lewin 1961).

SEM and EDS investigations of the AZ2 sediments sections reveal two species of centric diatoms, *Stephanodiscus* sp. and *Aulacoseira lirata* (Figure 5.10). *Stephanodiscus* is a polymorphic and one of the most diverse genera of phytoplankton. It's variability is dependent on valve size and/or ecological conditions (Theriot, Stoermer, 1981), Some *Stephanodiscus* under different ecological condition can and do exist either singly or

colonially with only a little variation in valve morphology (Stoermer et al., 1999). Because of their ability to adapt and change with conditions (Julius et al., 2010). This allows for past trophic conditions to be inferred by the different levels of available dissolved silica from the morphology of specimens preserved in sediments (Stoermer et al., 1999). *Stephanodiscus* can be found in fresh water and thrives in thermally stratified lakes. It can adapt to be successful with low Si, but requires both high phosphorous and high light conditions. It is the dominant species in winter and spring when increased turbulence suspends these relatively heavy diatoms. In Qarun Lake, Egypt domination of *Stephanodiscus* is indicative of high lake levels and increased nutrient load from freshwater inputs from Nile River flooding (Marks et al. 2017).

Aulacoseira is a planktonic freshwater diatom species found in most waters, but thrive in inland waters like lakes and ponds or rivers (Edlund *et al.*, 2008). They require high amounts of sunlight. An alkaliphilous species, or tolerant of alkaline waters. *Aulacoseira* is common in eutrophic lakes of higher temperatures and associated with warmer climates (Ehrlich, 1973; Stoermer et al., 1975; Camburn et al., 1986). It has high growth rates and therefore high demand for available silica (Kilham & Kilham 1971). They are suggestive of stable conditions, common in spring and dominant in summer. The occurrence of *Aulacoseira* with *Stephanodiscus* in low abundance indicates warm eutrophic conditions of freshwater with slightly higher salinity and alkalinity (Marks et al. 2017).

The extensive literature suggests the diatom species found in AZ2 sediments, *Stephanodiscus* and *Aulacoseira*, are subject to a range of conditions largely associated with seasonal changes in temperature and freshwater inputs. The Qarun Lake study is potentially analogous to the al-Azraq and indicates each taxa individually and in mixed conditions are indicative of different seasons (Marks et al., 2017). A detailed diatom study is required to further differentiate laminae by dominant diatom specie.

The condition of the diatoms is also informative. Some laminae consist almost entirely of diatoms with a majority of the matrix fragmented frustules. Valves appear to be broken, not dissolved. However, in Section 1, 2, and 3 there is extensive indication of post depositional halite encrustation which may be responsible for the degree of fragmentation (Figure 5.11). Further analysis into the post-depositional conditions is necessary.

Implications for Laminated Sediment

Multiple lines of evidence including: visual laminations of alternating color, grain size analysis, micro-scale fluctuations in geochemistry between wet and dry episodes, and the presence of two species of centric diatom in great quantity, which are seasonally different, all support the determination of the Al-Azraq laminations as seasonal rhythmites. The light colored laminated are composed of silt, diatoms, and organic material from the warmer spring-summer season and a darker layer composed of clay and terrestrial silica from the cooler winter season ranging in thickness from 0 .5 to 1.5 cm. Whether these coupled deposits can be defined as annual varves is not yet established as the specific species of calcium and sulfur are yet to be determined. Determining if all laminations are seasonal rhythmites is also not definitive and will be further investigated with micro-facies analysis. It is reasonable to presume there is a great deal of variation in depositional sequences and timing throughout the evolution of this paleolake (Ahmad, Davies, 2021). Age control is also necessary at the micro-scale to support the seasonal determination and to better place these sediments into the wider paleoenvironmental context of the Dead Sea basin laminated sediments and beyond.

Implications of Paleoenvironmental Variability and Regional Implications

The lacustrine sediments of the Al-Azraq basin demonstrate a wide range of paleoenvironments influenced basin evolution and shift in climate regime (Ahmad, Davies 2017, 2021). The laminated sediments investigated here contribute additional understanding

to the paleoenvironmental history of the basin and broader region. The rhythmites indicate both long-term stability of the paleoenvironment, and also signal abrupt changes in climate impacting the watershed (Kemp, 2003). The long-term stability of the regional climate regime is reflected in the meters of laminated sediment, of which only three short sections were examined in detail here. This is supported by the long record of steady alternating fluctuations of Ca and Si, as well as the consistency in the micro-scale short period and consistent low amplitude. The presence of meters of diatomite in the Al-Azraq first reported by Al'ali (2009), is expressed in 11 meters of AZ2 lacustrine sediments.

There is also evidence of abrupt changes in temperature and precipitation regime. The range of sediment grain size throughout the core while overall falling within the sandy silt range, show horizons of clays, aeolian, phases, and episodes of high water levels and drying episodes. Within the three sections examined here a significant potential climate shift is recorded in Section 2 below 80 mm with abrupt change of pattern and shift to different thresholds. Additional evidence of changes in climate is revealed by the EDS analysis of diatom samples showing extensive halite encrusting diatom frustules post-deposition. This indicates a period of high temperature. It also has implication for other carbonates and the sequence of evaporation.

Wet winters and dry summers characterize the climate of the eastern Mediterranean basin. The Jordan Plateau and eastern Mediterranean regional falls within a climatic transition zone between the fluctuations of the Northern jet Stream (NJS) and Subtropical Jet Stream (STJ). Throughout the Paleocene these circulation patterns have shifted in dominance producing more or less moisture between glaciations and non-glacial periods. The Dead Sea and its precursor lakes have long been viewed as one of the best gauges of precipitation history for the region (Neev et al., 1967, Migowsk, 2006). A study by Migowsk indicate two major wet phases along with a number of abrupt arid phases in the Jordan Valley and Dead

Sea region. The recent work by Ben Dor (2019) continue to demonstrate the regional import of laminated sediment. While the work by Lopez et al. (2016) and responses by Bookman (2020) stress the need to examine the basis for determining coupled laminae as seasonal deposition. It is reasonable to assume not all rhythmites represent strictly annual deposition, but rather seasonal being a wet and dry season. It is known from the present day Al-Azraq basing there are some years without any precipitation, and research has noted several very wet phases in the Dead Sea where water levels during the Holocene rose above 400 m bmsl, Neev and Emery (1967). It should be pointed out that the Dead Sea is a very large and very deep basin where it is unlikely annual depositional layers will cover the entire basin.

One line of critic of the annual designation of Dead Sea varves relies on demonstrating the source of pollen is not seasonal, but washed in and mixed from the surrounding watershed or aeolian in origin. However, in the Al-Azraq basin biological evidence for seasonality comes from *in situ* diatom production which is tied directly to lake environmental conditions (Gasse, 1994; Gasse et al., 1983; Gasse, et al. 1997). The diatom species found in the AZ2 laminations, *Stephanodiscus sp.* and *Aulacoseira lirata* are deposited in late summer earl winter, after the water settles down, the elongated centric diatoms tend to be spring and early summer, respectfully. The formation of a matrix bed of diatom frustules (Si, O) in matrix of crushed frustules, Fe-Mg-Al clay, and encrusted with halite (NaCl) indicate arid conditions occurring post-deposition.

From a smaller playa basin, Lake Qarun in the Feiyum Oasis west of the Nile River in Egypt perhaps more similar to the Al-Azraq, comes an additional study of note f (Marks et al. 2016; Zalat et al., 2017). The laminated sediments from this sediment core are also dominated by *Aulacoseira* spp. and *Stephanodiscus* spp. assemblages, but *Cyclostephanos dubius* and *Cyclotella meneghiniana* are also common. Two main factors in diatom

preservation at Quran are lake levels and salt levels. These would suggest similar climate conditions across the transitional region of the eastern Mediterranean (Flower, 2009).

7. CONCLUSIONS

Conclusions

The results of this investigation demonstrate the presence of laminated sediments and through robust examination by multiple analyses determine them to be seasonal rhythmites. These sediments reflect significant changes in depositional processes, moisture fluxes, and temperature regimes. These records document recurring processes and abrupt changes in the climate of the Quaternary evolution of this ancient saline lake. The sediment and mineralogical analysis of the AZ2 core sediments indicate changes in energy, environment, episodes of tectonic activity, terrestrial and aeolian inputs, depositional changes, and high evaporation phases. AZ2 core records approximately 11 meters with laminated sediments having alternating laminae of light and dark deposits composed of clays, silts, and diatoms. The detailed analyses of three sections of laminates provides a window into fine resolution lake processes.

Arid lake sediments are a complex mix of autochthonous biotic (microbial reduction) and abiotic (reduction and precipitation) processes and allochthonous inputs from the surrounding watershed which bring terrestrial minerals and organic detritus into the basin (Gierlowski-Kordesch, 2010). Calcium and silica are major components within the AZ2 sediments and rhythmites. Calcium is high throughout catchment (basalt and carbonate sources) and from aeolian sources. Is it also produced through evaporation within the lake. Silica also has multiple origins from erosion in the watershed and the biogenic productivity of diatoms. Mapping the rhythmite elements through XRF indicate variations are dominated by the seasonal deposition of additional terrigenous material, as seen primarily through Al, Fe, K, Sr and Ti. The Ca, Cl, S and to some extent a portion of Si are indicative of internal lake processes.

This research identifies the presence of laminae in AZ2 sediments and further demonstrates these laminated sediments are seasonal rhythmites. The rhythmites are composed of alternating calcium and silica. There are other signals in the element data requiring further investigation to identify the types of carbonates (calcite, aragonite, halite, gypsum, etc.), which will provide additional data on the seasonality signal. Additionally the presence of two species of differing seasonal express also supports seasonal differences in depositional timing. This research demonstrates, contrary to Ben Dor (2016), the Dead Sea is not the only deep hypersaline lake in the region containing finely laminated rhythmites and the potential for a high resolution paleoenvironmental record. This research also suggests Qarun Lake, Egypt may also serve as an analog for the Al-Azraq paleolake sharing similar diatom sequences.

APPENDIX A

Grain Size Data

AZ2 Grain Size Raw Data						
Depth	Tot Clay	Tot silt	tot sand	Tot	Sheppard	Folk
5.51	10.44	64.77	24.78	100.00	SnSilt	SnSilt
5.55	8.43	68.90	22.66	99.99	SnSilt	SnSilt
5.59	9.16	66.81	24.03	100.00	SnSilt	SnSilt
5.64	11.28	64.56	24.16	100.00	SnSilt	SnSilt
5.68	7.83	60.72	31.45	99.99	SnSilt	SnSilt
5.70	8.15	61.31	30.55	100.01	SnSilt	SnSilt
5.72	14.57	64.22	21.21	100.00	SnSilt	SnSilt
5.79	11.16	60.38	28.47	100.00	SnSilt	SnSilt
5.83	9.33	64.15	26.52	100.00	SnSilt	SnSilt
5.89	11.40	64.42	24.18	100.00	SnSilt	SnSilt
5.94	9.39	54.56	36.04	100.00	SnSilt	SnSilt
6.00	12.76	65.63	21.63	100.02	SnSilt	SnSilt
6.05	12.39	69.20	18.41	100.00	SnSilt	SnSilt
6.09	11.94	57.40	30.66	100.00	SnSilt	SnSilt
6.51	9.61	59.58	30.80	100.00	SnSilt	SnSilt
6.56	11.58	60.99	27.44	100.01	SnSilt	SnSilt
6.61	10.03	65.38	24.59	99.99	SnSilt	SnSilt
6.68	11.58	63.32	25.09	99.99	SnSilt	SnSilt
6.75	11.79	51.01	37.21	100.01	SnSilt	SnSilt
6.82	19.81	64.70	15.51	100.02	ClayeySilt	SnSilt
6.88	17.87	57.04	25.10	100.02	SnSilt	SnSilt
6.94	15.36	60.90	23.75	100.01	SnSilt	SnSilt
6.99	20.50	66.81	12.69	100.00	ClayeySilt	SnSilt
7.00	16.60	59.39	24.00	99.99	SnSilt	SnSilt
7.10	9.61	59.58	30.80	100.00	SnSilt	SnSilt
7.15	9.61	59.58	30.80	100.00	SnSilt	SnSilt
7.30	9.61	59.58	30.80	100.00	SnSilt	SnSilt
7.34	9.61	59.58	30.80	100.00	SnSilt	SnSilt
7.39	9.61	59.58	30.80	100.00	SnSilt	SnSilt
7.42	9.61	59.58	30.80	100.00	SnSilt	SnSilt
7.52	10.74	60.73	28.52	99.99	SnSilt	SnSilt
7.57	8.55	64.18	27.27	100.00	SnSilt	SnSilt
7.64	12.06	62.38	25.55	99.99	SnSilt	SnSilt
7.68	10.35	61.51	28.14	100.00	SnSilt	SnSilt
8.02	18.52	71.87	9.60	99.99	ClayeySilt	Silt
8.09	10.45	62.16	27.38	99.99	SnSilt	SnSilt
8.22	14.16	66.95	18.88	99.99	SnSilt	SnSilt
8.26	13.97	67.76	18.27	100.00	SnSilt	SnSilt
8.51	10.53	62.98	26.47	99.99	SnSilt	SnSilt
8.56	40.04	49.23	10.74	100.01	SnSilt	SnSilt
8.67	10.34	59.23	30.42	100.00	SnSilt	SnSilt
8.70	15.60	67.48	16.92	100.00	SnSilt	SnSilt
8.74	14.15	68.40	17.45	99.99	SnSilt	SnSilt
8.90	14.97	65.36	19.67	100.00	SnSilt	SnSilt

9.09	15.75	60.31	23.94	100.00	SnSilt	SnSilt
9.83	13.00	58.51	28.48	99.99	SnSilt	SnSilt
9.89	9.72	55.82	34.46	99.99	SnSilt	SnSilt
9.92	8.99	51.98	39.04	100.01	SnSilt	SnSilt
9.97	8.59	65.76	25.66	100.01	SnSilt	SnSilt
10.06	3.26	59.12	37.63	100.01	SnSilt	SnSilt
10.10	3.12	50.87	46.01	100.00	SnSilt	SnSilt
10.18	3.11	53.48	43.40	100.00	SnSilt	SnSilt
10.22	2.00	49.19	48.82	100.01	SnSilt	SnSilt
10.26	2.52	52.12	45.39	100.02	SnSilt	SnSilt
10.32	6.54	62.99	30.47	100.00	SnSilt	SnSilt
10.38	3.03	62.06	34.90	100.00	SnSilt	SnSilt
10.47	6.85	63.32	29.85	100.01	SnSilt	SnSilt
10.53	9.09	71.27	19.64	100.00	SnSilt	SnSilt
11.00	2.03	62.95	35.02	100.00	SnSilt	SnSilt
11.04	1.77	67.32	30.92	100.01	SnSilt	SnSilt
11.10	1.62	56.31	42.07	100.00	SnSilt	SnSilt
11.20	1.06	58.77	40.17	100.00	SnSilt	SnSilt
11.25	0.57	59.52	39.90	100.00	SnSilt	SnSilt
11.32	1.03	52.89	46.09	100.01	SnSilt	SnSilt
11.42	2.52	67.46	30.02	100.00	SnSilt	SnSilt
11.49	0.87	49.04	50.09	99.99	SiltySand	SiltySand
12.60	4.31	61.52	34.19	100.02	SnSilt	SnSilt
12.65	3.11	68.55	28.34	100.00	SnSilt	SnSilt
12.67	2.76	57.44	39.81	100.00	SnSilt	SnSilt
12.69	3.55	54.99	41.47	100.01	SnSilt	SnSilt
12.75	4.08	60.38	35.54	100.00	SnSilt	SnSilt
12.78	8.46	54.82	36.74	100.01	SnSilt	SnSilt
12.86	7.92	57.86	34.22	100.00	SnSilt	SnSilt
12.88	8.46	54.82	36.74	100.01	SnSilt	SnSilt
12.89	8.46	54.82	36.74	100.01	SnSilt	SnSilt
13.01	8.46	54.82	36.74	100.01	SnSilt	SnSilt
14.01	8.46	54.82	36.74	100.01	SnSilt	SnSilt
14.04	8.46	54.82	36.74	100.01	SnSilt	SnSilt
14.10	8.46	54.82	36.74	100.01	SnSilt	SnSilt
14.11	8.46	54.82	36.74	100.01	SnSilt	SnSilt
14.16	8.46	54.82	36.74	100.01	SnSilt	SnSilt
14.23	8.46	54.82	36.74	100.01	SnSilt	SnSilt
14.31	6.31	50.85	42.83	99.99	SnSilt	SnSilt
14.38	8.46	54.82	36.74	100.01	SnSilt	SnSilt
14.46	8.46	54.82	36.74	100.01	SnSilt	SnSilt
14.56	8.46	54.82	36.74	100.01	SnSilt	SnSilt
14.63	8.46	54.82	36.74	100.01	SnSilt	SnSilt
14.68	8.46	54.82	36.74	100.01	SnSilt	SnSilt
15.77	6.24	83.57	10.20	100.00	Silt	SnSilt
15.84	5.51	72.69	21.80	100.00	SnSilt	SnSilt

15.86	7.27	67.25	25.48	100.00	SnSilt	SnSilt
17.03	10.66	67.55	21.80	100.01	SnSilt	SnSilt
17.08	5.85	66.41	27.76	100.01	SnSilt	SnSilt
17.12	6.18	65.93	27.84	99.95	SnSilt	SnSilt
17.18	7.38	62.11	30.29	99.78	SnSilt	SnSilt
17.21	10.15	62.96	26.89	100.00	SnSilt	SnSilt
17.30	13.08	68.44	18.44	99.96	SnSilt	SnSilt
17.38	7.36	65.66	26.98	100.00	SnSilt	SnSilt
17.42	9.46	67.17	23.37	99.99	SnSilt	SnSilt
17.45	5.52	68.09	26.38	99.99	SnSilt	SnSilt
17.50	7.62	70.75	21.65	100.02	SnSilt	SnSilt
17.59	9.22	69.15	21.64	100.01	SnSilt	SnSilt
17.66	9.92	76.34	13.73	99.99	Silt	SnSilt
17.71	6.62	57.68	35.71	100.01	SnSilt	SnSilt
17.76	8.53	69.36	22.10	99.99	SnSilt	SnSilt
17.81	5.78	61.55	32.67	100.00	SnSilt	SnSilt
17.85	7.55	74.21	18.23	99.99	SnSilt	SnSilt
17.94	5.90	53.98	40.12	100.00	SnSilt	SnSilt
18.00	7.43	73.64	18.92	99.99	SnSilt	SnSilt
18.06	8.69	56.96	34.38	100.03	SnSilt	SnSilt
18.14	10.69	58.51	30.83	100.03	SnSilt	SnSilt
18.20	8.66	49.29	42.04	99.99	SnSilt	SnSilt
19.02	7.71	65.70	26.60	100.01	SnSilt	SnSilt
19.09	6.58	64.77	28.66	100.01	SnSilt	SnSilt
19.16	9.32	73.90	16.77	99.99	SnSilt	SnSilt
19.20	7.24	54.63	38.12	99.99	SnSilt	SnSilt
19.23	9.57	67.07	23.36	100.00	SnSilt	SnSilt
19.30	6.50	60.38	33.66	100.54	SnSilt	SnSilt
19.33	10.37	74.14	15.50	100.01	SnSilt	SnSilt
19.41	8.45	57.28	34.26	99.99	SnSilt	SnSilt
20.50	11.56	67.53	20.91	100.00	SnSilt	SnSilt
20.57	14.24	66.00	19.77	100.01	SnSilt	SnSilt
20.61	12.67	64.35	22.97	100.00	SnSilt	SnSilt
22.00	14.41	72.27	13.33	100.00	ClayeySilt	SnSilt
22.04	14.12	71.94	13.93	99.99	ClayeySilt	SnSilt
22.05	15.20	67.72	17.08	100.00	SnSilt	SnSilt
22.20	12.82	68.86	18.33	100.00	SnSilt	SnSilt
22.28	16.07	74.64	9.29	100.00	ClayeySilt	Silt
22.38	11.50	50.89	37.59	99.98	SnSilt	SnSilt
22.44	17.01	69.81	13.17	99.99	SnSilt	SnSilt
22.54	11.55	52.07	36.38	100.00	SnSilt	SnSilt
22.56	16.55	62.27	21.18	100.00	SnSilt	SnSilt
22.62	9.75	55.75	34.50	100.00	SnSilt	SnSilt
22.64	12.97	56.88	30.14	100.00	SnSilt	SnSilt
22.92	8.87	46.95	44.58	100.40	SnSilt	SnSilt
23.03	11.05	55.83	33.54	100.41	SnSilt	SnSilt

23.05	10.60	72.08	17.70	100.38	SnSilt	SnSilt
23.15	11.54	43.03	46.02	100.59	SnSilt	SnSilt
23.29	7.22	51.99	18.93	78.14	SnSilt	SnSilt
23.34	7.59	64.43	28.32	100.34	SnSilt	SnSilt
23.56	11.55	76.70	11.72	99.97	Silt	SnSilt
23.59	11.55	76.70	11.72	99.97	Silt	SnSilt
23.62	7.87	72.54	19.56	99.97	SnSilt	SnSilt
23.66	8.27	70.39	21.33	99.99	SnSilt	SnSilt
23.69	6.72	39.78	53.47	99.98	SiltySand	SiltySand
23.73	11.61	63.01	25.35	99.97	SnSilt	SnSilt
23.76	10.33	69.29	20.36	99.98	SnSilt	SnSilt
23.78	16.30	66.09	17.57	99.96	SnSilt	SnSilt
23.81	16.93	53.34	29.68	99.95	SnSilt	SnSilt
25.24	11.32	85.33	3.35	100.00	Silt	Silt
25.28	13.75	81.95	4.30	100.00	Silt	Silt
25.29	10.49	80.17	9.34	100.00	Silt	Silt
25.32	16.39	83.49	0.11	99.99	Silt	Silt
25.34	18.23	79.42	2.34	100.00	Silt	Silt
25.38	15.65	80.67	3.68	100.00	Silt	Silt
25.41	14.21	82.40	3.39	100.00	Silt	Silt
25.43	16.13	80.07	3.80	100.00	Silt	Silt
25.44	12.20	73.66	14.13	99.99	SnSilt	SnSilt
25.45	13.00	78.85	8.15	100.00	SnSilt	SnSilt
25.46	11.76	83.24	4.99	99.99	Silt	Silt
25.48	12.63	79.03	8.34	100.01	Silt	Silt
25.50	11.66	56.10	32.23	99.99	SnSilt	SnSilt
25.51	13.20	82.93	3.87	100.00	Silt	Silt
25.55	13.09	77.94	8.95	99.99	Silt	Silt
25.92	11.76	70.79	17.46	100.00	SnSilt	SnSilt
35.24	18.43	76.60	4.97	99.99	Silt	Silt
35.34	14.60	72.56	12.83	100.00	ClayeySilt	SnSilt
35.45	11.92	73.32	14.75	100.00	SnSilt	SnSilt
35.54	12.47	71.65	15.88	99.99	SnSilt	SnSilt
35.64	12.73	71.58	15.70	100.01	SnSilt	SnSilt
35.68	13.76	73.72	12.49	99.97	ClayeySilt	SnSilt
35.76	13.53	76.67	9.81	100.00	Silt	Silt
35.87	13.90	77.03	9.08	100.01	Silt	Silt
35.96	27.59	55.21	17.19	99.99	ClayeySilt	SandyMud
35.98	11.89	65.80	22.31	100.00	SnSilt	SnSilt

APPENDIX B

X-Ray Florescence Raw Data

SECTION 1 XRF Raw Data

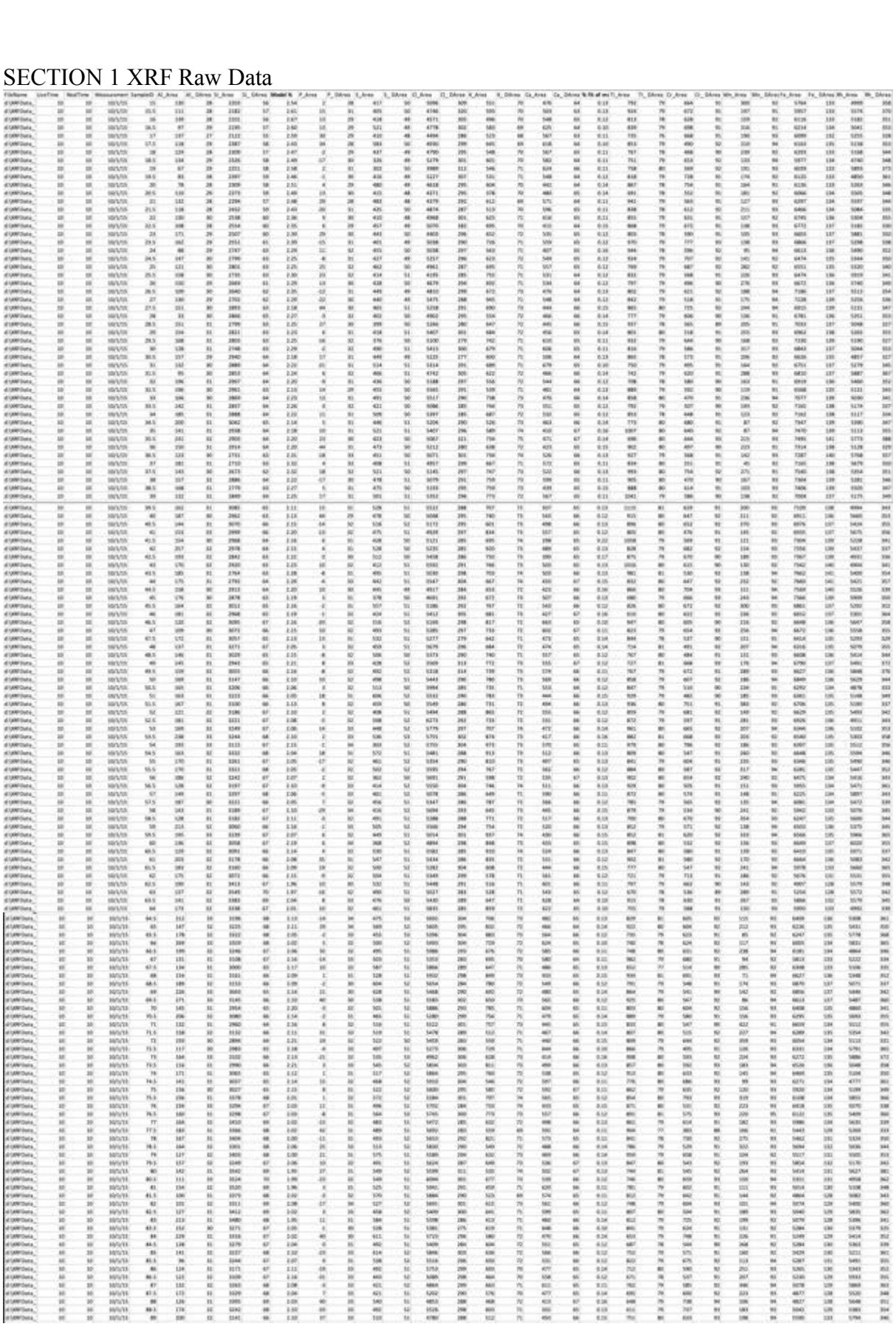

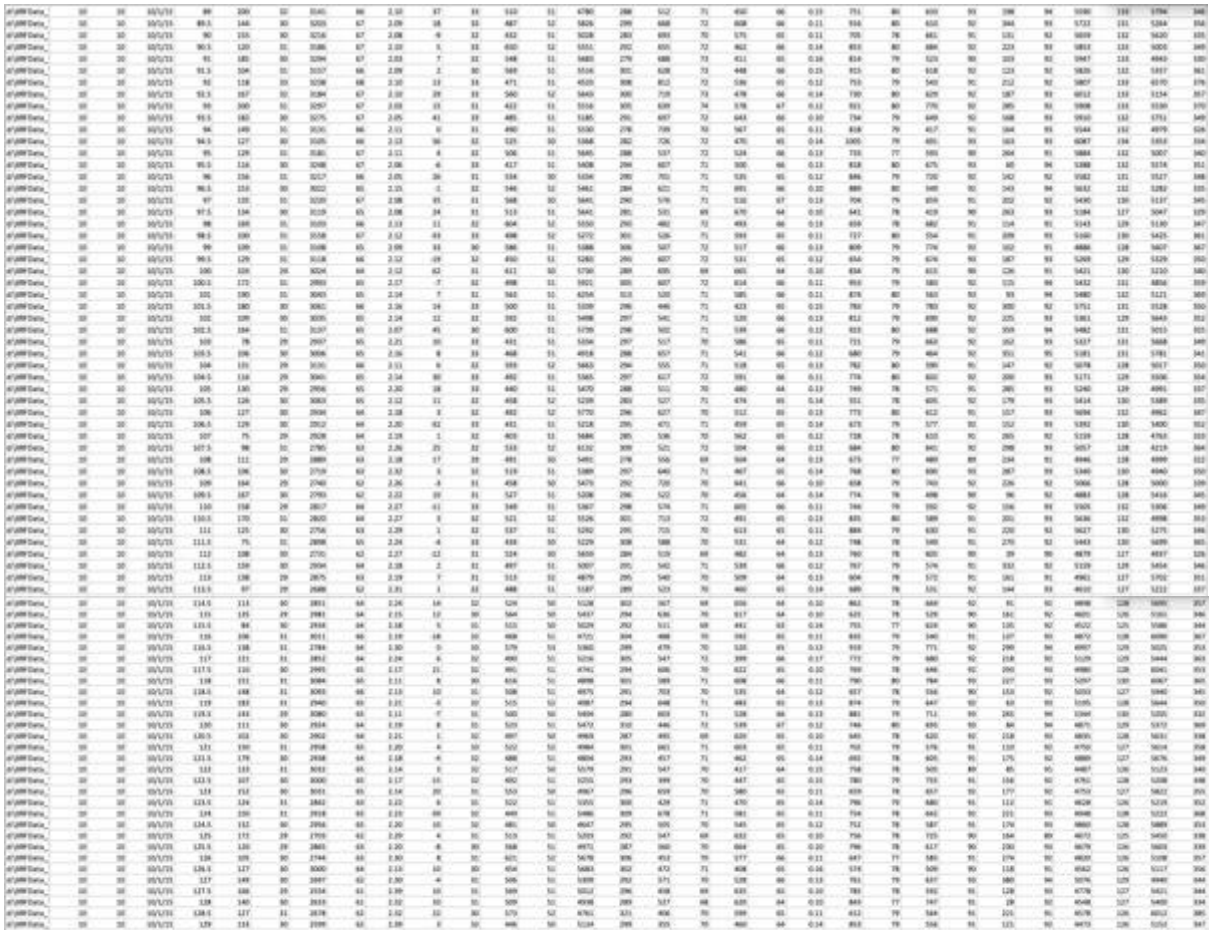

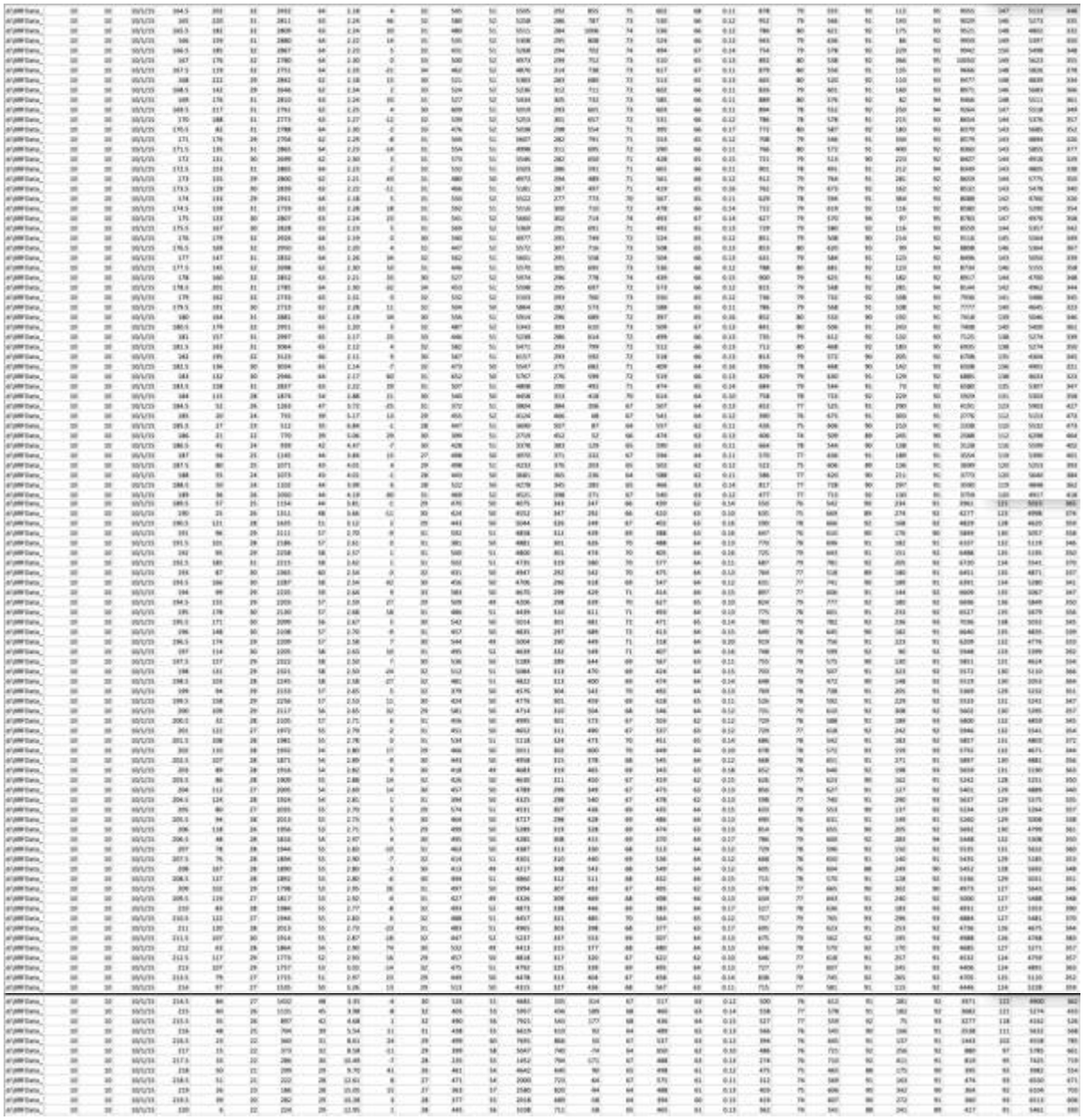

SECTION 2 XRF Raw Data

FileName	LiveTim	RealTi	Measured	Sampl	Al_Are	Al_ DA	Si_Are	Si_ DA	P_Area	P_ DAr	S_Area	S_ DAr	Cl_Area	Cl_ DA	K_Area	K_ DAr	Ca_Are	Ca_ DA	Ti_Are	Ti_ DA	Cr_Are	Cr_ DA	Mn_Ar	Mn_ D	Fe_Are	Fe_ DA	Rh_Are	Rh_ DA
d:\XRF Data_Tube	10	10	10/6/15	8	45	26	860	42	29	32	496	55	6545	523	365	67	876	66	417	78	553	92	281	93	2470	111	5475	496
d:\XRF Data_Tube	10	10	10/6/15	8.5	55	27	1098	45	10	31	493	53	5743	402	142	67	618	66	453	76	609	91	190	93	3328	118	4492	405
d:\XRF Data_Tube	10	10	10/6/15	9	104	28	1636	52	5	31	498	52	4491	324	466	70	841	68	820	79	617	92	239	94	4865	127	5239	361
d:\XRF Data_Tube	10	10	10/6/15	9.5	205	29	2329	58	10	30	541	52	4677	282	629	70	766	68	838	80	579	91	144	92	5805	131	5181	325
d:\XRF Data_Tube	10	10	10/6/15	10	204	30	2433	60	12	32	578	52	4183	272	646	71	771	68	661	80	527	92	190	94	5853	132	5138	319
d:\XRF Data_Tube	10	10	10/6/15	10.5	155	29	2516	60	7	31	617	51	4517	278	576	72	843	69	875	80	576	92	140	93	5772	133	5221	327
d:\XRF Data_Tube	10	10	10/6/15	11	205	32	2641	62	-4	32	482	52	4380	279	730	72	790	70	783	81	544	92	208	94	5674	132	5127	332
d:\XRF Data_Tube	10	10	10/6/15	11.5	161	31	2502	61	19	33	525	51	4446	276	675	73	898	70	993	81	717	93	197	92	5409	131	4918	325
d:\XRF Data_Tube	10	10	10/6/15	12	234	31	2620	62	-27	31	489	51	4571	271	860	73	799	67	867	80	539	92	227	94	5443	131	4921	319
d:\XRF Data_Tube	10	10	10/6/15	12.5	167	30	2413	59	-11	31	509	51	4302	279	601	73	678	68	966	82	725	93	285	93	5583	132	5172	330
d:\XRF Data_Tube	10	10	10/6/15	13	141	30	2537	60	3	30	527	50	4171	259	807	71	797	67	835	80	636	93	188	94	5471	132	5054	306
d:\XRF Data_Tube	10	10	10/6/15	13.5	134	30	2567	61	6	31	491	50	4146	276	698	73	707	69	777	80	554	91	147	92	5458	131	5109	328
d:\XRF Data_Tube	10	10	10/6/15	14	114	31	2627	62	-15	32	447	50	3939	283	681	71	746	68	982	80	564	91	225	94	5837	132	5661	343
d:\XRF Data_Tube	10	10	10/6/15	14.5	178	30	2487	61	-3	32	575	51	4485	274	685	71	784	68	940	80	661	93	160	94	5772	132	5010	322
d:\XRF Data_Tube	10	10	10/6/15	15	157	31	2656	63	2	32	543	50	4166	272	658	75	623	69	976	81	639	92	79	93	5709	132	4948	328
d:\XRF Data_Tube	10	10	10/6/15	15.5	209	32	2789	63	28	31	441	50	4422	273	835	73	760	68	856	81	655	92	214	92	5613	132	4949	327
d:\XRF Data_Tube	10	10	10/6/15	16	231	30	2706	62	8	31	530	50	4236	284	699	74	745	70	973	81	621	93	119	95	5395	132	5325	344
d:\XRF Data_Tube	10	10	10/6/15	16.5	202	31	2906	64	17	32	521	49	4545	256	759	73	853	68	949	79	700	91	74	91	5591	130	4697	305
d:\XRF Data_Tube	10	10	10/6/15	17	201	31	2801	63	54	31	571	50	4384	266	743	73	643	68	920	79	602	91	119	92	5329	130	4981	317
d:\XRF Data_Tube	10	10	10/6/15	17.5	169	33	2813	65	12	33	555	50	4001	277	846	75	801	70	949	82	521	92	179	94	5983	134	5226	339
d:\XRF Data_Tube	10	10	10/6/15	18	205	32	2717	63	-8	33	434	50	4227	272	805	74	642	69	982	80	550	91	204	93	5690	132	5010	325
d:\XRF Data_Tube	10	10	10/6/15	18.5	219	33	2720	63	0	32	533	51	4338	284	880	74	722	69	807	82	609	92	216	92	5797	132	5171	341
d:\XRF Data_Tube	10	10	10/6/15	19	208	32	2833	63	-13	31	582	51	4440	271	718	74	767	70	792	80	502	92	153	93	5897	133	4746	327
d:\XRF Data_Tube	10	10	10/6/15	19.5	214	33	2706	63	20	32	617	53	3930	277	671	72	992	71	873	81	733	91	219	91	5528	131	5409	334
d:\XRF Data_Tube	10	10	10/6/15	20	201	31	2659	62	4	31	669	52	4501	260	635	73	947	71	876	80	672	91	170	91	6079	133	4402	310
d:\XRF Data_Tube	10	10	10/6/15	20.5	221	31	2750	63	6	33	684	53	4030	249	923	73	991	70	753	79	563	90	67	92	6500	136	4998	298
d:\XRF Data_Tube	10	10	10/6/15	21	235	32	2688	62	7	31	628	53	4205	259	790	74	846	70	901	80	620	92	184	93	6167	133	4966	308
d:\XRF Data_Tube	10	10	10/6/15	21.5	232	33	2731	64	-1	33	681	53	4185	279	836	74	1029	71	1072	80	557	92	303	94	5845	133	4999	340
d:\XRF Data_Tube	10	10	10/6/15	22	201	31	2730	63	23	31	771	52	4711	261	727	73	964	70	819	80	671	92	203	93	5796	132	4455	309
d:\XRF Data_Tube	10	10	10/6/15	22.5	269	33	2653	63	-28	33	507	52	4521	273	764	73	880	70	660	79	500	91	138	93	5720	131	4778	324
d:\XRF Data_Tube	10	10	10/6/15	23	239	31	2607	61	31	31	609	51	4342	261	708	73	723	69	919	80	728	93	250	93	5543	132	4850	310
d:\XRF Data_Tube	10	10	10/6/15	23.5	210	31	2682	62	50	31	601	51	4679	267	817	74	839	69	934	80	707	92	247	93	5598	131	4797	317
d:\XRF Data_Tube	10	10	10/6/15	24	236	32	2730	62	9	30	589	52	4743	284	653	74	842	70	945	81	550	91	281	92	5740	131	4786	342
d:\XRF Data_Tube	10	10	10/6/15	24.5	211	32	2585	62	0	32	577	51	3912	281	608	73	770	68	883	80	403	91	209	94	5350	130	5433	338
d:\XRF Data_Tube	10	10	10/6/15	25	205	30	2579	60	-8	31	520	51	4263	261	743	71	772	68	846	80	642	91	133	92	5323	129	4963	308
d:\XRF Data_Tube	10	10	10/6/15	25.5	184	31	2670	62	-13	31	525	51	4079	269	783	74	779	68	889	80	590	92	338	92	5441	130	5136	323
d:\XRF Data_Tube	10	10	10/6/15	26	142	32	2551	62	-9	33	524	51	4377	268	843	71	767	67	805	79	446	90	48	91	5035	129	4718	315
d:\XRF Data_Tube	10	10	10/6/15	26.5	190	31	2730	62	45	32	558	51	4146	267	702	73	762	69	912	82	676	93	261	93	5495	131	5012	323
d:\XRF Data_Tube	10	10	10/6/15	27	185	31	2774	63	11	31	569	52	4045	279	713	73	743	69	897	80	605	91	304	93	5060	129	5390	340
d:\XRF Data_Tube	10	10	10/6/15	27.5	173	31	2625	62	32	32	673	51	4374	272	745	74	755	69	860	80	434	91	170	92	5255	130	4777	326
d:\XRF Data_Tube	10	10	10/6/15	28	152	31	2594	62	4	32	624	51	4031	272	672	73	860	69	910	79	669	92	241	92	5575	130	5241	327
d:\XRF Data_Tube	10	10	10/6/15	28.5	163	31	2507	61	-9	33	521	51	4197	273	656	73	792	68	1018	79	603	91	99	92	5342	130	4994	323
d:\XRF Data_Tube	10	10	10/6/15	29	175	30	2529	60	-3	31	556	52	4116	265	743	72	861	68	820	78	488	91	197	93	5563	131	5061	315
d:\XRF Data_Tube	10	10	10/6/15	29.5	191	30	2395	59	11	30	823	52	4045	259	677	72	800	68	869	78	622	91	117	92	6100	133	5136	306
d:\XRF Data_Tube	10	10	10/6/15	30	193	30	2689	62	-26	30	597	51	4511	262	740	72	929	69	840	80	670	91	292	91	6421	133	4782	313
d:\XRF Data_Tube	10	10	10/6/15	30.5	218	32	2524	61	13	32	550	50	4560	269	799	72	819	69	800	80	636	91	224	92	6008	132	4838	316
d:\XRF Data_Tube	10	10	10/6/15	31	216	32	2556	62	7	32	484	50	3928	275	834	73	729	68	827	80	535	91	261	92	5800	131	5473	326
d:\XRF Data_Tube	10	10	10/6/15	31.5	172	31	2499	61	3	31	518	51	4260	267	786	73	725	68	903	79	475	90	149	92	5911	133	5193	315
d:\XRF Data_Tube	10	10	10/6/15	32	182	32	2506	61	12	33	492	51	4361	264	785	73	923	68	945	79	577	89	246	91	5852	131	4623	309
d:\XRF Data_Tube	10	10	10/6/15	32.5	204	32	2487	61	-8	31	559	52	4136	275	672	73	830	69	785	79	784	91	113	91	5657	131	5077	326
d:\XRF Data_Tube	10	10	10/6/15	33	239	31	2515	60	20	31	712	51	4486	271	782	73	881	69	862	80	704	90	407	91	5804	131	4734	322
d:\XRF Data_Tube	10	10	10/6/15	33.5	210	32	2447	61	35	32	575	51	4013	272	822	72	850	68	817	79	510	89	110	91	5675	131	5207	319
d:\XRF Data_Tube	10	10	10/6/15	34	244	31	2676	62	10	32	549	52	4279	288	769	76	832	70	844	81	541	91	156	92	5756	130	4821	349
d:\XRF Data_Tube	10	10	10/6/15	34.5	193	30	2507	60	14	30	565	52	4573	271	1062	72	998	68	883	81	763	92	308	92	5794	131	4963	318
d:\XRF Data_Tube	10	10	10/6/15	35	227	32	2496	61	11	32	537	52	4405	284	589	74	758	69	707	80	573	92	86	93	5668	131	4780	339
d:\XRF Data_Tube	10	10	10/6/15	35.5	196	32	2493	61	-1	33	485	51	4568	287	721	73	767	69	773	80	684	92	181	93	5459	131	4937	337
d:\XRF Data_Tube	10	10	10/6/15	36	177	31	2486	61	-20	32	497	50	4151	292	610	72	612	68	889	79	528	90	212	92	5456	130	5607	347
d:\XRF Data_Tube	10	10	10/6/15	36.5	165	32	2532	61	-13	32	393	50	4261	281	633	72	775	68	769	79	629	92	154	93	5247	130	5135	333
d:\XRF Data_Tube	10	10	10/6/15	37	166	31	2524	61	10	32	488	51	4325	279	629	73	780	68	887	79	666	91	184	92	5331	130	5016	330
d:\XRF Data_Tube	10	10	10/6/15	37.5	218	30	2570	60	10	29	604	50	3974	262	630	72	749	68	837	80	789	92	327	93	5750	132	5166	313
d:\XRF Data_Tube	10	10	10/6/15	38	201	31	2544	61	-3	31	518	52	3702	275	797	72	881	67	785	80	590	92	157	93	5757	132	5560	331
d:\XRF Data_Tube	10	10	10/6/15	38.5	209	32	2541	61	41	30	651	51	3899	287	805	73	789	68	860	82	548	93	202	95	5771	131	5484	350
d:\XRF Data_Tube	10	10	10/6/15	39	230	33	2563	61	34	31	671	51	3884	265	614	72	868	68	825	79	628	90	245	91	5379	129	5061	315
d:\XRF Data_Tube	10	10	10/6/15	39.5	176	31	2309	59	-19	33	682	54	4129	278	692	73	1091	72	799	79	551	91	277	92	5521	130	4845	330
d:\XRF Data_Tube	10	10	10/6/15	40	205	31	2460	61	-6	32	888	54	4268	273	538	72	1096	72	771	78	593	90	44	91	5402	129	4935	324
d:\XRF Data_Tube	10	10	10/6/15	40.5	211	30	2377	59	3	33	859	55	3769	246	658	72	1281	73	990	79	623	90	195	92	5206	128	5026	292
d:\XRF Data_Tube	10	10	10/6/15	41	139	30	2471	61	-7	32	829	55	4147	263	597	72	1398	74	865	78	610	90	181	91	5394	130	4749	315
d:\XRF Data_Tube	10	10	10/6/15	41.5	146	30	2469	61	-19	32	906	55	4113	261	774	71	1280	72	624	78	466	90	170	91	5918	132	5055	312
d:\XRF Data_Tube	10	10	10/6/15	42	260	31	2325	58	1	30	696	53	4239	267	633	71	1139	71	901	79	541	91	198	93	5719	132	4641	316
d:\XRF Data_Tube	10	10	10/6/15	42.5	188	30	2272	58	39	30	787	53	3646	271	710	70	956	68	583	78	510	90	66	91	6248	134	5477	322
d:\XRF Data_Tube	10	10	10/6/15	43	187	30	2294	58	7	31	907	55	4314	265	662	71	745	68	837	79	501	90	95	92	6711	136	4656	312
d:\XRF Data_Tube	10	10	10/6/15	43.5	238	31	2421	60	5	31	513	51	4057	265	653	72	720	67	701	79	664	89	242	90	6270	134	4966	311
d:\XRF Data_Tube	10	10	10/6/15	44	220	32	2470	60	-2	32	565	51	4469	272	728	72	702	68	804	79	473	90	197	92	5501	131	4696	320
d:\XRF Data_Tube	10	10	10/6/15	44.5	215	31	2473	61	10	32	638	51	4025	279	707	73	960	70	894	79	701	91	206	92	5244	130	5232	334
d:\XRF Data_Tube	10	10	10/6/15	45	163	31	2473	60	5	31	608	51	4382	270	739	72	961	70	757	79	689	93	209	94	5293	128	4673	321
d:\XRF Data_Tube	10	10	10/6/15	45.5	226	32	2469	60	5	30	679	53	4299	276	721	73	803	70	799	80	646	91	173	92	5289	130	5034	329
d:\XRF Data_Tube	10	10	10/6/15	46	151	31	2354	59	30	31	692	51	3681	268	590	71	818	69	880	79	710	91	250	91	5252	129	5396	319
d:\XRF Data_Tube	10	10	10/6/15	46.5	169	30	2532	60	-15	30	613	51	4285	265	702	73	857	70	681	79	477	91	250	93	5463	130	4563	318
d:\XRF Data_Tube	10	10	10/6/15	47	181	31	2440	60	-2	31	712	53	4437	267	699	71	1032	70	818	79	527	90	251	92	5252	129	4645	315
d:\XRF Data_Tube	10	10	10/6/15	47.5	139	29	2331	58	-2	31	622	52	4463	266	626	71	894	69	941	79	549	91	162	93	5580	131	4550	311
d:\XRF Data_Tube	10	10	10/6/15	48	176	29	2227	58	27	31	530	48	4073	256	686	70	676	67	781	78	420	89	102	92	5267	129	4885	294
d:\XRF Data_Tube	10	10	10/6/15	48.5	178	30	2312	58	34	29	489	49	4128	263	742	71	715	66	873	79	595	91	115	93	5309	130	4856	308
d:\XRF Data_Tube	10	10	10/6/15	49	165	30	2392	59	24	30	541	50	3798	270	758	71	652	67	761	78	629	91	137	92	5127	129	5348	321
d:\XRF Data_Tube	10	10	10/6/15	49.5	155	30	2412	60	-10	30	434	48	4261	274	601	70	904	68	837	78	562	91	112	93	5150	129	4947	323
d:\XRF Data_Tube	10	10	10/6/15	50	215	32	2407	60	10	31	612	51	3837	286	648	72	647	67	790	80	615	91	244	92	5074	128	5489	341
d:\XRF Data_Tube	10	10	10/6/15	50.5	192	31	2413	59	-2	30	510	50	4017	282	670	71	736	67	843	79	447	91	116	93	5144	130	5401	337
d:\XRF Data_Tube	10	10	10/6/15	51	199	31	2619	61	-4	30	481	51	4176	280	705	72	725	67	879	80	645	91	236	92	5360	129	5005	338
d:\XRF Data_Tube	10	10	10/6/15	51.5	165	30	2531	61	3	32	537	50	3971	284	794	72	896	69	795	79	717	92	229	92	5255	129	5440	342
d:\XRF Data_Tube	10	10	10/6/15	52	194	30	2443	60	-6	32	581	52	4324	269	660	70	822	67	801	79	519	90	223	92	5248	129	4861	315
d:\XRF Data_Tube	10	10	10/6/15	52.5	216	31	2585	61	11	31	605	51	4515	273	609	73	712	69	831	79	637	92	105	93	5499	130	4481	325
d:\XRF Data_Tube	10	10	10/6/15	53	170	31	2635	62	-5	32	549	49	4322	251	722	71	849	68	815	79	447	90	181	93	5534	132	4709	296
d:\XRF Data_Tube	10	10	10/6/15	53.5	189	30	2642	62	9	32	622	50	3860	262	791	73	902	69	860	80	591	92	220	93	5582	130	5235	317
d:\XRF Data_Tube	10	10	10/6/15	54	150	30	2542	61	16	30	540	51	4039	264	633	71	982	68	808	78	572	90	150	91	5189	129	5091	314
d:\XRF Data_Tube	10	10	10/6/15	54.5	191	30	2459	59	29	30	659	51	4461	271	596	72	977	71	884	80	720	92	303	92	5923	131	4824	323
d:\XRF Data_Tube	10	10	10/6/15	55	217	31	2602	61	-9	31	597	50	4182	258	895	73	983	69	863	80	557	91	108	93	5770	133	4870	308
d:\XRF Data_Tube	10	10	10/6/15	55.5	193	30	2594	60	25	31	563	51	4096	260	857	73	1051	69	823	78	623	90	103	91	5761	132	5057	310
d:\XRF Data_Tube	10	10	10/6/15	56	184	32	2653	62	4	32	562	51	3918	273	869	74	929	70	894	81	677	91	137	92	5904	133	5255	331
d:\XRF Data_Tube	10	10	10/6/15	56.5	226	31	2644	61	2	31	503	51	4132	270	755	72	776	68	881	79	497	89	248	92	5954	132	5125	323
d:\XRF Data_Tube	10	10	10/6/15	57	220	33	2551	62	-8	32	508	51	4204	274	759	73	805	69	798	79	615	91	141	92	6023	134	4980	326

d:\XRFData_Tube	10	10	10/6/15	57.5	243	30	2474	59	32	31	489	50	4153	267	840	72	841	68	949	80	583	91	495	93	6005	132	5234	313
d:\XRFData_Tube	10	10	10/6/15	58	144	31	2505	61	-8	32	543	51	4121	264	774	71	986	68	946	79	769	91	280	92	5895	132	5107	312
d:\XRFData_Tube	10	10	10/6/15	58.5	168	31	2647	62	-1	32	452	51	4592	273	786	73	833	69	899	79	704	91	138	91	6078	133	4593	324
d:\XRFData_Tube	10	10	10/6/15	59	220	32	2588	62	4	31	609	50	4370	271	706	73	790	69	825	79	516	92	307	94	6096	134	4764	322
d:\XRFData_Tube	10	10	10/6/15	59.5	250	32	2611	61	-4	31	408	51	4334	275	639	73	820	68	876	80	607	91	379	93	6199	134	5037	329
d:\XRFData_Tube	10	10	10/6/15	60	169	31	2812	64	-6	32	509	51	4141	277	792	73	735	69	873	81	591	92	169	93	6016	133	5415	336
d:\XRFData_Tube	10	10	10/6/15	60.5	146	31	2461	61	14	33	372	49	4330	270	612	72	828	68	752	78	604	91	201	92	5655	131	4682	318
d:\XRFData_Tube	10	10	10/6/15	61	95	28	1869	54	3	30	435	49	3340	286	559	70	741	66	680	78	568	91	164	92	4788	127	5624	333
d:\XRFData_Tube	10	10	10/6/15	61.5	122	26	1430	48	6	29	382	48	3741	289	422	67	713	65	617	76	545	89	189	90	4365	123	4865	313
d:\XRFData_Tube	10	10	10/6/15	62	142	30	2170	57	7	31	532	50	3537	292	634	73	781	68	841	80	605	92	166	93	5573	132	5645	352
d:\XRFData_Tube	10	10	10/6/15	62.5	166	31	2537	60	34	31	537	51	4138	280	708	74	805	70	785	80	620	93	154	95	6174	133	5089	338
d:\XRFData_Tube	10	10	10/6/15	63	203	31	2561	61	22	31	622	51	4212	264	805	74	978	70	905	80	536	91	127	93	6022	133	4769	314
d:\XRFData_Tube	10	10	10/6/15	63.5	252	32	2557	61	25	31	679	51	4452	262	825	75	1039	71	888	80	635	92	517	94	6333	134	4797	310
d:\XRFData_Tube	10	10	10/6/15	64	261	34	2870	64	-4	31	518	51	4483	277	837	75	904	71	1012	81	581	92	491	95	6734	135	4954	334
d:\XRFData_Tube	10	10	10/6/15	64.5	289	34	2840	64	3	31	596	50	4220	281	904	75	804	71	1122	81	558	91	235	93	6745	137	5408	340
d:\XRFData_Tube	10	10	10/6/15	65	305	33	2955	64	-15	32	500	51	4516	272	1017	75	888	70	951	81	608	92	211	94	6837	138	5265	327
d:\XRFData_Tube	10	10	10/6/15	65.5	197	33	3008	66	-1	32	460	50	4266	266	888	76	682	69	1158	81	579	91	133	93	6533	137	5172	320
d:\XRFData_Tube	10	10	10/6/15	66	252	33	2941	65	-15	32	402	50	4390	265	975	75	790	70	832	81	477	91	302	93	6863	137	5209	318
d:\XRFData_Tube	10	10	10/6/15	66.5	310	35	2957	66	7	34	432	51	4530	279	1057	77	680	70	988	81	698	92	145	92	6814	137	5153	334
d:\XRFData_Tube	10	10	10/6/15	67	252	32	2993	65	0	32	416	51	4468	279	837	76	762	70	1003	83	577	93	216	94	6903	138	5322	338
d:\XRFData_Tube	10	10	10/6/15	67.5	213	34	3140	67	32	32	521	51	4341	266	987	77	916	70	1141	82	637	92	204	96	7248	140	5235	324
d:\XRFData_Tube	10	10	10/6/15	68	348	34	3165	67	10	33	412	51	4378	267	1229	77	852	70	963	83	517	92	213	94	7425	141	5289	324
d:\XRFData_Tube	10	10	10/6/15	68.5	255	34	3165	68	15	35	505	51	4554	269	1163	78	834	71	1005	82	641	92	267	94	7401	140	5131	325
d:\XRFData_Tube	10	10	10/6/15	69	219	33	3192	67	-2	32	467	51	4762	260	960	75	936	71	1128	81	640	93	111	94	7163	138	4804	314
d:\XRFData_Tube	10	10	10/6/15	69.5	255	34	3173	68	7	34	488	51	4249	273	977	77	798	70	1086	82	613	93	87	94	7067	138	5515	333
d:\XRFData_Tube	10	10	10/6/15	70	323	35	3274	67	9	32	575	52	4599	274	952	76	745	71	929	82	476	93	125	94	7240	140	5123	335
d:\XRFData_Tube	10	10	10/6/15	70.5	240	33	3219	67	11	32	515	50	4546	260	873	75	714	70	954	82	635	92	222	95	6883	138	5206	315
d:\XRFData_Tube	10	10	10/6/15	71	270	33	3153	67	-7	33	477	52	4572	265	1107	77	751	70	872	82	595	92	155	93	6980	138	5182	318
d:\XRFData_Tube	10	10	10/6/15	71.5	307	34	3118	66	35	33	538	51	4097	256	1071	78	710	70	990	83	515	91	205	93	7687	140	5438	310
d:\XRFData_Tube	10	10	10/6/15	72	248	34	3190	67	7	32	546	51	4716	266	971	76	910	71	1186	82	746	93	75	93	7361	139	5078	321
d:\XRFData_Tube	10	10	10/6/15	72.5	219	34	3091	67	12	32	551	51	4346	274	1022	76	899	71	934	82	620	93	221	94	6861	138	5544	332
d:\XRFData_Tube	10	10	10/6/15	73	228	34	3116	67	-5	33	485	51	4423	277	863	74	993	70	1072	81	746	92	265	94	6669	137	5547	336
d:\XRFData_Tube	10	10	10/6/15	73.5	226	32	3143	67	-4	33	530	53	3829	279	968	75	875	70	893	81	552	91	233	93	6490	136	6456	340
d:\XRFData_Tube	10	10	10/6/15	74	210	35	3214	69	-22	34	490	52	4446	280	919	76	864	71	1012	81	578	91	187	94	6462	136	5457	341
d:\XRFData_Tube	10	10	10/6/15	74.5	288	34	3095	66	18	31	594	51	4819	273	1037	76	864	70	957	81	545	91	147	93	6463	136	5104	326
d:\XRFData_Tube	10	10	10/6/15	75	302	33	3096	66	-7	32	575	52	4615	263	1132	74	916	69	827	81	561	93	230	94	6562	137	5249	315
d:\XRFData_Tube	10	10	10/6/15	75.5	199	33	3203	68	-6	35	497	52	4693	267	851	75	818	71	940	80	514	91	214	93	6630	136	5087	320
d:\XRFData_Tube	10	10	10/6/15	76	303	34	3153	67	47	33	435	50	4445	275	889	76	781	71	994	81	664	92	139	93	6600	138	5588	331
d:\XRFData_Tube	10	10	10/6/15	76.5	222	34	3137	67	10	32	558	52	4347	284	840	75	973	71	1049	82	481	93	134	95	6678	137	5661	347
d:\XRFData_Tube	10	10	10/6/15	77	199	33	3173	67	20	31	523	50	4656	263	857	75	876	71	918	82	540	92	223	94	6390	137	4999	317
d:\XRFData_Tube	10	10	10/6/15	77.5	253	32	3270	66	46	30	582	52	4693	262	882	75	798	70	821	81	633	93	300	95	6547	136	5231	316
d:\XRFData_Tube	10	10	10/6/15	78	274	33	3261	67	36	32	584	52	4757	272	758	76	794	70	1061	82	709	92	100	93	6544	137	5255	328
d:\XRFData_Tube	10	10	10/6/15	78.5	253	34	3251	67	21	32	573	51	4672	275	1060	76	950	71	1093	82	592	93	164	95	6723	138	5273	335
d:\XRFData_Tube	10	10	10/6/15	79	206	33	3166	67	39	33	623	52	4648	267	805	75	919	71	994	81	642	93	158	94	7557	142	4980	323
d:\XRFData_Tube	10	10	10/6/15	79.5	194	32	3128	66	3	32	640	53	4590	265	956	75	867	70	882	81	568	92	146	94	7792	142	5119	320
d:\XRFData_Tube	10	10	10/6/15	80	242	32	3097	66	18	34	759	54	4396	266	827	75	979	71	892	81	585	93	294	94	8274	142	5194	325
d:\XRFData_Tube	10	10	10/6/15	80.5	221	34	3035	66	2	33	695	53	4466	262	932	75	964	70	976	81	619	92	239	93	7601	140	5236	315
d:\XRFData_Tube	10	10	10/6/15	81	179	34	3157	68	-23	34	570	53	4376	278	1074	75	1160	72	853	81	618	92	106	93	6980	139	5632	339
d:\XRFData_Tube	10	10	10/6/15	81.5	246	33	3010	65	34	32	582	52	4939	265	783	74	969	71	1044	80	775	91	232	90	6716	136	4971	314
d:\XRFData_Tube	10	10	10/6/15	82	217	32	2954	66	-17	34	729	54	4923	272	905	75	1226	73	972	80	652	91	151	92	6413	136	4759	325
d:\XRFData_Tube	10	10	10/6/15	82.5	227	34	3143	68	-7	34	647	54	3878	281	925	75	1075	72	970	81	550	92	152	93	6635	137	6023	346
d:\XRFData_Tube	10	10	10/6/15	83	266	32	3158	66	-27	32	1000	57	4695	260	812	76	1300	76	1075	81	754	91	449	92	6566	135	5065	316
d:\XRFData_Tube	10	10	10/6/15	83.5	286	33	2921	65	-19	33	1444	61	4408	271	688	76	1930	81	922	83	747	94	154	95	6480	137	5457	333
d:\XRFData_Tube	10	10	10/6/15	84	196	31	2638	62	-4	33	1327	61	4772	268	627	74	1816	80	819	81	531	92	161	93	5733	133	4858	319
d:\XRFData_Tube	10	10	10/6/15	84.5	219	30	2405	60	-22	34	1235	61	4376	265	516	73	1993	80	645	79	470	91	88	93	5390	131	4919	314
d:\XRFData_Tube	10	10	10/6/15	85	186	31	2494	61	4	33	1463	61	4579	264	575	72	2009	79	868	79	472	90	116	93	5252	130	4951	315
d:\XRFData_Tube	10	10	10/6/15	85.5	189	30	2473	61	2	34	1287	60	4703	264	600	73	1750	78	901	81	619	92	177	93	5413	130	4676	312
d:\XRFData_Tube	10	10	10/6/15	86	156	31	2431	60	3	31	590	53	4624	286	720	72	823	71	840	83	583	93	137	94	5263	132	4877	338
d:\XRFData_Tube	10	10	10/6/15	86.5	203	32	2378	60	20	32	628	52	3646	297	520	73	742	69	901	80	527	91	337	93	5097	129	5863	355
d:\XRFData_Tube	10	10	10/6/15	87	125	31	2323	60	10	32	685	53	4292	275	603	73	1056	72	930	81	656	92	274	93	5041	128	4914	323
d:\XRFData_Tube	10	10	10/6/15	87.5	155	30	2369	59	9	31	912	56	4073	276	453	70	1275	73	726	79	582	91	82	91	4858	127	5613	326
d:\XRFData_Tube	10	10	10/6/15	88	182	31	2146	58	15	34	1352	61	4110	270	481	73	1782	80	746	79	720	92	144	93	4813	127	5298	319
d:\XRFData_Tube	10	10	10/6/15	88.5	152	31	2166	58	-30	33	1379	61	3979	265	454	72	1867	79	622	79	451	91	129	93	4650	127	5195	315
d:\XRFData_Tube	10	10	10/6/15	89	174	31	2025	57	-23	34	1294	61	4089	277	460	71	1895	78	730	81	667	94	130	95	4904	129	5084	328
d:\XRFData_Tube	10	10	10/6/15	89.5	129	30	2114	57	-2	33	1311	61	4375	273	339	71	1968	79	759	80	561	92	194	93	4842	127	4895	322
d:\XRFData_Tube	10	10	10/6/15	90	165	31	2019	56	-2	32	1467	61	4596	275	457	73	1842	80	687	80	710	93	126	93	4582	126	4516	324
d:\XRFData_Tube	10	10	10/6/15	90.5	140	31	2071	57	-22	33	1129	59	4387	271	536	71	1590	75	805	79	620	92	122	92	4441	125	4744	315
d:\XRFData_Tube	10	10	10/6/15	91	143	30	1905	55	10	33	1153	58	4059	290	450	71	1727	77	646	80	670	93	178	94	4527	125	5445	339
d:\XRFData_Tube	10	10	10/6/15	91.5	149	29	1829	54	-13	32	1319	61	3959	275	519	70	2070	78	652	79	661	92	162	93	4317	125	5230	323
d:\XRFData_Tube	10	10	10/6/15	92	164	29	1704	53	-8	33	1742	64	3900	269	277	70	2383	83	652	79	568	92	151	94	4348	125	5146	318
d:\XRFData_Tube	10	10	10/6/15	92.5	94	28	1565	52	-4	35	1989	67	3825	260	232	69	3203	88	612	78	475	90	236	93	4183	122	4994	310
d:\XRFData_Tube	10	10	10/6/15	93	78	29	1516	51	-21	34	2219	70	3788	263	206	71	3346	90	719	78	548	91	202	92	4128	122	5170	319
d:\XRFData_Tube	10	10	10/6/15	93.5	85	30	1411	51	-5	35	2542	72	4047	257	236	70	3566	91	596	77	589	91	88	92	3742	120	4873	308
d:\XRFData_Tube	10	10	10/6/15	94	48	27	1537	51	-31	33	2238	70	4133	256	137	69	3485	90	616	76	477	90	189	92	3804	119	4748	306
d:\XRFData_Tube	10	10	10/6/15	94.5	67	28	1344	49	-6	32	2416	70	3952	265	34	70	3765	92	846	77	557	90	264	90	3870	119	5231	319
d:\XRFData_Tube	10	10	10/6/15	95	36	27	1288	48	-22	33	2218	69	3591	265	123	68	3369	89	625	78	544	91	231	93	3442	118	5019	320
d:\XRFData_Tube	10	10	10/6/15	95.5	143	28	1470	50	11	32	1486	63	4397	279	250	70	2458	83	571	76	566	90	181	91	3791	119	4402	320
d:\XRFData_Tube	10	10	10/6/15	96	124	29	1752	52	46	30	896	54	3955	300	316	70	1212	73	615	80	572	92	210	93	4259	125	5154	348
d:\XRFData_Tube	10	10	10/6/15	96.5	149	28	1656	51	-19	31	806	54	4192	282	399	69	1208	72	657	78	626	90	121	91	4262	123	4621	315
d:\XRFData_Tube	10	10	10/6/15	97	153	28	1604	50	56	30	1161	56	4091	297	310	70	1552	75	714	78	724	91	326	90	4125	122	5056	342
d:\XRFData_Tube	10	10	10/6/15	97.5	119	28	1378	48	37	31	1311	58	4590	290	246	70	1858	79	614	78	608	91	260	91	3975	120	4543	324
d:\XRFData_Tube	10	10	10/6/15	98	50	27	1439	49	-8	31	1537	62	3878	280	289	69	2321	81	609	78	676	92	175	91	3720	119	5094	327
d:\XRFData_Tube	10	10	10/6/15	98.5	100	27	1437	49	-34	31	1643	63	3646	266	255	67	2712	83	576	77	513	90	155	91	3374	117	5123	314
d:\XRFData_Tube	10	10	10/6/15	99	88	26	1214	47	-39	33	2002	67	4178	271	85	68	3470	90	665	78	553	90	123	91	3208	115	4721	317
d:\XRFData_Tube	10	10	10/6/15	99.5	75	25	1204	46	16	33	2097	66	3705	259	231	68	3488	89	646	77	602	91	179	91	2970	114	4861	308
d:\XRFData_Tube	10	10	10/6/15	100	43	26	1166	47	-36	34	1855	66	3659	266	206	68	3069	86	554	77	540	90	133	91	3067	115	4882	312
d:\XRFData_Tube	10	10	10/6/15	100.5	96	27	1326	48	55	32	1740	65	3622	275	242	69	3179	87	489	78	692	91	341	92	3528	117	5140	327
d:\XRFData_Tube	10	10	10/6/15	101	96	26	1291	47	-12	31	1158	59	3754	292	59	68	1818	78	640	78	750	92	273	91	3479	118	5210	328
d:\XRFData_Tube	10	10	10/6/15	101.5	125	28	1441	49	7	31	1204	60	4160	295	280	69	2060	79	700	77	562	92	182	94	3271	117	4804	339
d:\XRFData_Tube	10	10	10/6/15	102	98	27	1172	46	-2	32	1627	62	4116	274	148	67	2769	85	542	76	573	89	160	90	2790	112	4804	308
d:\XRFData_Tube	10	10	10/6/15	102.5	106	27	1120	46	-37	34	1791	66	3734	280	174	68	2913	86	421	77	530	89	226	91	3181	115	4976	325
d:\XRFData_Tube	10	10	10/6/15	103	44	28	1176	47	-6	33	1713	65	3817	270	198	69	2870	86	571	78	571	90	208	92	3418	117	4696	314
d:\XRFData_Tube	10	10	10/6/15	103.5	54	26	1260	47	1	32	1647	64	3532	277	195	68	2537	84	533	78	577	91	269	92	3250	117	5287	322
d:\XRFData_Tube	10	10	10/6/15	104	83	28	1566	49	6	29	1306	60	3629	296	183	70	1953	79	714	78	572	91	235	92	3675	120	5351	351
d:\XRFData_Tube	10	10	10/6/15	104.5	132	27	1402	49	-3	31	1113	59	3786	301	242	68	1767	77	663	78	613	91	135	92	3498	119	5285	343
d:\XRFData_Tube	10	10	10/6/15	105	105	26	1409	48	17	31	998	56	3635	307	291	69	1327	74	635	78	737	92	258	91	3949	120	5551	346
d:\XRFData_Tube	10	10	10/6/15	105.5	66	28	1443	50	-20	31	623	53	4233	320	379	69	930	68	705	78	588	91	154	92	3871	122	4856	353
d:\XRFData_Tube	10	10	10/6/15	106	74	27	1604	50	9	29	549	51	3999	322	449	69	757	67	585	78	613	91	270	92	3735	120	5515	359
d:\XRFData_Tube	10	10	10/6/15	106.5	91	27	1495	50	-15	30	495	50	3385	302	528	68	636	65	632	78	662	92	121	91	3539	121	5480	336
d:\XRFData_Tube	10	10	10/6/15	107	73	27	1595	50	7	29	502	49	4047	296	338	68	558	65	624	77	392	88	239	91	3411	118	4965	324

d:\XRF Data_Tube	10	10	10/6/15	107.5	76	28	1595	51	-5	31	497	51	3975	316	395	70	589	66	641	80	692	94	118	93	3535	120	4968	356
d:\XRF Data_Tube	10	10	10/6/15	108	107	28	1495	50	16	31	442	50	3839	310	387	70	530	66	815	78	595	91	128	92	3570	120	5170	338
d:\XRF Data_Tube	10	10	10/6/15	108.5	90	26	1526	50	-6	29	584	51	3858	315	379	69	719	67	735	79	600	92	63	92	3672	121	5258	354
d:\XRF Data_Tube	10	10	10/6/15	109	75	25	1553	50	33	30	546	50	4276	293	403	68	869	67	644	78	591	90	127	92	3385	118	4748	319
d:\XRF Data_Tube	10	10	10/6/15	109.5	93	29	1430	50	0	31	479	51	3984	346	415	69	630	66	621	78	639	91	261	91	3442	117	5333	377
d:\XRF Data_Tube	10	10	10/6/15	110	73	26	1323	48	9	31	487	50	4034	319	362	68	544	65	660	79	529	91	208	92	3596	120	5129	342
d:\XRF Data_Tube	10	10	10/6/15	110.5	75	26	1523	49	1	30	421	51	3648	318	531	69	722	66	592	78	547	91	279	92	3595	120	5619	356
d:\XRF Data_Tube	10	10	10/6/15	111	94	27	1415	49	-23	32	1040	57	3427	287	239	70	1471	75	741	78	609	91	252	93	3578	119	5075	328
d:\XRF Data_Tube	10	10	10/6/15	111.5	123	28	1484	49	14	30	1016	57	3957	297	260	69	1373	74	543	78	578	91	236	91	3786	120	5036	335
d:\XRF Data_Tube	10	10	10/6/15	112	145	28	1456	50	-28	32	1030	57	3610	296	266	69	1585	75	685	77	575	90	169	91	3629	120	5366	338
d:\XRF Data_Tube	10	10	10/6/15	112.5	90	28	1435	49	15	32	946	55	4485	290	361	70	1163	72	612	77	615	91	355	93	3839	120	4338	319
d:\XRF Data_Tube	10	10	10/6/15	113	82	27	1567	51	-17	31	888	55	3840	294	419	69	1146	71	519	78	613	91	164	91	3771	120	5077	333
d:\XRF Data_Tube	10	10	10/6/15	113.5	130	28	1424	50	-2	33	795	54	3909	302	339	67	1182	70	598	78	521	90	208	92	3522	120	4898	330
d:\XRF Data_Tube	10	10	10/6/15	114	105	27	1498	49	10	30	796	54	3956	315	280	68	1018	70	569	79	589	91	228	92	3440	119	5335	352
d:\XRF Data_Tube	10	10	10/6/15	114.5	117	28	1536	50	-5	31	618	53	3695	323	220	68	927	69	631	80	620	93	225	93	3704	121	5421	367
d:\XRF Data_Tube	10	10	10/6/15	115	138	27	1543	49	4	29	609	52	3873	287	368	68	805	67	588	78	581	90	84	91	3305	118	4875	314
d:\XRF Data_Tube	10	10	10/6/15	115.5	124	28	1440	49	19	31	698	53	3917	330	303	69	859	69	721	79	563	91	186	92	3634	121	5256	366
d:\XRF Data_Tube	10	10	10/6/15	116	96	26	1331	48	-4	31	770	55	3930	330	423	68	1375	72	749	78	530	91	136	93	3250	118	5373	364
d:\XRF Data_Tube	10	10	10/6/15	116.5	60	25	1210	45	6	30	976	57	3553	288	298	67	1681	74	570	78	620	91	291	92	3281	116	5155	320
d:\XRF Data_Tube	10	10	10/6/15	117	38	24	1031	44	-26	31	922	56	3225	293	51	66	1812	76	555	76	684	91	199	92	2966	114	5364	318
d:\XRF Data_Tube	10	10	10/6/15	117.5	15	25	1022	43	28	29	1244	59	3618	307	166	67	2108	78	600	77	661	91	189	91	2666	112	5235	343
d:\XRF Data_Tube	10	10	10/6/15	118	72	24	1016	42	44	30	876	55	3982	325	41	66	1373	73	574	77	766	93	145	93	3088	115	4843	348
d:\XRF Data_Tube	10	10	10/6/15	118.5	38	24	858	41	16	29	980	57	3359	336	23	66	1503	74	396	75	531	90	166	91	2380	109	5435	360
d:\XRF Data_Tube	10	10	10/6/15	119	91	27	1291	47	1	30	1183	59	3702	298	299	68	1718	76	555	78	646	91	308	91	3246	117	5190	337
d:\XRF Data_Tube	10	10	10/6/15	119.5	45	27	1485	51	-2	33	1951	66	3834	254	220	68	3255	88	489	78	587	90	76	91	3462	117	4835	302
d:\XRF Data_Tube	10	10	10/6/15	120	48	28	1424	51	-27	34	1845	66	3495	261	342	67	3477	89	528	77	553	91	234	94	3511	119	5348	312
d:\XRF Data_Tube	10	10	10/6/15	120.5	98	29	1673	52	-16	32	1653	63	4425	266	326	69	2551	82	861	78	599	91	148	91	3929	120	4462	311
d:\XRF Data_Tube	10	10	10/6/15	121	70	29	1484	51	3	33	1914	66	3945	259	335	69	3032	86	589	77	504	90	105	91	3674	119	4910	305
d:\XRF Data_Tube	10	10	10/6/15	121.5	106	28	1592	51	-16	33	1873	66	4041	259	356	69	3317	88	714	78	638	91	151	91	3998	121	4803	308
d:\XRF Data_Tube	10	10	10/6/15	122	115	29	1550	52	-37	34	2359	70	3901	259	196	69	3718	93	611	78	524	89	163	90	3582	118	5034	313
d:\XRF Data_Tube	10	10	10/6/15	122.5	91	28	1557	52	-27	34	2369	71	3415	259	219	70	4162	95	554	78	571	90	226	92	3687	118	5360	320
d:\XRF Data_Tube	10	10	10/6/15	123	83	29	1579	52	-32	34	2290	70	3624	248	213	70	4069	94	591	77	530	90	130	91	3706	119	5020	302
d:\XRF Data_Tube	10	10	10/6/15	123.5	78	28	1555	51	-12	33	2595	71	4119	235	300	69	4057	93	630	77	507	89	193	90	4022	120	4331	284
d:\XRF Data_Tube	10	10	10/6/15	124	186	28	1769	53	15	33	2321	70	3714	254	297	69	4136	93	557	78	596	90	272	90	3785	119	5068	315
d:\XRF Data_Tube	10	10	10/6/15	124.5	115	28	1782	53	-14	32	2141	68	3914	241	277	70	3582	90	657	77	500	89	103	91	4150	121	4559	291
d:\XRF Data_Tube	10	10	10/6/15	125	121	28	1766	53	-6	34	2479	71	4016	242	339	69	4024	92	571	77	545	90	160	91	4119	121	4596	294
d:\XRF Data_Tube	10	10	10/6/15	125.5	123	29	1625	53	-17	35	2549	72	3686	240	338	69	4577	96	522	77	714	91	234	91	4025	121	4943	294
d:\XRF Data_Tube	10	10	10/6/15	126	74	29	1776	55	-30	35	2289	69	3920	247	304	70	3919	94	708	79	551	91	115	92	4350	123	4733	301
d:\XRF Data_Tube	10	10	10/6/15	126.5	129	31	1769	55	-6	35	2597	72	4008	239	199	70	4137	95	600	78	592	89	107	89	4322	121	4751	290
d:\XRF Data_Tube	10	10	10/6/15	127	118	30	1987	57	-17	35	2495	72	3930	250	286	72	3966	94	750	78	603	91	134	91	4417	124	4905	310
d:\XRF Data_Tube	10	10	10/6/15	127.5	178	30	2040	57	-21	34	1966	66	3906	239	438	70	3178	88	724	79	572	90	310	90	4676	124	5009	287
d:\XRF Data_Tube	10	10	10/6/15	128	140	30	2041	57	-1	35	2289	69	3472	245	299	71	3951	93	678	78	812	92	129	91	4835	125	5430	303
d:\XRF Data_Tube	10	10	10/6/15	128.5	156	30	2159	59	-46	36	2136	70	4038	253	509	73	3862	93	692	78	582	90	189	92	4612	125	4720	312
d:\XRF Data_Tube	10	10	10/6/15	129	159	31	2189	59	-31	35	1966	66	3965	247	313	71	3138	89	602	78	492	90	130	91	4945	127	5066	299
d:\XRF Data_Tube	10	10	10/6/15	129.5	214	30	2264	59	-14	33	1786	65	4545	253	388	72	2946	88	730	79	490	90	76	92	4896	127	4415	305
d:\XRF Data_Tube	10	10	10/6/15	130	180	31	2386	60	37	33	1153	59	4397	264	567	72	2103	80	697	80	607	91	260	93	5040	129	4672	314
d:\XRF Data_Tube	10	10	10/6/15	130.5	148	31	2486	61	-8	33	1273	60	4091	266	552	73	2245	82	771	80	650	92	85	92	5410	129	5043	325
d:\XRF Data_Tube	10	10	10/6/15	131	210	30	2313	59	20	34	2138	68	4104	248	197	73	3764	94	738	79	636	91	203	92	4864	125	4765	304
d:\XRF Data_Tube	10	10	10/6/15	131.5	175	31	2229	58	9	34	2613	72	4267	239	246	71	4682	99	602	79	524	90	283	90	4577	124	4578	294
d:\XRF Data_Tube	10	10	10/6/15	132	203	32	2572	62	5	33	1595	63	4395	259	593	73	2502	84	622	79	543	90	241	91	5408	129	4755	314
d:\XRF Data_Tube	10	10	10/6/15	132.5	183	32	2577	61	33	33	1686	62	4193	262	519	73	2442	84	805	80	533	91	180	93	5322	130	4886	324
d:\XRF Data_Tube	10	10	10/6/15	133	234	31	2658	62	23	32	1457	61	4254	263	435	73	2220	83	708	80	681	93	149	93	5486	131	5214	321
d:\XRF Data_Tube	10	10	10/6/15	133.5	210	32	2742	64	-8	34	1026	59	4130	267	447	73	1800	79	808	80	765	91	291	92	5349	131	4949	325
d:\XRF Data_Tube	10	10	10/6/15	134	228	30	2707	62	13	33	1084	57	4498	258	622	73	1520	76	927	80	497	91	352	94	5426	130	4552	309
d:\XRF Data_Tube	10	10	10/6/15	134.5	155	30	2527	61	-8	33	977	57	4456	265	522	72	1646	78	689	80	479	92	268	94	5602	132	4794	315
d:\XRF Data_Tube	10	10	10/6/15	135	178	31	2518	62	-2	35	1482	62	4130	271	504	73	2680	84	752	80	555	92	119	92	5408	130	5153	333
d:\XRF Data_Tube	10	10	10/6/15	135.5	186	30	2404	60	-27	34	1755	66	4117	255	398	72	3823	92	699	79	689	92	190	93	5303	129	4910	315
d:\XRF Data_Tube	10	10	10/6/15	136	266	32	2647	62	10	32	1303	61	4227	262	605	72	2231	82	816	80	591	92	81	93	5949	133	4995	320
d:\XRF Data_Tube	10	10	10/6/15	136.5	214	31	2830	64	-13	33	1155	60	4261	267	767	75	1939	80	695	80	538	92	220	93	5895	132	5181	326
d:\XRF Data_Tube	10	10	10/6/15	137	177	31	2743	63	-14	34	1266	61	4359	264	661	74	2433	83	904	81	526	92	317	95	5944	133	5092	322
d:\XRF Data_Tube	10	10	10/6/15	137.5	218	32	2660	62	-5	32	1643	62	4438	253	646	74	2745	86	915	81	671	92	163	92	6068	134	4924	310
d:\XRF Data_Tube	10	10	10/6/15	138	217	32	3030	66	-11	34	1197	60	4381	260	660	74	2137	81	909	81	748	93	243	93	6342	135	4863	319
d:\XRF Data_Tube	10	10	10/6/15	138.5	183	31	3008	66	5	34	1205	60	4332	255	788	73	2161	81	670	81	562	93	57	94	6080	135	4855	314
d:\XRF Data_Tube	10	10	10/6/15	139	198	32	3013	66	-4	32	1230	58	4007	253	552	73	1704	78	824	81	565	91	67	92	6251	134	5403	309
d:\XRF Data_Tube	10	10	10/6/15	139.5	248	32	3059	66	-3	33	1144	58	4300	250	785	73	1920	79	935	82	692	93	413	93	6778	136	5100	304
d:\XRF Data_Tube	10	10	10/6/15	140	179	34	2950	67	-26	35	1152	60	4425	271	706	74	1979	80	798	81	632	92	208	93	7008	138	5235	330
d:\XRF Data_Tube	10	10	10/6/15	140.5	190	33	3112	67	13	34	1084	58	4883	267	689	75	1624	79	908	82	583	93	195	94	6919	139	4897	323
d:\XRF Data_Tube	10	10	10/6/15	141	208	33	3276	68	-18	33	952	56	4160	272	794	75	1473	76	931	83	702	94	102	95	7187	140	5610	337
d:\XRF Data_Tube	10	10	10/6/15	141.5	230	32	3216	67	-7	34	1416	62	4747	259	740	76	2321	84	845	82	623	93	299	94	6886	137	4696	319
d:\XRF Data_Tube	10	10	10/6/15	142	250	33	3280	68	-6	34	1370	62	4712	276	821	77	2213	84	863	82	569	93	182	93	6924	136	5351	340
d:\XRF Data_Tube	10	10	10/6/15	142.5	252	32	3175	66	34	31	1400	61	4636	251	642	76	2159	83	943	81	638	92	211	93	6957	138	4764	307
d:\XRF Data_Tube	10	10	10/6/15	143	188	32	3124	67	-16	35	1719	65	4464	260	573	75	3177	88	1015	80	567	92	217	94	6786	136	5207	323
d:\XRF Data_Tube	10	10	10/6/15	143.5	205	31	2992	66	-15	34	1493	62	4787	246	684	75	2769	86	905	81	550	91	371	94	6513	135	4507	299
d:\XRF Data_Tube	10	10	10/6/15	144	244	33	3108	67	-10	35	1207	61	4698	261	898	74	2096	80	844	82	599	92	154	93	6697	136	5035	318
d:\XRF Data_Tube	10	10	10/6/15	144.5	147	33	3166	68	-5	34	1226	59	4337	261	699	75	1612	79	991	83	618	93	151	95	6606	138	5425	318
d:\XRF Data_Tube	10	10	10/6/15	145	262	32	3324	69	-31	35	1423	62	5063	261	688	76	2387	83	1075	82	613	93	72	94	6547	137	4686	321
d:\XRF Data_Tube	10	10	10/6/15	145.5	247	33	3270	68	20	35	1574	63	4555	256	592	75	2376	85	793	81	585	93	213	94	6568	137	5133	316
d:\XRF Data_Tube	10	10	10/6/15	146	242	34	3456	70	-29	35	999	58	4655	261	836	76	1754	79	811	82	619	94	182	95	6766	139	5026	321
d:\XRF Data_Tube	10	10	10/6/15	146.5	158	33	3562	70	-7	33	1317	61	4429	256	746	75	1870	80	905	82	656	92	161	93	7066	140	5337	318
d:\XRF Data_Tube	10	10	10/6/15	147	227	33	3583	71	-27	36	1294	62	4220	257	758	75	2140	81	976	80	740	92	67	93	8166	144	5685	319
d:\XRF Data_Tube	10	10	10/6/15	147.5	148	32	3112	67	14	35	1501	63	4450	258	535	73	2445	83	879	80	646	93	197	94	9522	148	4900	318
d:\XRF Data_Tube	10	10	10/6/15	148	173	31	2728	63	12	32	1224	59	4053	253	425	71	1630	77	815	80	510	92	129	93	12596	159	5437	307
d:\XRF Data_Tube	10	10	10/6/15	148.5	154	29	2378	59	-14	32	714	54	4491	270	603	70	1011	69	776	79	614	93	163	94	10493	152	4794	317
d:\XRF Data_Tube	10	10	10/6/15	149	74	27	1897	54	27	30	583	53	3840	284	290	68	1063	69	580	78	552	91	198	93	4769	127	5082	328
d:\XRF Data_Tube	10	10	10/6/15	149.5	100	25	981	42	3	29	567	52	3660	379	49	66	837	67	614	77	508	90	171	92	2843	115	5602	398
d:\XRF Data_Tube	10	10	10/6/15	150	39	22	520	34	-3	28	396	52	3475	518	-44	65	669	65	424	78	840	93	234	90	1747	106	5638	499
d:\XRF Data_Tube	10	10	10/6/15	150.5	24	23	386	33	12	29	472	54	3500	584	-61	68	683	65	434	77	539	91	192	92	1256	101	5376	524
d:\XRF Data_Tube	10	10	10/6/15	151	17	22	322	31	3	29	606	59	4051	657	21	65	680	64	495	78	602	92	266	93	795	98	5328	603
d:\XRF Data_Tube	10	10	10/6/15	151.5	10	22	283	30	7	29	479	58	3659	736	-113	68	488	63	418	76	688	92	246	91	570	94	5448	651
d:\XRF Data_Tube	10	10	10/6/15	152	17	21	275	30	11	29	394	54	1244	772	-115	69	506	64	321	77	628	93	200	92	418	95	7431	728
d:\XRF Data_Tube	10	10	10/6/15	152.5	8	23	260	30	-1	28	429	56	3144	717	54	66	624	61	328	74	663	92	212	92	381	94	5833	630
d:\XRF Data_Tube	10	10	10/6/15	153	17	23	301	31	-12	29	447	58	4200	701	-100	66	602	64	503	77	713	92	231	92	286	93	4896	620

SECTION 3 XRF Raw Data

FileName	LiveTim	RealTir	Measure	Sample	Al_Area	Al_ DAres	Si_Area	Si_ DAres	model %	P_Area	P_ DAres	S_Area	S_ DAres	Cl_Area	Cl_ DAres	K_Area	K_ DAres	Ca_Area	Ca_ DAres	model %	Ti_Area	Ti_ DAres	Cr_Area	Cr_ DAres	Mn_Area	Mn_ DAres	Fe_Area	Fe_ DAres	Rh_Area	Rh_ DAres
d:\XRF\Data_T	10	10	10/7/15	0.5	23	22	252	31	12.30	24	29	336	57	2046	863	43	68	507	63	12.43	390	78	544	93	200	93	442	95	6828	766
d:\XRF\Data_T	10	10	10/7/15	1	22	23	263	30	11.41	9	29	343	56	3060	710	-89	66	555	61	10.99	441	76	696	92	260	92	352	93	5493	587
d:\XRF\Data_T	10	10	10/7/15	1.5	36	22	286	30	10.49	-7	29	325	57	3137	728	3	66	657	63	9.59	459	77	748	93	231	92	529	95	5764	650
d:\XRF\Data_T	10	10	10/7/15	2	36	22	268	29	10.82	8	27	443	55	4173	661	-129	64	544	62	11.40	430	75	747	91	239	90	598	93	4409	578
d:\XRF\Data_T	10	10	10/7/15	2.5	27	22	256	29	11.33	-6	29	400	56	2727	700	-57	66	585	62	10.60	404	77	625	92	147	92	466	94	5811	620
d:\XRF\Data_T	10	10	10/7/15	3	29	22	285	30	10.53	47	28	496	54	2828	667	-31	66	639	62	9.70	373	75	599	91	246	92	500	93	5935	587
d:\XRF\Data_T	10	10	10/7/15	3.5	33	22	381	32	8.40	-9	29	794	56	2878	417	28	65	1313	71	5.41	385	76	687	90	392	90	1076	97	5545	402
d:\XRF\Data_T	10	10	10/7/15	4	62	25	732	40	5.46	-17	32	1357	62	3592	288	199	65	2604	80	3.07	503	74	635	89	95	89	1677	103	4771	315
d:\XRF\Data_T	10	10	10/7/15	4.5	78	27	1184	47	3.97	-36	33	1605	63	3700	276	129	67	2697	84	3.11	656	76	594	90	237	91	2975	113	4794	329
d:\XRF\Data_T	10	10	10/7/15	5	151	27	1697	51	3.01	33	30	1141	58	4144	280	459	69	1604	74	4.61	454	75	486	88	137	90	3657	117	4456	323
d:\XRF\Data_T	10	10	10/7/15	5.5	135	28	1625	52	3.20	-3	33	537	52	3904	311	548	70	643	66	10.26	653	79	478	91	247	93	4152	123	5260	345
d:\XRF\Data_T	10	10	10/7/15	6	113	27	1772	52	2.93	4	30	625	52	3943	303	447	70	764	67	8.77	700	80	563	93	207	95	4155	125	5080	348
d:\XRF\Data_T	10	10	10/7/15	6.5	111	29	1821	53	2.91	-3	30	649	52	3562	310	605	71	785	67	8.54	800	81	481	93	169	95	4452	125	5449	366
d:\XRF\Data_T	10	10	10/7/15	7	147	28	1733	52	3.00	24	31	564	50	4390	305	560	71	761	66	8.67	748	80	589	92	177	93	4540	126	4612	346
d:\XRF\Data_T	10	10	10/7/15	7.5	102	29	1823	54	2.96	7	30	521	52	3884	304	696	70	599	64	10.68	827	80	623	92	147	93	4672	126	5373	350
d:\XRF\Data_T	10	10	10/7/15	8	165	30	1911	54	2.83	34	31	512	50	3821	293	622	71	599	66	11.02	716	79	480	91	145	93	4491	126	4987	338
d:\XRF\Data_T	10	10	10/7/15	8.5	146	29	1939	54	2.78	15	28	600	51	4127	301	508	72	604	67	11.09	676	79	492	91	330	93	4464	126	4946	352
d:\XRF\Data_T	10	10	10/7/15	9	116	28	1931	54	2.80	-3	29	459	49	4099	286	626	70	643	66	10.26	783	79	642	92	294	93	4378	124	4794	331
d:\XRF\Data_T	10	10	10/7/15	9.5	66	28	1975	56	2.84	-14	31	456	51	3739	298	429	71	668	67	10.03	792	79	887	92	252	91	4306	123	5399	352
d:\XRF\Data_T	10	10	10/7/15	10	104	28	1818	53	2.92	1	29	503	49	4179	287	542	70	638	65	10.19	648	79	729	92	304	91	4396	125	4772	327
d:\XRF\Data_T	10	10	10/7/15	10.5	150	28	1850	53	2.86	12	29	462	49	4301	282	476	69	556	65	11.69	721	78	481	90	224	92	4372	124	4712	318
d:\XRF\Data_T	10	10	10/7/15	11	145	31	1883	55	2.92	-5	32	563	51	4133	309	478	72	503	68	13.52	845	79	831	93	299	93	4390	124	4925	357
d:\XRF\Data_T	10	10	10/7/15	11.5	97	29	1869	55	2.94	-16	32	378	50	3944	281	688	69	701	65	9.27	638	77	603	91	173	92	4312	124	5145	318
d:\XRF\Data_T	10	10	10/7/15	12	129	29	1867	54	2.89	22	30	515	49	4006	286	577	70	670	65	9.70	545	77	599	90	248	91	4214	123	5121	324
d:\XRF\Data_T	10	10	10/7/15	12.5	142	30	1957	56	2.86	-12	32	425	51	4023	318	639	71	577	66	11.44	758	77	620	91	157	91	4447	125	5369	370
d:\XRF\Data_T	10	10	10/7/15	13	117	28	1899	55	2.90	-6	32	443	51	4499	287	588	70	496	65	13.10	789	78	642	91	373	92	4494	124	4664	322
d:\XRF\Data_T	10	10	10/7/15	13.5	188	29	2036	55	2.70	-7	31	540	51	3881	297	717	70	707	66	9.34	687	80	667	92	186	92	4445	125	5271	349
d:\XRF\Data_T	10	10	10/7/15	14	148	29	1921	54	2.81	11	30	490	50	3709	288	477	71	478	64	13.39	596	77	634	90	227	89	4400	124	5315	331
d:\XRF\Data_T	10	10	10/7/15	14.5	146	30	2001	55	2.75	18	29	612	51	3976	306	802	72	619	65	10.50	906	80	608	92	247	93	4349	125	5239	360
d:\XRF\Data_T	10	10	10/7/15	15	126	29	1932	55	2.85	-10	31	439	51	3985	299	563	71	523	65	12.43	655	78	553	91	193	93	4497	125	5255	347
d:\XRF\Data_T	10	10	10/7/15	15.5	98	29	2181	57	2.61	-18	31	471	50	3572	293	628	71	681	66	9.69	769	80	717	93	284	93	4493	126	5585	353
d:\XRF\Data_T	10	10	10/7/15	16	165	29	2161	57	2.64	3	31	548	51	4050	285	582	70	522	65	13.45	882	79	732	92	204	92	4481	125	4934	334
d:\XRF\Data_T	10	10	10/7/15	16.5	119	29	1941	55	2.83	9	31	590	50	4125	296	559	70	528	65	13.31	751	78	548	91	154	93	4346	125	4989	338
d:\XRF\Data_T	10	10	10/7/15	17	55	30	1948	56	2.87	5	32	524	51	4072	296	641	71	614	66	10.75	709	78	650	91	155	93	4304	124	4825	343
d:\XRF\Data_T	10	10	10/7/15	17.5	161	30	2060	56	2.72	-13	32	444	52	3576	294	589	72	553	66	11.93	699	80	644	93	133	93	4515	126	5198	349
d:\XRF\Data_T	10	10	10/7/15	18	109	29	1947	56	2.88	-25	33	421	51	4078	305	601	70	596	67	11.24	880	80	708	92	84	93	4671	126	5201	352
d:\XRF\Data_T	10	10	10/7/15	18.5	148	29	2060	57	2.77	23	32	531	51	3992	298	576	71	638	67	10.50	812	78	745	93	145	93	4929	127	5153	348
d:\XRF\Data_T	10	10	10/7/15	19	169	30	2204	57	2.59	12	30	548	50	4195	281	608	71	521	66	13.67	673	79	653	92	195	93	4687	127	4635	331
d:\XRF\Data_T	10	10	10/7/15	19.5	120	30	2200	58	2.64	5	31	575	51	3923	296	503	71	583	67	11.49	799	79	653	92	240	94	4850	128	5198	352
d:\XRF\Data_T	10	10	10/7/15	20	144	30	2075	57	2.75	9	31	810	54	4131	285	481	69	617	66	10.70	564	78	597	90	171	92	4283	133	4904	335
E:\XRF\Data_T	10	10	10/7/15	20.5	141	29	2026	56	2.76	2	32	796	54	3631	290	437	70	648	66	10.19	789	79	727	92	203	93	6405	134	5550	342
E:\XRF\Data_T	10	10	10/7/15	21	137	30	2055	57	2.77	-12	32	695	53	4425	288	494	71	672	68	10.12	747	78	757	93	138	93	6078	133	4608	334
E:\XRF\Data_T	10	10	10/7/15	21.5	156	29	2191	57	2.60	10	30	599	51	4030	271	618	70	666	66	9.91	661	79	618	91	183	92	5305	128	4998	317
E:\XRF\Data_T	10	10	10/7/15	22	146	29	2131	57	2.67	-11	31	698	52	4032	271	587	69	593	65	10.96	724	78	675	91	111	93	5375	130	5052	317
E:\XRF\Data_T	10	10	10/7/15	22.5	173	29	2167	56	2.58	14	30	750	53	4113	279	659	71	581	66	11.36	656	78	558	91	105	92	5387	130	5144	327
E:\XRF\Data_T	10	10	10/7/15	23	135	30	2132	57	2.67	-7	30	702	52	4014	285	577	71	741	66	8.91	728	78	669	90	100	91	5136	128	5111	333
E:\XRF\Data_T	10	10	10/7/15	23.5	139	29	2212	58	2.62	-7	32	517	51	4493	271	698	69	752	65	8.64	687	78	525	90	193	91	4387	124	4562	311
E:\XRF\Data_T	10	10	10/7/15	24	99	29	2229	58	2.60	16	31	503	50	4035	279	567	70	645	64	9.92	766	79	522	90	183	91	4662	125	4959	328
E:\XRF\Data_T	10	10	10/7/15	24.5	156	30	2220	58	2.61	-12	31	395	50	4138	283	479	70	690	67	9.71	763	78	527	91	57	93	4550	126	4933	331
E:\XRF\Data_T	10	10	10/7/15	25	123	30	2159	57	2.64	2	30	410	49	3671	275	600	69	760	66	8.68	810	78	607	91	312	93	4583	126	5298	322
E:\XRF\Data_T	10	10	10/7/15	25.5	140	30	2155	57	2.65	-13	31	590	50	4055	282	676	70	732	66	9.02	844	79	603	90	382	91	4527	125	4804	328
E:\XRF\Data_T	10	10	10/7/15	26	97	30	2112	57	2.70	25	31	553	50	4106	271	646	70	690	65	9.42	715	78	596	90	257	91	4747	125	4833	314
E:\XRF\Data_T	10	10	10/7/15	26.5	157	30	2281	59	2.59	-22	32	509	51	4117	289	674	70	766	66	8.62	803	79	591	92	255	93	4524	125	5085	341
E:\XRF\Data_T	10	10	10/7/15	27	120	29	2240	58	2.59	-1	31	544	50	4182	272	541	71	587	67	11.41	610	78	497	90	157	90	4667	125	4822	316
E:\XRF\Data_T	10	10	10/7/15	27.5	167	30	2150	58	2.70	-12	32	527	51	3982	281	614	72	676	67	9.91	694	78	709	91	159	92	4575	125	4642	329
E:\XRF\Data_T	10	10	10/7/15	28	169	30	2218	57	2.57	10	31	483	51	4159	269	609	70	700	66	9.43	671	77	613	90	74	91	4651	126	4651	313
E:\XRF\Data_T	10	10	10/7/15	28.5	202	31	2222	58	2.61	13	31	580	52	3972	296	659	72	687	67	9.75	689	78	592	90	237	91	4804	125	5316	348
E:\XRF\Data_T	10	10	10/7/15	29	151	30	2336	59	2.53	-14	31	565	52	3873	277	540	72	485	67	13.81	665	79	524	92	129	93	4820	128	4914	332
E:\XRF\Data_T	10	10	10/7/15	29.5	150	30	2210	58	2.62	15	31	721	52	4366	282	612	72	703	68	9.67	564	78	754	92	256	92	4824	126	4663	332
E:\XRF\Data_T	10	10	10/7/15	30	129	28	2108	57	2.70	-14	32	647	53	4033	278	534	71	921	69	7.49	731	79	495	91	104	93	4548	126	4798	327
E:\XRF\Data_T	10	10	10/7/15	30.5	87	29	2095	56	2.67	14	29	699	52	4181	277	657	70	1080	70	6.48	795	79	492	90	86	91	4575	125	4741	324
E:\XRF\Data_T	10	10	10/7/15	31	111	30	2321	59	2.54	-13	32	610	52	3758	296	534	73	781	70	8.96	929	79	785	92	385	92	4967	127	5346	361
E:\XRF\Data_T	10	10	10/7/15	31.5	176	30	2377	59	2.48	11	30	561	51	4204	283	524	70	735	67	9.12	681	79	627	91	309	91	4936	127	5021	335
E:\XRF\Data_T	10	10	10/7/15	32	115	30	2341	60	2.56	-7	33	479	51	3773	297	662	72	665	68	10.23	742	80	605	92	209	92	4911	127	5535	356
E:\XRF\Data_T	10	10	10/7/15	32.5	130	29	2422	59	2.44	22	29	522	50	4211	278	583	72	652	67	10.28	991	77	810	91	239	91	4864	126	5042	332
E:\XRF\Data_T	10	10	10/7/15	33	151	30	2507	60	2.39	-12	30	589	51	4234	284	667	73	739	69	9.34	766	79	721	92	242	91	4893	127	4825	344
E:\XRF\Data_T	10	10	10/7/15	33.5	142	30	2356	59	2.50	8	31	548	50	4091	276	606	71	661	67	10.14	743	78	799	92	126	92	4944	127	4978	328
E:\XRF\Data_T	10	10	10/7/15	34	145	30	2306	59	2.56	15	31	576	50	3752	264	669	71	657	66	10.05	761	78	750	92	104	92	5180	127	5127	312
E:\XRF\Data_T	10	10	10/7/15	34.5	152	29	2266	58	2.56	15	30	542	50	4085	276	639	71	723	68	9.41	711	78	672	90	178	89	4880	125	5125	323
E:\XRF\Data_T	10	10	10/7/15	35	155	30	2305	59	2.56	-12	33	510	51	3886	294	691	71	764	67	8.77	684	79	603	91	43	92	4963	128	5473	349
E:\XRF\Data_T	10	10	10/7/15	35.5	149	30	2237	59	2.64	-5	32	494	51	3520	299	684	72	689	68	9.87	849	79	551	92	201	93	5068	128	5656	359
E:\XRF\Data_T	10	10	10/7/15	36	148	29	2334	58	2.49	14	30	503	51	3833	275	516	70	636	66	10.38	729	78	565	91	147	92	5030	128	5318	326
E:\XRF\Data_T	10	10	10/7/15	36.5	178	30	2346	59	2.51	-1	31	584	51	4731	267	722	70	760	66	8.68	919	78	556	90	130	92	5159	128	4302	310
E:\XRF\Data_T	10	10	10/7/15	37	178	31	2485	60	2.41	8	30	496	50	3840	288	447	71	697	66	9.47	830	79	741	92	72	91	4924	127	5455	347
E:\XRF\Data_T	10	10	10/7/15	37.5	105	30	2503	60	2.40	44	30	745	51	4027	281	582	71	835	68	8.14	665	79	577	91	167	92	4987	128	5298	341
E:\XRF\Data_T	10	10	10/7/15	38	159	31	2395	60	2.51	-20	32	523	51	4081	290	672	71	727	66	9.08	639	78	529	91	169	93	4947	128	5190	345
E:\XRF\Data_T	10	10	10/7/15	38.5	111	31	2419	61	2.52	-29	33	448	51	3259	296	695	72	737	67	9.09	719	78	557	91	176	92	4945	128	5889	359
E:\XRF\Data_T	10	10	10/7/15	39	127	30	2465	60	2.43	-7	32	477	52	4096	293	758	72	692	67	9.68	650	79	683	92	61	91	5327	129	5306	349
E:\XRF\Data_T	10	10	10/7/15	39.5	195	31	2448	60	2.45	2	32	525	51	4170	275	767	72	634	66	10.41	664	79	548	91	217	92	5297	129	4954	325
E:\XRF\Data_T	10	10	10/7/15	40	144	29	2374	59	2.49	14	31	537	51	4023	282	636	72	598	67	11.20	821	79	532	90	220	92	5161	129	5306	335
E:\XRF\Data_T	10	10	10/7/15	40.5	165	31	2365	59	2.49	36	31	507	51	4130	286	755	73	546	67	12.27	800	78	583	90	210	92	5329	129	5342	338

d:\dW Data_T	10	10	10/7/15	41	146	31	2536	61	2.41	10	31	482	51	3711	279	674	72	650	66	10.15	981	78	667	90	215	92	5541	130	5641	338
d:\dW Data_T	10	10	10/7/15	41.5	192	32	2457	60	2.44	52	31	627	51	4204	277	845	72	618	66	10.68	758	78	471	90	163	92	5711	131	4956	328
d:\dW Data_T	10	10	10/7/15	42	155	31	2265	59	2.60	14	32	492	50	4396	280	850	72	684	66	9.65	788	79	618	91	177	92	5394	130	4651	326
d:\dW Data_T	10	10	10/7/15	42.5	173	32	2465	61	2.47	1	32	525	51	4068	283	625	73	514	66	12.84	785	78	679	91	148	91	5254	130	4948	338
d:\dW Data_T	10	10	10/7/15	43	240	33	2415	61	2.53	9	33	409	51	3728	293	894	74	712	67	9.41	949	80	631	92	216	93	5784	132	5460	352
d:\dW Data_T	10	10	10/7/15	43.5	215	32	2314	59	2.55	1	32	568	50	3937	278	816	72	590	66	11.19	875	79	630	91	137	91	5524	131	5108	328
d:\dW Data_T	10	10	10/7/15	44	156	32	2380	60	2.52	0	31	471	51	4263	295	828	74	694	68	9.80	889	80	599	92	177	93	5630	132	5033	354
d:\dW Data_T	10	10	10/7/15	44.5	167	31	2395	60	2.51	13	31	452	50	3818	286	817	75	529	67	12.67	973	81	621	94	164	95	6053	133	5399	344
d:\dW Data_T	10	10	10/7/15	45	205	33	2268	59	2.60	12	32	470	50	4043	296	902	73	589	67	11.38	865	80	582	91	276	92	5887	131	5321	349
d:\dW Data_T	10	10	10/7/15	45.5	211	31	2402	59	2.46	1	31	489	50	4178	272	764	73	641	67	10.45	803	79	475	91	109	93	5886	132	4866	322
d:\dW Data_T	10	10	10/7/15	46	134	30	2435	60	2.46	10	31	616	51	4247	272	679	72	551	67	12.16	898	79	620	91	189	93	5612	131	4739	324
d:\dW Data_T	10	10	10/7/15	46.5	140	30	2646	62	2.34	31	30	565	50	4176	281	655	73	609	66	10.84	789	79	628	91	144	92	5394	129	5035	341
d:\dW Data_T	10	10	10/7/15	47	228	30	2502	60	2.40	-1	31	477	51	4073	272	580	72	519	66	12.62	754	78	752	91	132	92	5534	130	5296	323
d:\dW Data_T	10	10	10/7/15	47.5	148	30	2544	60	2.36	19	30	597	50	4112	267	572	72	687	68	9.90	915	78	626	92	143	94	5225	130	5024	319
d:\dW Data_T	10	10	10/7/15	48	131	31	2561	62	2.42	-25	32	537	51	4109	277	591	73	541	67	12.38	782	79	544	90	178	92	5132	129	5011	333
d:\dW Data_T	10	10	10/7/15	48.5	221	32	2586	62	2.40	-26	31	523	52	4165	293	596	72	800	68	8.50	755	78	796	93	177	92	5411	129	5258	353
d:\dW Data_T	10	10	10/7/15	49	141	30	2508	61	2.43	0	32	564	51	4258	278	641	72	636	68	10.69	791	79	617	91	134	93	5067	129	5188	329
d:\dW Data_T	10	10	10/7/15	49.5	171	32	2639	62	2.35	-10	31	541	51	4511	287	720	72	626	67	10.70	770	79	734	92	160	93	5230	130	4887	343
d:\dW Data_T	10	10	10/7/15	50	196	32	2502	61	2.44	-33	33	603	52	4256	292	706	72	556	67	12.05	771	80	623	92	153	92	5143	130	5166	349
d:\dW Data_T	10	10	10/7/15	50.5	222	31	2606	61	2.34	0	31	682	52	4373	273	646	72	860	70	8.14	839	79	576	91	369	93	5367	130	4980	327
d:\dW Data_T	10	10	10/7/15	51	165	31	2623	62	2.36	5	32	811	54	4297	279	576	73	1017	72	7.08	838	79	668	92	107	92	4951	129	5069	337
d:\dW Data_T	10	10	10/7/15	51.5	156	31	2486	61	2.45	-6	33	736	53	4359	277	610	71	954	69	7.23	891	77	669	91	118	92	5218	129	4990	328
d:\dW Data_T	10	10	10/7/15	52	159	30	2688	62	2.31	7	32	596	52	4172	273	566	72	725	69	9.52	783	79	732	92	160	92	5288	130	5143	328
d:\dW Data_T	10	10	10/7/15	52.5	205	31	2642	62	2.35	-29	32	472	52	4176	284	694	73	636	67	10.53	682	80	597	92	198	93	5452	130	5287	340
d:\dW Data_T	10	10	10/7/15	53	192	31	2551	61	2.39	-1	30	510	50	4529	273	746	71	778	66	8.48	742	77	629	90	265	92	5242	129	4951	321
d:\dW Data_T	10	10	10/7/15	53.5	206	31	2452	60	2.45	21	32	542	51	4243	288	696	74	609	67	11.00	890	81	661	92	265	94	5573	131	4991	345
d:\dW Data_T	10	10	10/7/15	54	181	32	2466	60	2.43	44	31	562	51	4814	287	847	73	626	67	10.70	855	79	644	92	78	93	5519	131	4543	337
d:\dW Data_T	10	10	10/7/15	54.5	168	29	2597	61	2.35	-5	31	532	50	4035	274	700	72	769	68	8.84	674	78	642	91	203	92	5269	129	5182	329
d:\dW Data_T	10	10	10/7/15	55	176	31	2457	61	2.48	-7	33	420	50	4181	277	607	71	737	67	9.09	853	79	553	90	168	93	5335	130	5099	325
d:\dW Data_T	10	10	10/7/15	55.5	177	32	2538	62	2.44	-4	33	642	52	3995	291	473	72	674	68	10.09	840	79	706	93	144	94	6029	134	5369	354
d:\dW Data_T	10	10	10/7/15	56	183	30	2551	59	2.31	47	29	603	51	4359	267	635	71	617	67	10.86	643	78	702	91	231	91	6035	133	4712	319
d:\dW Data_T	10	10	10/7/15	56.5	131	31	2547	61	2.39	29	30	655	51	4275	291	721	72	671	67	9.99	637	80	728	93	194	93	6188	134	5254	350
d:\dW Data_T	10	10	10/7/15	57	211	31	2497	61	2.44	-12	31	754	53	3937	270	650	71	634	66	10.41	697	78	554	91	155	93	6851	137	5367	322
d:\dW Data_T	10	10	10/7/15	57.5	173	30	2570	61	2.37	27	31	675	52	4170	274	568	73	548	67	12.23	883	78	544	92	69	93	6544	136	5144	329
d:\dW Data_T	10	10	10/7/15	58	183	31	2791	63	2.26	19	31	666	53	4246	276	639	73	553	67	12.12	818	78	651	91	170	92	6186	134	5131	332
d:\dW Data_T	10	10	10/7/15	58.5	145	32	2713	62	2.29	25	31	603	51	4489	276	674	72	686	68	9.91	740	79	796	93	178	92	6276	134	4976	332
d:\dW Data_T	10	10	10/7/15	59	222	32	2585	62	2.40	-6	32	764	55	4204	275	785	72	1142	71	6.22	942	80	668	92	216	94	5903	132	5165	331
d:\dW Data_T	10	10	10/7/15	59.5	176	31	2662	62	2.33	-13	32	598	52	4510	268	676	73	851	69	8.11	852	80	497	91	313	93	5752	131	4795	318
d:\dW Data_T	10	10	10/7/15	60	179	31	2750	63	2.29	-14	31	594	53	4317	271	593	73	625	70	11.20	872	81	680	93	175	94	5877	134	4964	328
d:\dW Data_T	10	10	10/7/15	60.5	216	32	2698	62	2.30	-4	31	558	52	4358	283	765	73	654	68	10.40	834	81	587	92	119	93	5657	132	5205	341
d:\dW Data_T	10	10	10/7/15	61	216	32	2731	63	2.31	28	32	549	50	4180	265	595	72	673	67	9.96	837	79	735	91	186	90	5445	131	4725	318
d:\dW Data_T	10	10	10/7/15	61.5	184	32	2776	64	2.31	25	33	642	52	4648	280	660	73	566	68	12.01	812	80	661	92	359	92	5657	131	4853	335
d:\dW Data_T	10	10	10/7/15	62	156	32	2694	63	2.34	20	32	600	52	4742	278	694	72	640	67	10.47	806	80	786	92	64	93	5863	133	4847	328
d:\dW Data_T	10	10	10/7/15	62.5	147	31	2818	63	2.24	-2	31	625	52	4190	276	725	74	718	68	9.47	763	80	648	91	94	93	6028	134	5289	337
d:\dW Data_T	10	10	10/7/15	63	198	31	2692	63	2.34	-2	33	492	51	4712	280	584	73	666	69	10.36	811	81	595	92	300	94	5846	132	4912	333
d:\dW Data_T	10	10	10/7/15	63.5	184	30	2639	62	2.35	-8	33	555	53	4087	274	646	72	824	68	8.25	743	78	509	91	36	92	5425	131	5484	327
d:\dW Data_T	10	10	10/7/15	64	217	31	2859	64	2.24	23	32	585	52	4587	266	708	72	606	67	11.06	910	80	639	92	189	92	5989	132	4819	318
d:\dW Data_T	10	10	10/7/15	64.5	163	33	2758	64	2.32	0	34	535	53	4774	292	750	74	704	69	9.80	860	80	578	92	146	93	5753	132	4774	351
d:\dW Data_T	10	10	10/7/15	65	136	31	2719	63	2.32	-13	33	749	54	4229	273	662	74	881	70	7.95	930	80	662	92	253	94	6154	134	5012	331
d:\dW Data_T	10	10	10/7/15	65.5	217	32	2787	63	2.26	-4	32	666	54	4360	276	665	73	900	71	7.89	830	80	676	92	62	93	6536	136	5204	333
d:\dW Data_T	10	10	10/7/15	66	232	33	2718	63	2.32	30	33	794	55	4700	280	634	72	856	70	8.18	722	79	704	91	288	92	6865	137	4985	333
d:\dW Data_T	10	10	10/7/15	66.5	179	32	2724	63	2.31	-7	32	751	54	4514	286	633	73	839	69	8.22	821	81	767	94	286	94	6618	137	5715	349
d:\dW Data_T	10	10	10/7/15	67	169	32	2784	64	2.30	20	33	601	54	4106	286	680	74	727	70	9.63	898	80	622	91	253	92	6568	136	5458	350
d:\dW Data_T	10	10	10/7/15	67.5	202	33	2691	64	2.38	7	34	655	54	4605	292	833	75	883	70	7.93	874	81	737	93	137	93	6246	135	4795	351
d:\dW Data_T	10	10	10/7/15	68	205	32	2916	65	2.23	9	33	506	52	4138	276	616	74	719	70	9.74	941	80	553	92	89	93	5876	134	5569	335
d:\dW Data_T	10	10	10/7/15	68.5	192	30	2770	63	2.27	-7	32	541	51	4251	264	779	71	865	67	7.75	967	79	580	90	231	92	6025	133	5132	315
d:\dW Data_T	10	10	10/7/15	69	213	33	2850	64	2.25	12	31	657	52	4305	285	789	73	741	69	9.31	772	80	570	92	164	93	6247	135	5499	344
d:\dW Data_T	10	10	10/7/15	69.5	185	33	2859	65	2.27	-23	33	598	52	4270	283	833	73	612	67	10.95	814	80	629	91	174	92	6722	136	5368	342
d:\dW Data_T	10	10	10/7/15	70	259	33	2791	64	2.29	-11	33	589	53	4509	281	850	73	650	66	10.15	994	81	611	92	166	94	6827	138	5161	338
d:\dW Data_T	10	10	10/7/15	70.5	205	34	2932	66	2.25	-17	33	494	52	4379	285	802	74	664	67	10.09	793	79	563	91	121	93	6326	135	5249	343
d:\dW Data_T	10	10	10/7/15	71	201	33	3065	66	2.15	-18	33	565	53	4119	272	699	72	731	68	9.30	774	81	635	92	180	94	6055	135	5253	334
d:\dW Data_T	10	10	10/7/15	71.5	208	32	3018	65	2.15	28	31	557	50	4353	270	628	72	747	69	9.24	832	79	794	93	181	92	5995	133	5126	327
d:\dW Data_T	10	10	10/7/15	72	147	30	2580	61	2.36	8	33	849	55	4406	259	657	72	1510	75	4.97	693	78	530	90	84	93	5787	132	4766	309
d:\dW Data_T	10	10	10/7/15	72.5	199	31	2615	62	2.37	10	32	713	53	4276	270	572	72	945	71	7.51	762	80	569	91	214	92	5739	131	4949	322
d:\dW Data_T	10	10	10/7/15	73	143	31	2572	62	2.41	2	32	585	52	4538	268	730	73	888	69	7.77	1014	81	632	92	264	93	6031	133	4349	319
d:\dW Data_T	10	10	10/7/15	73.5	230	32	2721	64	2.35	17	34	525	53	4166	291	695	74	681	68	9.99	732	79	731	92	117	93	5928	134	5252	351
d:\dW Data_T	10	10	10/7/15	74	191	32	2892	65	2.25	-7	35	643	55	3975	288	556	75	1107	73	6.59	782	80	641	93	252	94	6111	135	5544	356
d:\dW Data_T	10	10	10/7/15	74.5	203	32	2903	64	2.20	-4	31	712	52	4544	275	641	74	738	70	9.49	815	81	658	93	167	93	5906	134	4763	334
d:\dW Data_T	10	10	10/7/15	75	161	31	2839	64	2.25	1	33	530	52	4015	273	624	73	762	68	8.92	688	80	546	92	252	93	5983	134	5561	330
d:\dW Data_T	10	10	10/7/15	75.5	213	31	2853	64	2.24	2	33	666	54	4215	281	749	72	922	70	7.59	784	80	595	91	98	92	5609	133	5473	339
d:\dW Data_T	10	10	10/7/15	76	212	32	2995	65	2.17	11	32	657	52	4610	272	729	73	938	70	7.46	813	79	546	92	109	93	5923	133	4758	330
d:\dW Data_T	10	10	10/7/15	76.5	206	33	2939	65	2.21	30	32	604	51	4431	281	603	74	618	68	11.00	765	81	526	93	106	94	5708	134	5286	341
d:\dW Data_T	10	10	10/7/15	77	241	33	2874	64	2.23	7	33	624	52	4596	271	803	74	750	69	9.20	904	81	619	93	192	93	6056	134	4915	325
d:\dW Data_T	10	10	10/7/15	77.5	309	34	2925	65	2.22	-9	32	456	52	4880	280	933	75	626	67	10.70	776	80	539	91	146	93	6199	134	4821	334
d:\dW Data_T	10	10	10/7/15	78	264	33	3114	66	2.12	24	32	560	53	4232	277	907	75	530	67	12.64	953	81	672	93	188	92	6104	134	5291	339
d:\dW Data_T	10	10	10/7/15	78.5	235	32	2974	65	2.19	5	32	498	51	4408	276	688	74	460	68	14.78	888	80	586	92	350	94	6202	134	5297	333
d:\dW Data_T	10	10	10/7/15	79	260	33	3013	65	2.16	-7	32	523	53	4252	285	822	74	734	69	9.53	1018	81	560	92	185	93	6042	134	5460	347
d:\dW Data_T	10	10	10/7/15	79.5	192	33	2980	64	2.15	64	30	681	51	4612	273	891	73	732	67	9.15	898	80	484	91	115	92	5943	133	4912	330
d:\dW Data_T	10	10	10/7/15	80	206	33	2971	65	2.19	-9	32	515	53	4771	292	730	75	644	68	10.56	850	80	635	93	137	94	6112	135	5016	356
d:\dW Data_T	10	10	10/7/15	80.5	208	32	2995	66	2.20	28	33	559	52	4328	280	741	74	625	68	10.88	890	80	514	91	220	93	6193	133	5401	338
d:\dW Data_T	10	10	10/7/15	81	174	32	2909	65	2.23	-5	32	628	52	4639	278	706	74	706	68	9.63	919	80	659	92	104	93	6120	135	5003	335
d:\dW Data_T	10	10	10/7/15	81.5	210	31	2966	65	2.19	-3	32	477	51	4035	271	866	73	763	68	8.91	870	80	702	93	253	93	6253	136	5513	331

d:\dW Data_T	10	10	10/7/15	82	192	33	2990	66	2.21	-28	33	592	52	4745	279	789	75	693	68	9.81	901	79	690	92	219	93	6163	134	4820	337
d:\dW Data_T	10	10	10/7/15	82.5	228	32	3044	65	2.14	32	32	543	52	4655	278	703	74	627	68	10.85	902	80	624	92	336	92	6163	134	5210	335
d:\dW Data_T	10	10	10/7/15	83	229	33	3060	66	2.16	50	31	561	52	3883	272	858	75	805	69	8.57	690	80	644	93	207	94	6365	136	5748	335
d:\dW Data_T	10	10	10/7/15	83.5	220	32	3053	66	2.16	-2	32	755	54	4539	273	613	74	844	70	8.29	780	81	641	92	216	94	6590	137	5044	333
d:\dW Data_T	10	10	10/7/15	84	200	34	3000	66	2.20	-6	33	714	54	4283	284	629	75	640	70	10.94	960	81	493	92	143	93	6648	136	5335	347
d:\dW Data_T	10	10	10/7/15	84.5	198	33	2974	65	2.19	6	32	649	53	4476	279	655	74	659	69	10.47	942	80	567	91	133	92	6464	136	5244	339
d:\dW Data_T	10	10	10/7/15	85	250	33	3285	68	2.07	-9	33	575	53	4930	284	788	75	529	68	12.85	907	82	566	92	49	93	6629	137	4947	347
d:\dW Data_T	10	10	10/7/15	85.5	206	32	3181	66	2.07	-2	33	611	53	4791	270	849	75	527	67	12.71	759	80	547	91	98	93	6463	136	4834	328
d:\dW Data_T	10	10	10/7/15	86	278	32	3240	66	2.04	3	31	724	53	4206	269	830	75	686	68	9.91	898	81	688	92	307	92	6642	136	5558	332
d:\dW Data_T	10	10	10/7/15	86.5	245	33	3331	68	2.04	-9	32	598	52	4407	277	754	76	732	69	9.43	919	81	570	93	56	94	6528	136	5211	343
d:\dW Data_T	10	10	10/7/15	87	217	34	3269	69	2.11	-12	35	477	53	4388	278	748	76	633	69	10.90	1003	82	626	93	112	94	6348	137	5071	343
d:\dW Data_T	10	10	10/7/15	87.5	178	33	3248	68	2.09	-21	33	645	52	4454	272	811	73	825	68	8.24	857	80	700	93	137	94	6631	137	5263	334
d:\dW Data_T	10	10	10/7/15	88	170	33	3200	68	2.13	4	33	674	54	4719	279	880	75	727	69	9.49	912	82	469	91	136	93	6602	136	5114	342
d:\dW Data_T	10	10	10/7/15	88.5	148	32	3188	68	2.13	-8	34	531	53	3987	276	747	74	773	69	8.93	943	81	608	92	178	94	6713	137	5600	341
d:\dW Data_T	10	10	10/7/15	89	203	33	3112	67	2.15	-9	34	623	53	4658	286	802	75	644	69	10.71	777	81	715	94	243	94	6893	137	5215	348
d:\dW Data_T	10	10	10/7/15	89.5	197	32	3181	67	2.11	10	32	629	53	4156	271	829	73	550	67	12.18	949	81	649	92	199	92	7094	139	5490	333
d:\dW Data_T	10	10	10/7/15	90	281	32	3071	65	2.12	-4	31	582	51	4398	264	879	75	611	67	10.97	753	79	518	92	83	94	7483	141	5085	321
d:\dW Data_T	10	10	10/7/15	90.5	216	33	2904	65	2.24	-16	32	586	52	4619	282	752	74	457	67	14.66	1127	80	621	91	152	92	7159	139	5126	341
d:\dW Data_T	10	10	10/7/15	91	213	33	3015	66	2.19	-1	33	558	52	4604	277	804	75	668	68	10.18	909	81	593	92	89	93	7052	137	5042	335
d:\dW Data_T	10	10	10/7/15	91.5	196	33	3139	67	2.13	29	32	686	52	4660	273	905	75	674	69	10.24	897	81	682	91	210	93	7128	138	4982	332
d:\dW Data_T	10	10	10/7/15	92	188	33	3246	68	2.09	33	32	557	52	4228	277	867	75	708	69	9.75	902	81	609	92	122	94	6652	138	5542	342
d:\dW Data_T	10	10	10/7/15	92.5	222	33	3119	66	2.12	14	32	571	52	4831	265	718	74	568	68	11.97	983	79	691	91	168	91	6677	137	4741	318
d:\dW Data_T	10	10	10/7/15	93	226	33	3141	66	2.10	3	32	554	51	4763	274	951	75	667	66	9.90	910	80	589	92	197	94	6835	138	5186	332
d:\dW Data_T	10	10	10/7/15	93.5	312	35	3274	68	2.08	-6	33	504	51	4559	271	889	76	630	68	10.79	969	81	752	94	88	93	6793	138	4976	332
d:\dW Data_T	10	10	10/7/15	94	168	33	3140	67	2.13	-2	33	538	53	4876	269	884	75	614	67	10.91	831	80	658	92	153	93	6940	139	4881	324
d:\dW Data_T	10	10	10/7/15	94.5	205	34	3350	69	2.06	-1	33	494	52	4972	276	897	74	653	67	10.26	914	81	571	90	132	90	6814	137	4916	333
d:\dW Data_T	10	10	10/7/15	95	179	32	3389	68	2.01	4	32	482	52	4039	267	895	75	497	66	13.28	969	80	754	92	141	94	6596	137	5554	331
d:\dW Data_T	10	10	10/7/15	95.5	234	34	3432	69	2.01	0	32	540	52	4351	270	1006	74	745	69	9.26	925	82	686	93	273	94	6842	138	5551	333
d:\dW Data_T	10	10	10/7/15	96	176	33	3404	70	2.06	-9	35	491	52	4797	294	818	75	544	68	12.50	928	81	616	94	80	94	6987	139	5262	363
d:\dW Data_T	10	10	10/7/15	96.5	207	35	3245	69	2.13	-9	34	498	51	4094	277	662	75	551	68	12.34	1046	82	628	93	66	94	6788	137	5408	342
d:\dW Data_T	10	10	10/7/15	97	194	34	3447	70	2.03	22	33	586	52	4554	277	892	76	819	68	8.30	833	80	537	92	122	94	6660	137	5173	341
d:\dW Data_T	10	10	10/7/15	97.5	258	33	3510	70	1.99	-27	32	489	52	4538	277	841	75	637	68	10.68	978	81	619	92	176	94	6620	138	5274	342
d:\dW Data_T	10	10	10/7/15	98	258	34	3456	69	2.00	-9	32	550	52	5013	271	851	75	638	68	10.66	848	81	669	93	196	93	7173	140	4529	332
d:\dW Data_T	10	10	10/7/15	98.5	203	34	3342	69	2.06	-22	34	487	52	4608	282	771	76	612	68	11.11	889	81	509	92	94	93	6854	139	5363	345
d:\dW Data_T	10	10	10/7/15	99	247	33	3545	70	1.97	-15	33	500	52	4435	274	870	76	564	68	12.06	834	81	569	91	120	92	7121	138	5271	339
d:\dW Data_T	10	10	10/7/15	99.5	201	33	3549	70	1.97	1	33	572	52	4113	270	841	76	439	68	15.49	881	81	528	91	319	94	7077	139	5585	336
d:\dW Data_T	10	10	10/7/15	100	197	33	3446	70	2.03	-11	34	565	53	4016	270	984	75	723	68	9.41	873	80	531	91	156	93	7263	139	5756	333
d:\dW Data_T	10	10	10/7/15	100.5	241	34	3378	69	2.04	-23	33	562	53	4260	280	992	76	702	68	9.69	901	81	656	93	71	93	7388	140	5699	346
d:\dW Data_T	10	10	10/7/15	101	239	35	3373	69	2.05	24	33	529	52	4684	286	924	76	621	69	11.11	919	81	647	92	193	94	7669	140	5398	352
d:\dW Data_T	10	10	10/7/15	101.5	214	33	3492	70	2.00	-6	34	541	53	4353	266	836	75	656	68	10.37	1172	82	738	93	117	93	7287	140	5350	329
d:\dW Data_T	10	10	10/7/15	102	243	35	3429	69	2.01	2	32	589	53	4613	275	934	75	695	68	9.78	854	81	623	93	146	93	7450	140	5342	339
d:\dW Data_T	10	10	10/7/15	102.5	297	34	3379	68	2.01	37	31	679	54	4695	274	803	76	693	70	10.10	1094	81	631	93	34	94	7315	140	5210	336
d:\dW Data_T	10	10	10/7/15	103	233	34	3534	70	1.98	18	33	586	52	4546	269	1049	76	726	68	9.37	931	80	555	92	131	94	7365	141	5322	330
d:\dW Data_T	10	10	10/7/15	103.5	184	34	3410	69	2.02	-1	33	546	53	4268	281	887	76	607	69	11.37	1085	81	481	92	253	95	7671	140	5799	349
d:\dW Data_T	10	10	10/7/15	104	167	33	3438	70	2.04	10	34	529	53	4400	279	866	76	662	69	10.42	915	81	567	93	88	95	7487	142	5604	345
d:\dW Data_T	10	10	10/7/15	104.5	289	34	3466	70	2.02	-19	35	446	52	5133	270	875	77	552	70	12.68	986	81	597	91	280	93	7570	140	4594	329
d:\dW Data_T	10	10	10/7/15	105	244	35	3452	70	2.03	11	35	637	53	4517	276	970	76	653	68	10.41	833	81	601	92	214	94	7050	139	5385	338
d:\dW Data_T	10	10	10/7/15	105.5	177	33	3584	71	1.98	14	34	607	52	4332	273	947	74	788	69	8.76	908	80	486	92	260	93	7427	139	5819	338
d:\dW Data_T	10	10	10/7/15	106	266	34	3468	70	2.02	-4	33	628	54	4638	283	956	76	741	69	9.31	960	81	660	94	165	95	7642	142	5458	350
d:\dW Data_T	10	10	10/7/15	106.5	173	32	3545	70	1.97	51	33	847	55	4295	274	912	75	948	70	7.38	924	82	582	93	185	95	7816	142	5967	341
d:\dW Data_T	10	10	10/7/15	107	205	35	3500	70	2.00	-23	34	826	56	5173	291	929	77	691	69	9.99	880	83	665	94	431	95	8004	143	5138	361
d:\dW Data_T	10	10	10/7/15	107.5	246	35	3430	69	2.01	20	33	611	53	4849	269	897	76	736	69	9.38	915	82	584	92	173	93	7137	139	5039	327
d:\dW Data_T	10	10	10/7/15	108	178	34	3398	70	2.06	26	35	641	54	4564	277	1052	76	820	69	8.41	921	80	454	91	197	93	7241	139	5475	338
d:\dW Data_T	10	10	10/7/15	108.5	224	34	3470	70	2.02	9	35	709	55	4906	280	975	78	791	71	8.98	1023	81	605	92	62	93	7475	141	5183	343
d:\dW Data_T	10	10	10/7/15	109	194	34	3587	71	1.98	15	35	813	55	4891	281	852	77	1039	74	7.12	922	82	666	94	454	96	7788	141	5075	350
d:\dW Data_T	10	10	10/7/15	109.5	301	35	3503	69	1.97	55	32	739	55	4710	277	819	75	1122	73	6.51	1015	81	724	91	231	92	7560	140	5767	339
d:\dW Data_T	10	10	10/7/15	110	276	34	3462	69	1.99	19	31	692	53	5131	272	920	76	711	70	9.85	948	81	643	91	282	93	7385	140	4933	331
d:\dW Data_T	10	10	10/7/15	110.5	253	35	3531	71	2.01	18	33	791	55	4791	284	1008	76	930	71	7.63	911	81	501	93	136	94	7305	141	5494	350
d:\dW Data_T	10	10	10/7/15	111	247	35	3432	70	2.04	-7	33	714	54	4552	275	1107	76	837	70	8.36	854	82	717	94	126	94	7411	141	5388	339
d:\dW Data_T	10	10	10/7/15	111.5	247	35	3374	70	2.07	28	36	652	54	4599	274	946	76	855	70	8.19	949	81	569	92	164	93	7417	140	5583	332
d:\dW Data_T	10	10	10/7/15	112	290	34	3520	70	1.99	-17	35	745	56	4976	268	1080	77	910	71	7.80	1028	83	653	93	146	94	7846	142	4989	327
d:\dW Data_T	10	10	10/7/15	112.5	317	35	3565	70	1.96	11	32	768	56	4939	283	880	78	963	73	7.58	1096	83	572	94	179	95	7673	142	5306	353
d:\dW Data_T	10	10	10/7/15	113	277	35	3350	69	2.06	-3	34	668	54	4870	273	906	77	841	72	8.56	832	81	798	94	105	95	7455	142	5371	330
d:\dW Data_T	10	10	10/7/15	113.5	246	35	3612	71	1.97	5	33	800	55	4859	286	858	76	759	71	9.35	808	82	680	94	197	94	7530	141	5498	353
d:\dW Data_T	10	10	10/7/15	114	289	34	3632	70	1.93	7	32	797	55	4725	274	797	76	901	73	8.10	793	82	718	94	231	94	7344	141	5366	340
d:\dW Data_T	10	10	10/7/15	114.5	198	35	3427	70	2.04	-13	34	802	56	4696	290	919	77	1066	72	6.75	1000	83	591	93	55	94	7273	141	5339	361
d:\dW Data_T	10	10	10/7/15	115	237	35	3643	72	1.98	-17	35	612	54	4911	278	870	77	791	71	8.98	856	81	566	92	299	94	7300	139	5247	341
d:\dW Data_T	10	10	10/7/15	115.5	261	35	3598	72	2.00	-14	36	638	54	4415	285	1039	77	813	71	8.73	867	82	653	93	199	95	7439	141	5776	354
d:\dW Data_T	10	10	10/7/15	116	243	35	3502	70	2.00	23	32	707	55	4625	282	1121	77	888	70	7.88	914	81	605	92	215	93	7157	139	5772	349
d:\dW Data_T	10	10	10/7/15	116.5	300	35	3612	71	1.97	-8	33	723	54	5066	279	902	77	756	70	9.26	867	81	392	90	295	94	7900	142	5142	342
d:\dW Data_T	10	10	10/7/15	117	206	34	3385	70	2.07	-27	34	692	54	5168	279	1150	75	741	68	9.18	1018	82	658	94	315	95	7884	141	5158	337
d:\dW Data_T	10	10	10/7/15	117.5	223	33	3350	69	2.06	-18	34	636	54	4849	276	1040	76	716	69	9.64	1089	82	681	92	194	94	7500	141	5575	335
d:\dW Data_T	10	10	10/7/15	118	300	35	3388	70	2.07	-15	34	535	53	4669	276	1055	78	623	69	11.08	1083	82	577	92	164	94	7461	141	5371	336
d:\dW Data_T	10	10	10/7/15	118.5	200	34	3310	69	2.08	-19	34	619	54	4790	283	1066	77	678	69	10.18	1107	81	710	92	116	92	7348	140	5626	345
d:\dW Data_T	10	10	10/7/15	119	209	35	3480	70	2.01	28	33	687	54	4749	279	976	77	737	70	9.50	1033	83	649	94	146	95	7745	143	5345	343
d:\dW Data_T	10	10	10/7/15	119.5	235	35	3440	70	2.03	15	34	615	54	4759	282	901	78	652	70	10.74	954	82	537	92	211	94	7562	141	5564	344
d:\dW Data_T	10	10	10/7/15	120	268	35	3459	69	1.99	22	33	645	55	4900	284	1068	77	726	70	9.64	1000	81	621	92	149	93	7441	142	5448	347
d:\dW Data_T	10	10	10/7/15	120.5	233	35	3295	69	2.09	34	34	767	53	5355	286	1029	77	999	71	7.11	904	81	532	92	159	94	7322	140	4815	346
d:\dW Data_T	10	10	10/7/15	121	225	33	3412	69	2.02	18	33	684	55	4613	275	1021	78	855	72	8.42	1108	82	699	93	232	94	7836	142	5385	340
d:\dW Data_T	10	10	10/7/15	121.5	200	33	3263	69	2.11	1	34	704	54	4911	266	986	76	781	70	8.96	1069	80	480	91	98	93	7574	141	4836	321
d:\dW Data_T	10	10	10/7/15	122	227	32	2947	66	2.24	-5	35	1244	60	4675	280	535	77	2284	84	3.68	1021	80	621	91	198	92	6722	136	4962	345
d:\dW Data_T	10	10	10/7/15	122.5	156	32	2354	61	2.59	-8	36	2495	72	4789	250	497	74	1055	102	1.90	701	78	637	91	82	91	5632	130	4632	309

d:\ANFData_Ts	10	10	10/7/15	123	193	33	2900	66	2.28	-16	35	1314	61	4921	274	658	75	2838	86	3.03	928	81	626	92	93	93	6463	134	4797	334
d:\ANFData_Ts	10	10	10/7/15	123.5	203	34	3402	70	2.06	-19	33	629	53	4603	286	735	76	828	71	8.57	919	82	513	92	240	94	7158	140	5497	353
d:\ANFData_Ts	10	10	10/7/15	124	187	34	3428	70	2.04	1	34	592	53	3507	301	814	77	598	70	11.71	941	82	733	93	305	94	7567	141	6835	383
d:\ANFData_Ts	10	10	10/7/15	124.5	188	33	3300	68	2.06	30	34	482	52	4229	273	780	76	715	69	9.65	835	81	763	92	235	92	6892	138	5547	334
d:\ANFData_Ts	10	10	10/7/15	125	227	33	3257	67	2.08	20	32	636	53	4378	284	830	76	584	68	11.64	1018	81	478	92	252	94	6926	138	5897	348
d:\ANFData_Ts	10	10	10/7/15	125.5	278	34	3394	69	2.03	9	34	518	52	4283	279	919	76	615	69	11.22	1009	81	652	92	163	94	6979	139	5578	345
d:\ANFData_Ts	10	10	10/7/15	126	241	35	3383	70	2.07	-26	35	582	54	4263	287	884	76	687	70	10.19	919	83	632	94	216	93	7038	140	5890	355
d:\ANFData_Ts	10	10	10/7/15	126.5	288	33	3388	68	2.01	0	34	586	53	4867	266	943	77	638	70	10.97	872	80	594	93	158	95	7131	140	4915	323
d:\ANFData_Ts	10	10	10/7/15	127	199	34	3398	69	2.03	24	33	647	53	4490	271	1072	76	745	69	9.26	856	80	602	93	132	95	7207	139	5608	333
d:\ANFData_Ts	10	10	10/7/15	127.5	247	35	3422	70	2.05	9	33	768	55	4772	292	975	76	838	70	8.35	932	82	767	94	185	94	7161	139	5698	361
d:\ANFData_Ts	10	10	10/7/15	128	292	33	3466	69	1.99	26	33	679	53	4997	269	865	76	627	69	11.00	908	82	613	93	137	93	6974	139	4799	327
d:\ANFData_Ts	10	10	10/7/15	128.5	245	33	3326	69	2.07	6	35	642	54	4882	268	907	76	707	70	9.90	901	80	595	92	181	93	6927	137	4929	325
d:\ANFData_Ts	10	10	10/7/15	129	180	33	3220	68	2.11	-17	35	760	55	4580	262	870	75	999	72	7.21	1085	81	512	92	83	94	7178	139	5094	319
d:\ANFData_Ts	10	10	10/7/15	129.5	198	33	3504	70	2.00	20	33	705	54	4351	263	958	75	747	69	9.24	715	80	619	92	114	93	6620	137	5395	323
d:\ANFData_Ts	10	10	10/7/15	130	200	33	3404	70	2.06	10	34	606	52	4731	270	895	75	585	69	11.79	814	80	637	92	240	92	7202	139	5106	329
d:\ANFData_Ts	10	10	10/7/15	130.5	232	33	3270	68	2.08	62	33	666	52	4430	268	935	76	681	69	10.13	1003	82	610	93	201	94	7047	140	5333	329
d:\ANFData_Ts	10	10	10/7/15	131	254	34	3121	67	2.15	-3	33	507	52	4491	283	1079	78	703	68	9.67	1072	81	601	93	101	94	7396	140	5313	347
d:\ANFData_Ts	10	10	10/7/15	131.5	278	35	3239	69	2.13	-19	34	504	53	4886	298	1057	77	620	69	11.13	940	82	502	91	101	92	7145	138	5465	362
d:\ANFData_Ts	10	10	10/7/15	132	219	33	2965	65	2.19	4	32	652	52	4428	271	957	76	675	69	10.22	786	80	543	91	58	93	6898	139	5361	325
d:\ANFData_Ts	10	10	10/7/15	132.5	246	32	3000	65	2.17	-9	32	637	53	4907	279	821	76	633	69	10.90	1138	82	652	93	98	94	7088	139	4908	336
d:\ANFData_Ts	10	10	10/7/15	133	265	33	2905	65	2.24	9	33	569	52	4377	281	935	77	702	70	9.97	905	82	645	94	417	95	6968	138	5269	343
d:\ANFData_Ts	10	10	10/7/15	133.5	237	32	2970	65	2.19	9	31	611	52	4183	280	787	76	718	69	9.61	941	81	578	93	245	94	7086	138	5630	343
d:\ANFData_Ts	10	10	10/7/15	134	272	32	3036	65	2.14	0	32	540	52	4250	277	1015	75	701	67	9.56	944	81	617	93	144	94	6852	139	5637	336
d:\ANFData_Ts	10	10	10/7/15	134.5	210	35	2979	66	2.22	-12	33	535	52	4551	288	830	75	592	67	11.32	863	81	664	93	227	93	6885	139	5205	349
d:\ANFData_Ts	10	10	10/7/15	135	226	34	2836	65	2.29	6	33	504	52	4475	271	787	74	604	67	11.09	923	80	482	91	76	93	6821	138	5136	323
d:\ANFData_Ts	10	10	10/7/15	135.5	196	34	2970	66	2.22	-8	33	651	53	4440	283	963	77	596	68	11.41	937	81	669	92	206	93	6966	138	5246	345
d:\ANFData_Ts	10	10	10/7/15	136	181	33	2989	66	2.21	15	33	407	51	4462	278	995	76	572	67	11.71	857	80	525	91	168	92	7105	138	5337	336
d:\ANFData_Ts	10	10	10/7/15	136.5	210	32	3003	65	2.16	-11	32	501	51	4652	276	830	76	544	69	12.68	1037	81	682	93	106	93	7188	138	5141	334
d:\ANFData_Ts	10	10	10/7/15	137	193	32	3099	66	2.13	15	32	624	52	4442	270	1017	76	585	68	11.62	767	80	629	92	136	93	6938	138	5138	329
d:\ANFData_Ts	10	10	10/7/15	137.5	287	35	3024	66	2.18	3	33	458	52	4217	284	1157	75	593	67	11.30	936	81	515	91	96	92	7159	137	5813	343
d:\ANFData_Ts	10	10	10/7/15	138	246	33	3126	67	2.14	-17	32	630	53	4412	294	868	76	663	69	10.41	859	81	536	92	119	94	6817	138	5597	363
d:\ANFData_Ts	10	10	10/7/15	138.5	245	34	2948	65	2.20	25	31	674	53	4479	285	747	75	629	69	10.97	900	80	641	92	163	92	6871	137	5153	347
d:\ANFData_Ts	10	10	10/7/15	139	205	34	3022	66	2.18	-5	33	620	53	4294	287	824	76	679	69	10.16	1057	82	619	93	91	94	6563	136	5601	353
d:\ANFData_Ts	10	10	10/7/15	139.5	228	34	2966	65	2.19	4	32	624	53	4875	284	758	75	789	70	8.87	857	80	459	92	240	93	6681	136	5019	342
d:\ANFData_Ts	10	10	10/7/15	140	263	32	2740	62	2.26	33	31	881	55	4450	280	794	76	1077	74	6.87	820	81	652	92	152	93	6428	135	5065	340
d:\ANFData_Ts	10	10	10/7/15	140.5	177	32	2787	65	2.33	-17	34	709	55	4107	290	846	75	892	71	7.96	830	80	630	93	194	93	6608	136	5341	357
d:\ANFData_Ts	10	10	10/7/15	141	200	33	2862	64	2.24	12	31	586	52	4375	287	820	75	742	68	9.16	782	80	731	93	366	92	6265	135	5229	349
d:\ANFData_Ts	10	10	10/7/15	141.5	263	32	2985	65	2.18	2	31	717	54	4327	286	847	75	725	69	9.52	932	80	603	92	156	94	6246	136	5399	351
d:\ANFData_Ts	10	10	10/7/15	142	223	32	3078	66	2.14	1	33	560	53	4125	280	756	74	682	68	9.97	869	80	489	91	245	93	6280	135	5400	345
d:\ANFData_Ts	10	10	10/7/15	142.5	214	33	2925	65	2.22	-14	34	682	54	4926	277	807	74	615	68	11.06	1040	81	778	92	71	92	6399	135	4616	333
d:\ANFData_Ts	10	10	10/7/15	143	213	34	2835	64	2.26	-8	32	666	53	4414	278	869	75	654	69	10.55	839	80	534	92	135	94	6596	137	5053	338
d:\ANFData_Ts	10	10	10/7/15	143.5	262	34	2857	65	2.28	-25	33	658	54	4434	281	1010	74	869	69	7.94	869	81	695	93	140	93	6452	135	5213	339
d:\ANFData_Ts	10	10	10/7/15	144	232	32	2934	65	2.22	10	32	568	52	4538	269	785	75	823	68	8.26	921	81	601	93	210	95	6244	135	4696	326
d:\ANFData_Ts	10	10	10/7/15	144.5	197	32	2806	64	2.28	-6	33	539	53	4389	270	716	73	732	67	9.15	757	79	674	92	108	92	6286	135	5217	322
d:\ANFData_Ts	10	10	10/7/15	145	239	31	2870	63	2.20	10	31	629	53	4371	280	581	74	518	68	13.13	830	80	630	92	283	93	6475	135	5128	342
d:\ANFData_Ts	10	10	10/7/15	145.5	274	33	2911	64	2.20	-6	31	654	53	4914	274	811	75	573	68	11.87	802	79	824	92	180	91	6374	134	4541	329
d:\ANFData_Ts	10	10	10/7/15	146	213	33	2749	63	2.29	0	32	766	54	4587	274	740	73	882	70	7.94	812	79	595	92	203	93	6234	133	4904	329
d:\ANFData_Ts	10	10	10/7/15	146.5	173	31	2723	63	2.31	5	34	1018	57	4484	267	625	73	1412	75	5.31	960	79	556	91	197	93	5920	132	4855	322
d:\ANFData_Ts	10	10	10/7/15	147	205	32	2525	61	2.42	37	33	1350	60	4051	274	696	75	1804	78	4.32	742	79	690	91	179	92	5975	132	5367	334
d:\ANFData_Ts	10	10	10/7/15	147.5	227	32	2375	61	2.57	-10	35	1297	61	4187	268	622	74	2106	81	3.85	821	79	628	91	108	92	5536	130	4910	322
d:\ANFData_Ts	10	10	10/7/15	148	197	32	2328	60	2.58	-12	35	1650	64	4368	262	587	75	2503	85	3.40	706	78	574	90	99	90	5437	129	4623	317
d:\ANFData_Ts	10	10	10/7/15	148.5	195	31	2347	60	2.56	2	33	1635	64	3990	249	516	72	2622	84	3.20	775	78	445	88	77	90	5345	128	4662	302
d:\ANFData_Ts	10	10	10/7/15	149	171	30	2333	60	2.57	-7	34	1726	63	4364	268	389	73	2617	85	3.25	693	79	579	91	193	92	5433	128	4765	329
d:\ANFData_Ts	10	10	10/7/15	149.5	191	31	2446	60	2.45	-12	32	1245	60	3915	279	550	75	1902	80	4.21	767	79	598	92	166	93	5467	131	5303	343
d:\ANFData_Ts	10	10	10/7/15	150	155	32	2473	62	2.51	-37	35	1216	60	4555	277	401	74	1438	78	5.42	640	79	577	91	158	93	5703	131	4322	335
d:\ANFData_Ts	10	10	10/7/15	150.5	206	31	2476	60	2.42	33	30	1048	57	4467	268	529	72	1331	74	5.56	649	79	645	92	228	92	5873	132	4504	322
d:\ANFData_Ts	10	10	10/7/15	151	140	31	2359	59	2.50	27	32	961	57	3900	263	459	72	1159	74	6.38	673	79	552	91	70	92	5427	130	4872	315
d:\ANFData_Ts	10	10	10/7/15	151.5	169	30	2345	60	2.56	1	33	943	56	3817	271	565	72	1024	72	7.03	899	79	560	90	349	92	5562	130	5291	323
d:\ANFData_Ts	10	10	10/7/15	152	178	31	2486	61	2.45	8	33	843	55	4114	274	611	72	1044	72	6.90	861	79	625	91	201	93	5476	131	5088	329
d:\ANFData_Ts	10	10	10/7/15	152.5	141	31	2491	61	2.45	27	33	909	56	4326	277	505	73	1230	74	6.02	622	79	608	91	282	91	5495	130	4783	334
d:\ANFData_Ts	10	10	10/7/15	153	226	32	2381	60	2.52	-14	31	716	52	4556	281	805	71	781	67	8.58	755	77	673	90	171	91	5482	129	4889	329
d:\ANFData_Ts	10	10	10/7/15	153.5	115	32	2560	62	2.42	17	33	675	54	4037	300	733	74	882	68	7.71	1011	80	692	93	241	92	5730	132	5532	367
d:\ANFData_Ts	10	10	10/7/15	154	183	31	2569	61	2.37	12	31	654	52	4194	273	602	72	730	69	9.45	844	79	765	91	243	90	5621	130	4828	328
d:\ANFData_Ts	10	10	10/7/15	154.5	162	30	2491	61	2.45	-5	32	562	52	4132	277	537	72	708	67	9.46	771	79	478	90	106	92	5334	129	4928	331
d:\ANFData_Ts	10	10	10/7/15	155	222	31	2422	59	2.46	54	30	721	52	4269	272	670	71	863	69	8.00	838	78	720	90	102	91	5270	129	4913	322
d:\ANFData_Ts	10	10	10/7/15	155.5	184	30	2356	60	2.55	-15	33	689	53	4270	278	541	71	743	67	9.02	722	79	587	91	161	93	5310	130	4915	327
d:\ANFData_Ts	10	10	10/7/15	156	158	29	2363	59	2.50	-8	30	702	52	3927	275	632	72	924	69	7.47	738	79	599	92	154	93	5526	130	5107	328
d:\ANFData_Ts	10	10	10/7/15	156.5	130	31	2375	59	2.59	-6	32	616	52	4289	276	598	71	742	67	9.03	804	78	697	92	164	92	5482	130	4770	325
d:\ANFData_Ts	10	10	10/7/15	157	197	31	2369	60	2.53	-2	32	712	53	4261	282	535	70	754	68	9.02	702	79	678	92	262	93	5171	129	4827	334
d:\ANFData_Ts	10	10	10/7/15	157.5	142	30	2134	57	2.67	-11	32	910	55	4134	276	473	70	1054	71	6.74	743	79	608	91	187	92	4721	126	4944	325
d:\ANFData_Ts	10	10	10/7/15	158	157	30	1980	56	2.83	-6	33	995	56	4085	283	447	71	1276	73	5.72	635	78	555	90	196	92	4822	126	4753	334
d:\ANFData_Ts	10	10	10/7/15	158.5	98	28	1838	54	2.94	9	31	1676	62	4149	258	346	70	2458	83	3.38	505	77	667	91	133	91	4527	124	4393	310
d:\ANFData_Ts	10	10	10/7/15	159	143	29	2068	56	2.71	11	31	1222	60	3844	274	372	71	1727	77	4.46	561	78	634	91	224	90	5078	127	5084	328
d:\ANFData_Ts	10	10	10/7/15	159.5	117	29	2066	57	2.76	-14	32	1024	56	4112	291	451	71	1438	74	5.15	638	78	632	91	346	92	4960	127	4927	348
d:\ANFData_Ts	10	10	10/7/15	160	146	29	2067	56	2.71	19	31	827	54	4166	274	477	71	1163	72	6.19	625	79	620	91	181	92	4944	127	4601	323
d:\ANFData_Ts	10	10	10/7/15	160.5	138	31	2057	57	2.77	-23	32	725	53	3926	289	488	71	855	69	8.07	721	78	686	92	305	92	5065	127	5148	339
d:\ANFData_Ts	10	10	10/7/15	161	134	30	2059	57	2.77	7	31	801	53	3936	279	577	70	954	68	7.13	705	77	636	91	146	92	4778	126	4852	326
d:\ANFData_Ts	10	10	10/7/15	161.5	150	30	2202	58	2.63	17	31	777	53	4529	292	465	71	798	69	8.65	786	79	750	92	200	93	4845	128	4550	346
d:\ANFData_Ts	10	10	10/7/15	162	105	30	2134	58	2.72	-17	33	542	52	4105	295	452	70	645	67	10.39	720	79	675	92	370	91	5315	128	5111	346
d:\ANFData_Ts	10	10	10/7/15	162.5	176	29	2111	57	2.70	25	32	627	52	3451	277	453	69	745	66	8.86	855	78	562	90	221	91	5128	127	5557	326
d:\ANFData_Ts	10	10	10/7/15	163	218	30	2134	57	2.67	-19	32	606	52	4606	285	580	70	651	66	10.14	757	79	575	91	315	91	5086	127	4533	327
d:\ANFData_Ts	10	10	10/7/15	163.5	119	30	2055	57	2.77	-8	32	593	52	3675	289	632	71	663	66	9.95	676	78	396	90	174	92	4598	126	5015	336

d:\WRF Data_Ti	10	10	10/7/15	164	135	30	2151	57	2.65	16	31	636	53	3457	299	617	70	751	66	8.79	724	79	698	91	194	90	4930	127	5688	360
d:\WRF Data_Ti	10	10	10/7/15	164.5	119	29	2062	55	2.67	17	29	656	51	4174	285	650	70	587	66	11.24	664	79	607	90	310	91	4793	125	4880	334
d:\WRF Data_Ti	10	10	10/7/15	165	112	28	1897	54	2.85	17	31	615	52	3737	286	692	70	939	69	7.35	651	77	539	90	146	92	4535	124	5169	332
d:\WRF Data_Ti	10	10	10/7/15	165.5	94	29	1677	55	2.78	17	29	638	52	4441	299	637	69	846	67	7.92	633	78	572	90	169	92	4562	125	4616	347
d:\WRF Data_Ti	10	10	10/7/15	166	96	28	1992	55	2.76	-1	31	585	51	3926	295	561	68	734	65	8.86	757	79	589	90	179	92	4671	126	5505	343
d:\WRF Data_Ti	10	10	10/7/15	166.5	128	28	1908	55	2.88	-7	32	570	52	4143	303	539	70	623	66	10.59	677	79	592	90	154	90	4865	126	4936	350
d:\WRF Data_Ti	10	10	10/7/15	167	85	28	2037	56	2.75	-3	30	595	51	3879	294	333	70	689	67	9.72	655	78	654	90	309	91	4636	125	5073	347
d:\WRF Data_Ti	10	10	10/7/15	167.5	85	29	1980	56	2.83	2	31	615	52	3980	309	508	70	740	67	9.05	740	79	544	90	57	91	4816	125	5137	366
d:\WRF Data_Ti	10	10	10/7/15	168	122	28	1834	53	2.89	20	30	585	51	4213	290	447	69	796	66	8.29	616	78	619	91	146	92	4768	127	4714	333
d:\WRF Data_Ti	10	10	10/7/15	168.5	147	28	1855	54	2.91	2	31	557	50	3733	291	476	69	635	66	10.39	635	78	549	91	237	93	4565	125	5120	335
d:\WRF Data_Ti	10	10	10/7/15	169	122	29	1842	54	2.93	-5	30	568	51	4150	300	422	70	663	66	9.95	811	77	758	91	104	91	4570	125	4977	344
d:\WRF Data_Ti	10	10	10/7/15	169.5	130	29	1809	54	2.99	0	32	640	52	4239	299	452	68	710	66	9.30	637	77	642	91	288	92	4433	124	4878	338
d:\WRF Data_Ti	10	10	10/7/15	170	101	28	1888	54	2.86	37	29	591	50	4119	291	545	69	758	67	8.84	568	79	627	92	146	93	4551	125	4808	336
d:\WRF Data_Ti	10	10	10/7/15	170.5	118	27	1847	53	2.87	33	30	588	51	3156	297	474	69	613	65	10.60	519	78	605	90	108	91	4452	125	5839	348
d:\WRF Data_Ti	10	10	10/7/15	171	122	28	1860	54	2.90	1	31	639	53	4140	306	368	70	582	67	11.51	670	77	695	90	100	90	4678	125	4981	353
d:\WRF Data_Ti	10	10	10/7/15	171.5	109	29	1728	53	3.07	-23	32	569	53	4890	298	380	69	851	68	7.99	621	77	631	91	210	92	5465	131	3888	335
d:\WRF Data_Ti	10	10	10/7/15	172	69	28	1737	53	3.05	38	32	508	51	3382	321	395	69	780	66	8.46	661	79	611	92	154	93	6742	136	5731	375
d:\WRF Data_Ti	10	10	10/7/15	172.5	144	27	1894	53	2.80	39	29	657	52	3918	284	399	70	753	67	8.90	648	78	591	91	299	91	6180	133	4831	330
d:\WRF Data_Ti	10	10	10/7/15	173	124	29	1948	55	2.82	11	31	639	52	4327	287	459	71	618	67	10.84	655	78	749	92	133	91	5348	128	4678	331
d:\WRF Data_Ti	10	10	10/7/15	173.5	87	29	1984	55	2.77	37	30	812	53	4264	288	465	70	764	68	8.90	581	78	648	91	242	92	4986	127	4601	338
d:\WRF Data_Ti	10	10	10/7/15	174	117	28	1858	54	2.91	-4	32	698	53	3935	289	512	69	794	67	8.44	690	78	702	91	247	91	6113	132	4995	334
d:\WRF Data_Ti	10	10	10/7/15	174.5	123	28	1920	55	2.86	14	31	580	52	3804	288	459	70	731	67	9.17	624	78	630	91	151	93	7061	137	5083	335
d:\WRF Data_Ti	10	10	10/7/15	175	118	28	1814	54	2.98	-14	31	742	53	4128	290	473	69	807	66	8.18	658	77	661	91	164	90	8678	144	4617	334
d:\WRF Data_Ti	10	10	10/7/15	175.5	143	29	1997	55	2.75	-7	30	721	52	3700	296	391	70	634	67	10.57	599	79	683	92	438	93	7603	139	5361	351
d:\WRF Data_Ti	10	10	10/7/15	176	133	28	1863	54	2.90	47	32	672	52	3700	293	419	68	833	67	8.04	698	78	695	90	255	90	5398	129	5338	338
d:\WRF Data_Ti	10	10	10/7/15	176.5	140	29	1907	54	2.83	27	31	570	52	4294	287	530	69	678	66	9.73	810	78	546	91	156	92	4943	128	4637	328
d:\WRF Data_Ti	10	10	10/7/15	177	93	29	1931	55	2.85	0	32	522	52	3884	313	523	70	730	66	9.04	739	79	732	92	215	92	5145	129	5274	368
d:\WRF Data_Ti	10	10	10/7/15	177.5	88	28	1790	53	2.96	-4	31	653	53	4394	304	369	70	552	66	11.96	780	78	577	92	158	92	5161	131	4669	348
d:\WRF Data_Ti	10	10	10/7/15	178	101	27	1856	54	2.91	-6	31	637	52	3963	279	416	69	697	67	9.61	629	79	453	90	141	93	5407	130	4719	322
d:\WRF Data_Ti	10	10	10/7/15	178.5	147	30	1838	54	2.94	-30	32	726	54	3970	311	430	71	874	70	8.01	606	79	654	92	187	93	5149	128	5085	364
d:\WRF Data_Ti	10	10	10/7/15	179	120	29	1834	55	3.00	-13	33	812	55	3908	295	500	70	1122	71	6.33	809	78	523	90	88	92	4997	128	5185	343
d:\WRF Data_Ti	10	10	10/7/15	179.5	127	28	2114	55	2.60	31	28	919	54	4196	274	300	71	1022	71	6.95	795	80	661	92	184	93	5437	129	4527	328
d:\WRF Data_Ti	10	10	10/7/15	180	119	29	2054	56	2.73	-4	31	840	55	4077	287	351	70	864	70	8.10	642	78	569	91	176	92	5469	129	4672	341

APPENDIX C

XRF Section Graphs of Major and Minor Elements

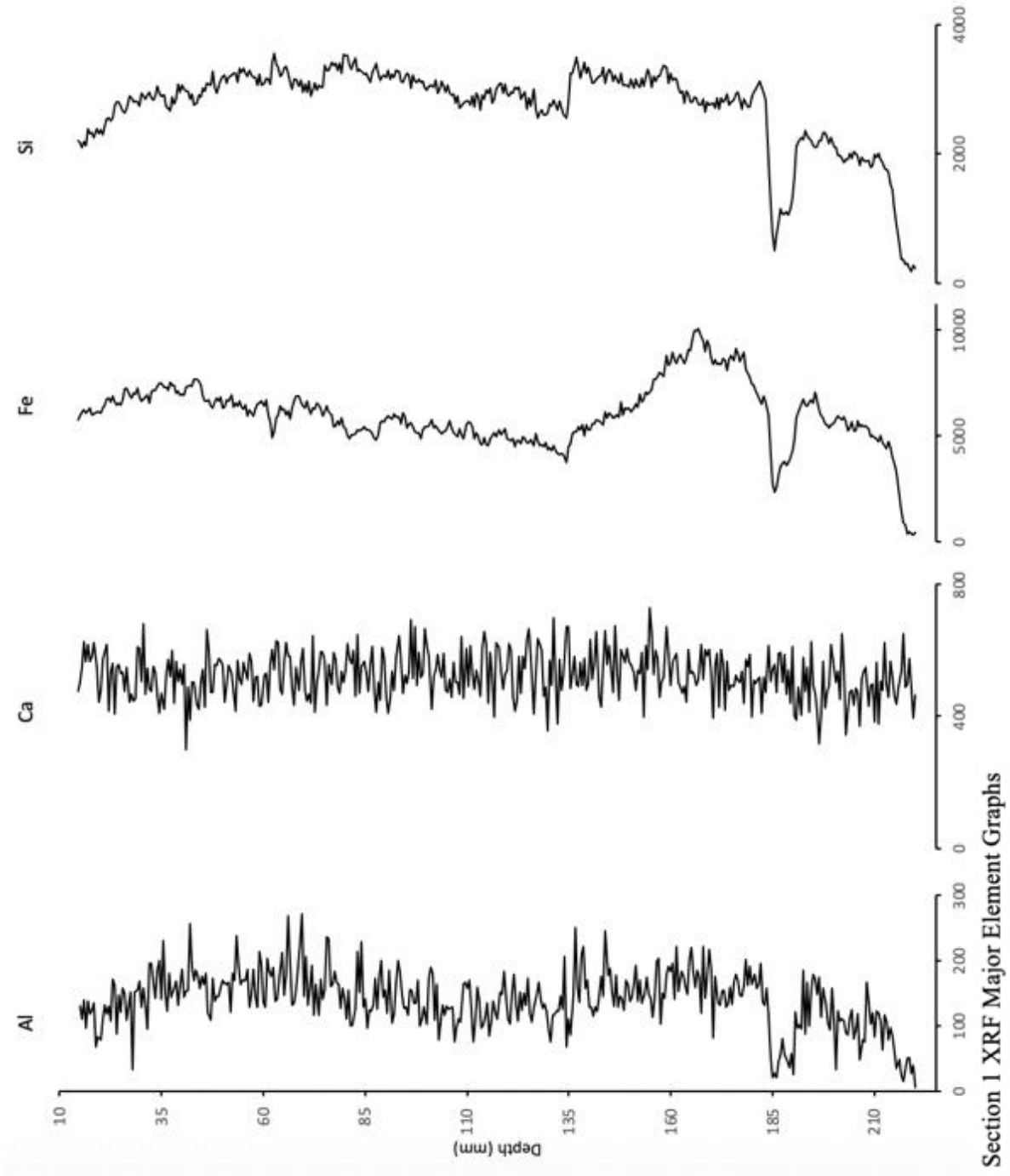

Section 1 XRF Major Element Graphs

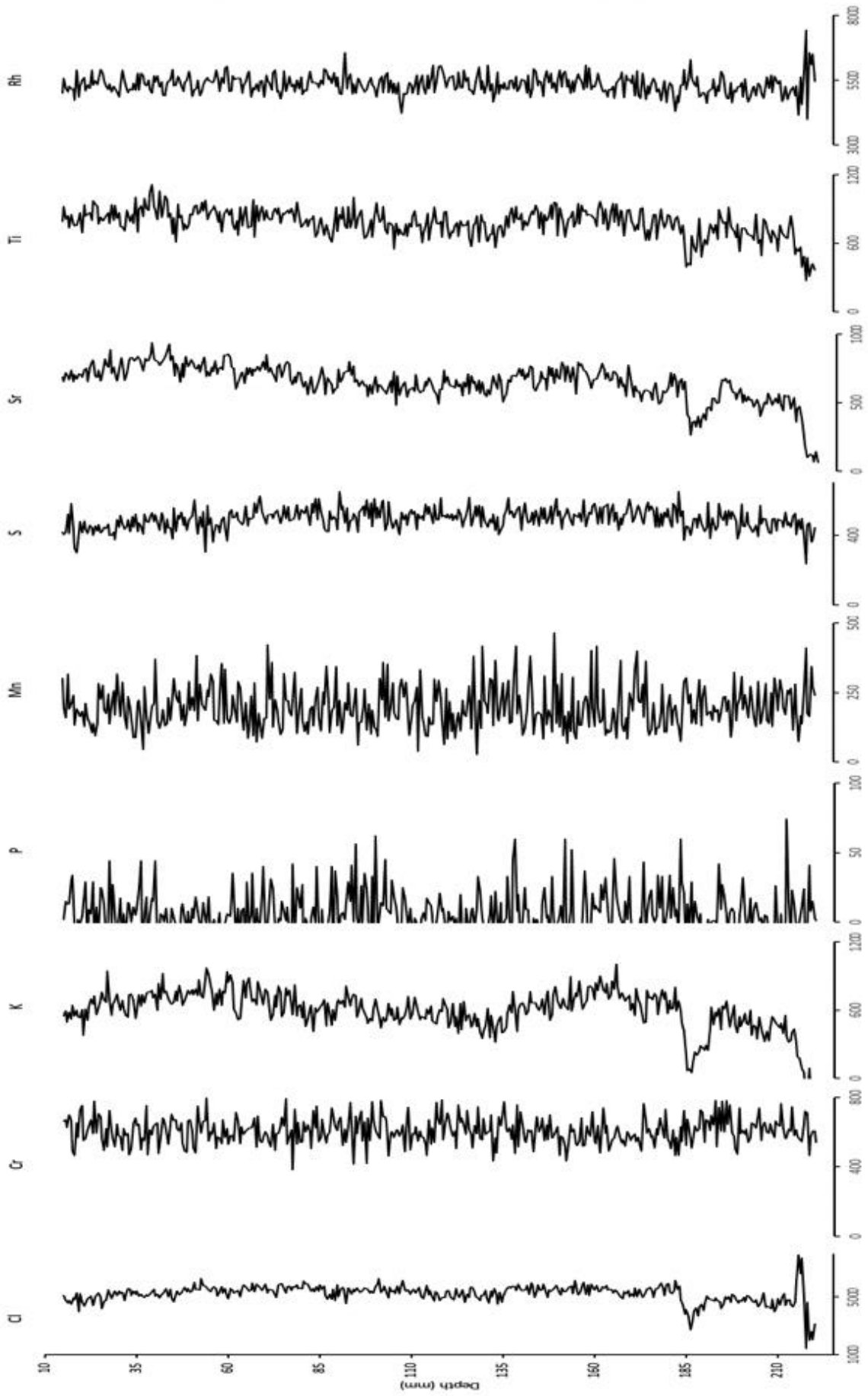

Section 1 XRF Minor Element Graphs

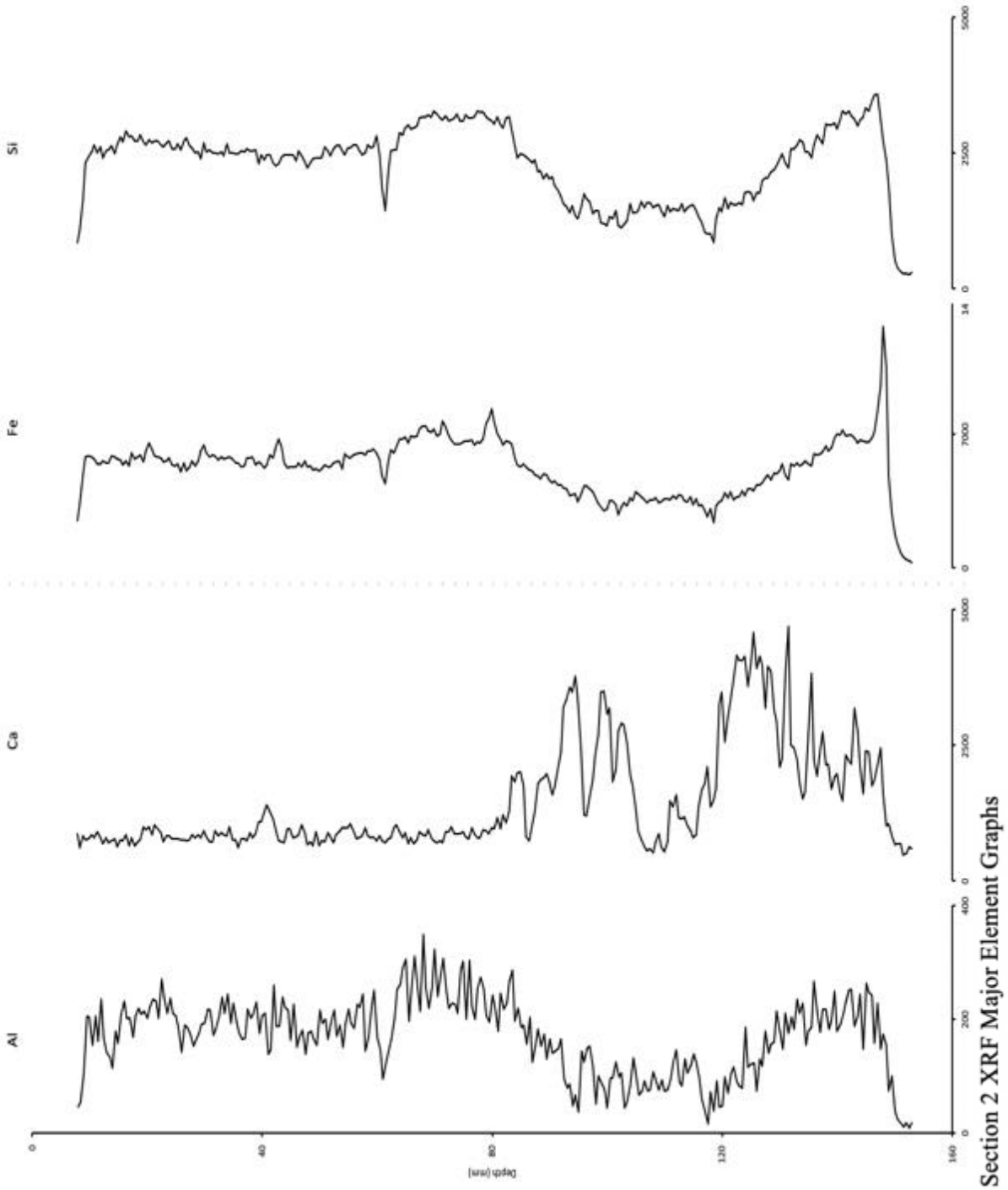

Section 2 XRF Major Element Graphs

Section 2 XRF Minor Element Graphs

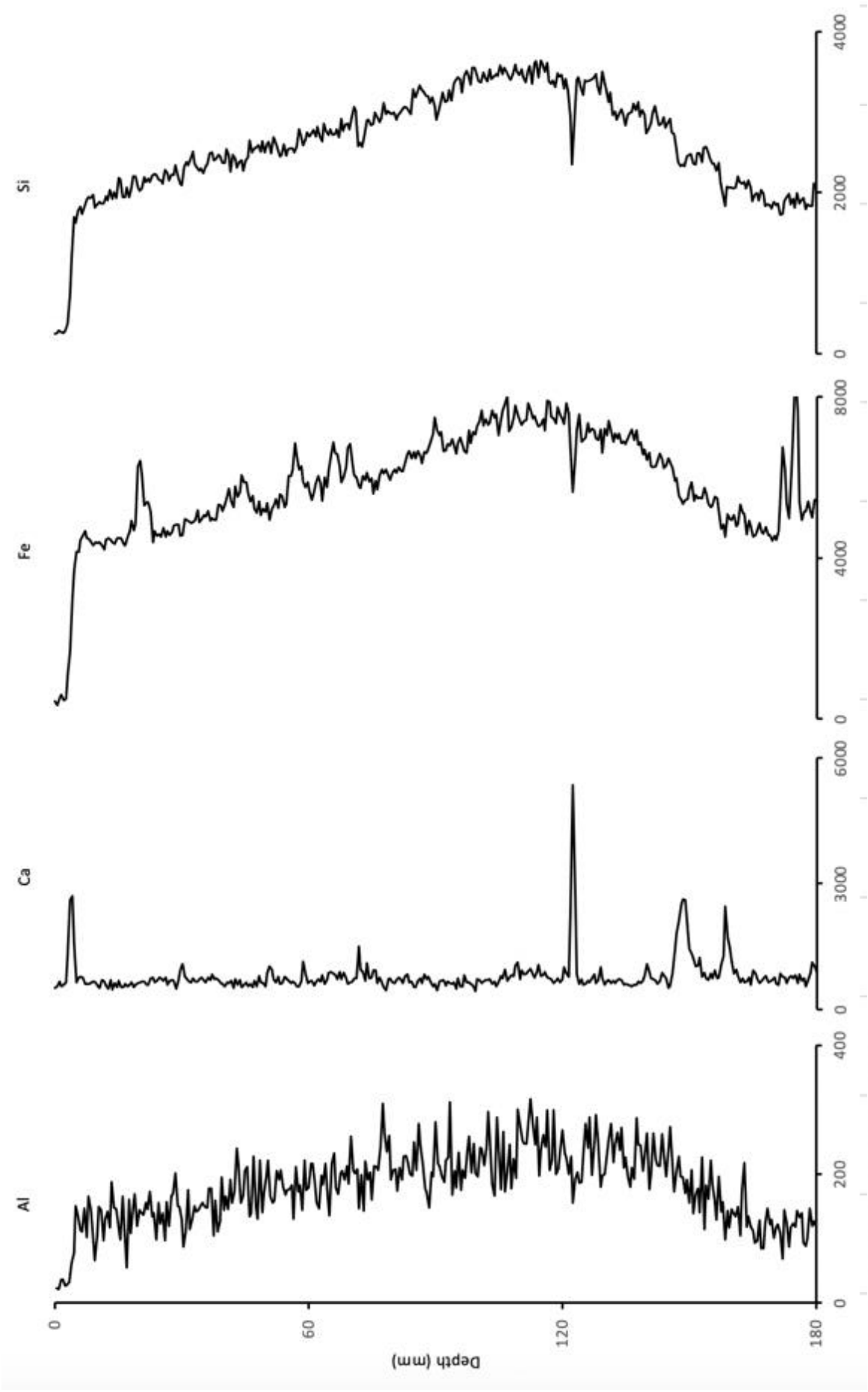

Section 3 XRF Major Element Graphs

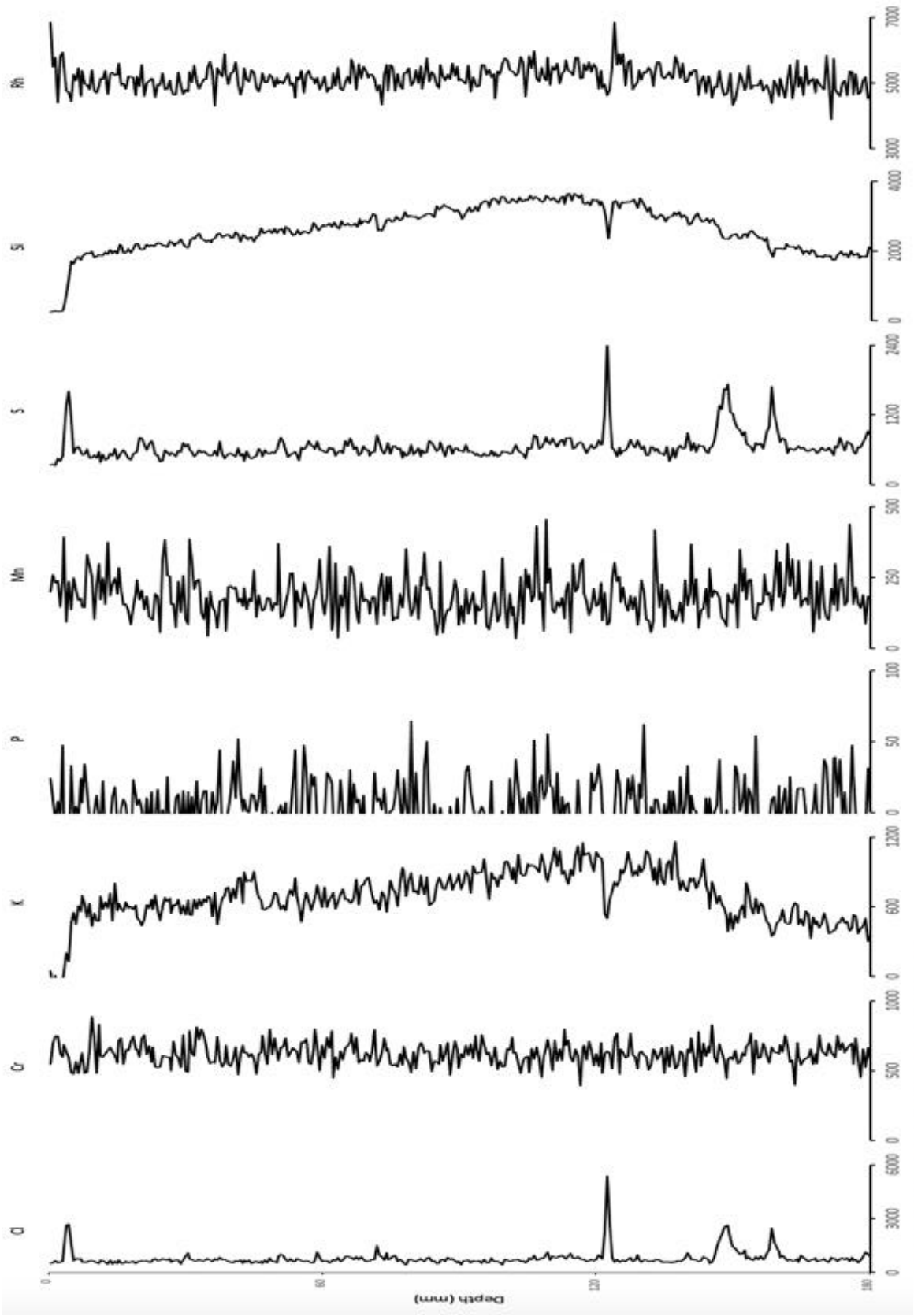

Section 3 XRF Minor Element Graphs

APPENDIX D

Scanning Electron Microscopy Diatom Images

Section 1 (14 -14.50 m)

Stephanodiscus sp.

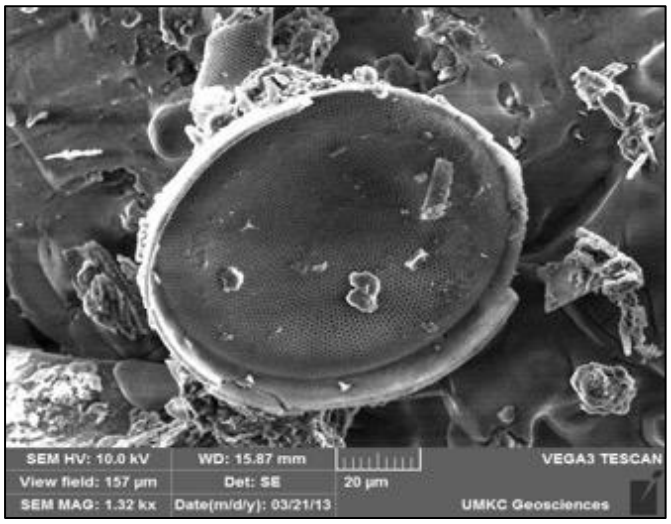

Stephanodiscus sp.

Stephanodiscus sp. and *Aulacoseira lirata*

Section 2 (19.62 - 19.76 m)

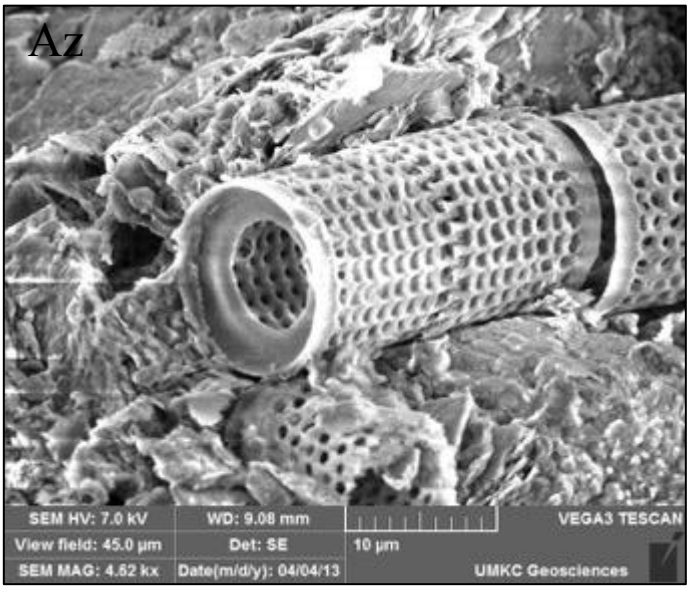

Aulacoseira lirata

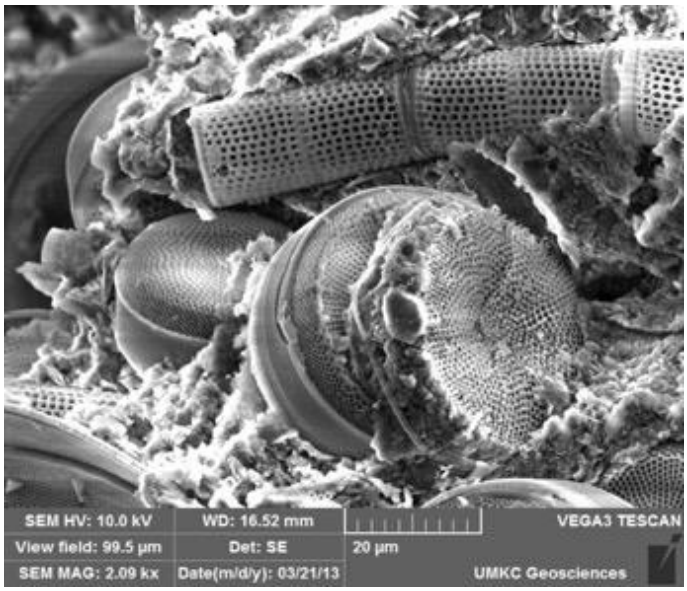

Aulacoseira lirata and Stephanodiscus sp.

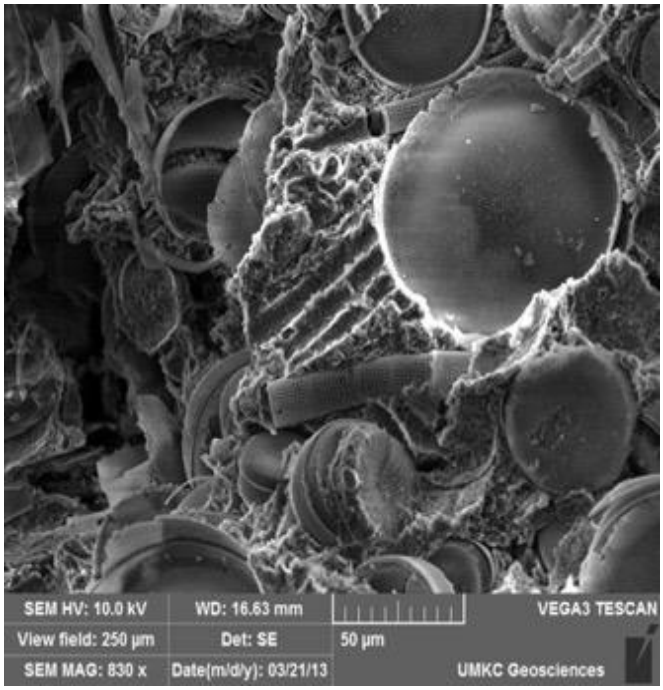

Aulacoseira lirata and *Stephanodiscus* sp.

Section 3 (20.05-20.14 m)

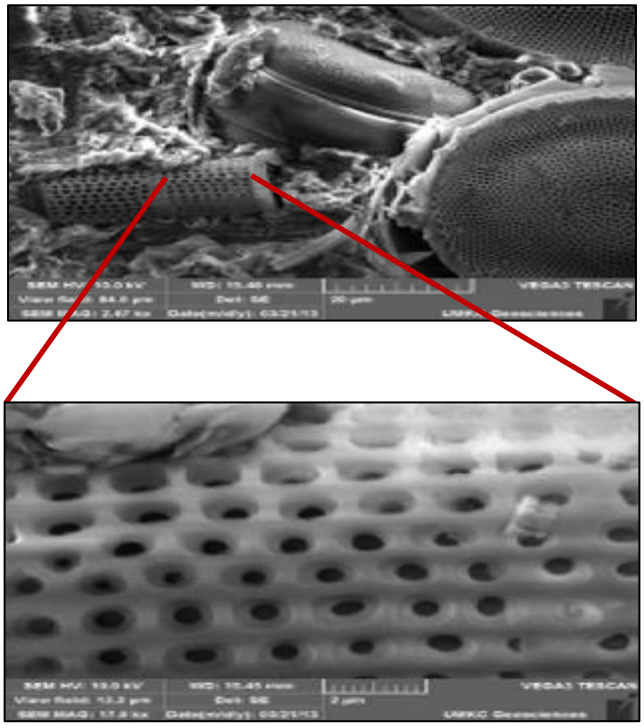

Aulacoseira lirata and *Stephanodiscus* sp.

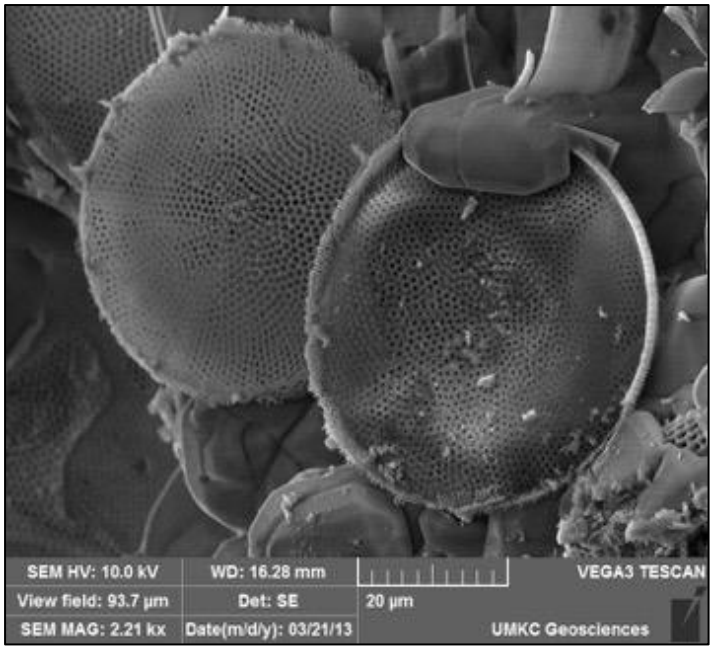

Stephanodiscus sp.

REFERENCES

Abed, A.M., Yasin, S., Sadaqa, R., Al-Hawari, Z., 2008. The paleoclimate of the eastern desert of Jordan during marine isotope stage 9. Quaternary Research. 69, 458-468.

Ahmad, K., Davies, C., 2021. Stable isotopic and geochemical analysis of lacustrine carbonates from the Al-Azraq basin, Jordan: implications for paleoenvironment and paleohydrology. Arabian Journal of Geosciences. 14, 470. https://doi.org/10.1007/s12517-021-06650-1

Ahmad, K., Davies, C., 2017. Stable isotope (δ13C and δ15N) based interpretation of organic matter sources and paleoenvironmental conditions in Al-Azraq basin, Jordan. Applied Geochemistry. 78, 49-60. 10.1016/j.apgeochem.2016.12.004

Ala'li, J., 1993. Exploration for Bentonite and other Minerals in Azraq Depression. Unpublished master's thesis, University of Jordan, Amman, Jordan.

Al Naber, M., 2016. Jordan – Azraq Basin Case Study. Groundwater governance in the Arab World. IWMI Project Publication. Report no. 12, pp. 106.

Anderson, R.Y., Dean, W.E., 1988. Lacustrine varve formation through time. Palaeogeography, Palaeoclimatology, Palaeoecology. 62, 215-235.

Archer, A.W., 1999. Modeling of tidal rhythmites using modern tidal periodicities and implications for short-term sedimentation rates, in: Sedimentary Modeling: Computer simulations and methods for improved parameter definition, Franseen, E.K., Watney, W.L., St. Kendall, C.G., Ross, W. (Eds.), Kansas Geological Survey Bulletin. 233, 185-194.

Battarbee, R.W., 1984. Diatom analysis and the acidification of lakes. Phil. Trans. R. Soc. Lond. B. 305, 451-477. doi.org/10.1098/rstb.1984.0070

Belmaker, R., Lazar, B., Stein, M., Taha, N., Bookman, R., 2019. Constraints on aragonite precipitation in the Dead Sea from geochemical measurements of flood plumes. Quaternary Science Reviews. 221, 105876.

Bender, F., 1974. Geology of Jordan. Gebruder Borntraeger, Berlin, pp. 196.

Brauer, A., Mangili, C., Moscariello, A., Witt, A., 2008. Palaeoclimatic implications from micro-facies data of a 5900 varve time series from the Piànico interglacial sediment record, southern Alps. Palaeogeography, Palaeoclimatology, Palaeoecology. 259, 121–135.

Ben Dor, Y., Neugebauer, I., Enzel, Y., Schwab, M.J., Tjallingii, R., Erel, Y., Brauer, A., 2020. Reply to comment on Ben Dor Y. et al. "Varves of the Dead Sea sedimentary record." Quaternary Science Reviews 215 (2019): 173–184. In Quaternary Science Reviews. 23, 1:1-5.

Ben Dor Y., Neugebauer, I., Enzel, Y., Schwab, M.J., Tjallingii, R., Erel, Y., Brauer, A., 2019. Varves of the Dead Sea sedimentary record. Quaternary Science Reviews. 215, 173-184.

Bloch, R., Littman, H., Elazari-Volcani, B., 1944. Occasional whiteness of the Dead Sea. Nature. 154, 402e403. https://doi.org/10.1038/154402a0.

Boggs, S., 2012. Principles of Sedimentology and Stratigraphy, 5th edition. Prentice Hall, Inc.

Bookman, R., 2020. Comment to: Ben Dor Y. et al. "Varves of the Dead Sea sedimentary record" Quaternary Science reviews 215 (2019): 173-184. Quaternary Science Reviews. 231, 1-3.

https://doi.org/10.1016/j.quascirev.2019.106064

Bostick, B.C., Theissen, K.M., Dunbar, R.B., Vairavamurthy, M.A., 2005. Record of redox status in laminated sediments from Lake Titicaca: A sulfur K-edge X-ray absorption near edge structure (XANES) study. Chemical Geology. 219, 163-174. https://doi.org/10.1016/j.chemgeo.2005.02.004.

Camburn, K.E., Kingston, J.C., 1986. The genus *Melosira* from soft-water lakes with special reference to northern Michigan, Wisconsin and Minnesota, in: Smol, J.P., Battarbee, R.W., Davis, R.B., Meriläinen, J. (Eds.), Diatoms and Lake Acidity, Dr W. Junk Publishers, Dordrecht, pp. 17-34.

Cane, G., 1972. A Paleoclimate reconstruction based on lacustrine sediments of the Azraq Basin, Jordan. Thesis, University of Ottowa, pp. 104.

Cordova, C.E., Nowell, A., Bisson, M., Ames, C.J.H., Pokines, J., Chang, M., al-Nahar, M., 2013. Interglacial and glacial desert refugia and the Middle Paleolithic of the Azraq Oasis, Jordan. Quaternary International. 300, 94-110.

Cordova, C.E., Rollefson, G.O., Kalchgruber, R., Wilke, P., Quintero, L., 2008. Natural and cultural stratigraphy of 'Ayn as-Sawda, Azraq Wetland Reserve: 2007 excavation report and discussion of finds. Annual of the Department of Antiquities of Jordan. 52,417-425.

Davies, C., 2005. Quaternary Paleoenvironments and Potential for Human Exploitation of the Jordan Plateau Desert Interior. Journal of Geoarchaeology. 20, 381-402.

Deutsche Welle., 2016. Syrian refugees build a city in Jordan desert. https://p.dw.com/p/1JL19. Accessed 07 July 2016

Dixit, S.S., Smol, J.P., Kingston, J.C., Charles, D.F., 1992. Diatoms: Powerful indicators of environmental change. Environmental Science and Technology. 26, 22–33.

Ehrlich, A., 1973. Quaternary diatoms of the Hula Basin (northern Israel). Geological Survey of Israel Bulletin. 58, 1-39.

Fitton, G., 1997. X-Ray fluorescence spectrometry, in: Modern Analytical Geochemistry: An Introduction to Quantitative Chemical Analysis for Earth, Environmental and Material Scientists, Gill, R. (Ed.), Addison Wesley Longman, UK.

Frances, A., 2015. Jordan's refugee crisis. Carnegie Endowment for International Peace. Sept 21, 2015. http://carnegieendowment.org/2015/09/21/jordan-s-refugee-crisis-pub-61338

Fritz, S., Juggins, S., Battarbee, R., Engstrom, D.R., 1991. Reconstruction of past changes in salinity and climate using a diatom-based transfer function. Nature. 352, 706-708. https://doi.org/10.1038/352706a0

Folk, R.L., 1974. Petrology of Sedimentary Rocks: Austin, Hemphill Publishing Company, pp. 182.

Folk, R.L., Ward, W.C., 1957. A study in the significance of grain size parameter. Journal of Petrology. 37, 327-354.

Gasse F., 1994. Lacustrine Diatoms for Reconstructing Past Hydrology and Climate, in: Long-Term Climatic Variations, Duplessy JC., Spyridakis MT. (Eds), NATO ASI Series (Series I: Global Environmental Change), vol 22. Springer, Berlin, Heidelberg. https://doi.org/10.1007/978-3-642-79066-9_15

Gasse, F., Barker, P., Gell, P.A., Fritz, S.C., Chalie, F., 1997. Diatom-inferred salinity in palaeolakes: An indirect tracer of climate change. Quaternary Science Reviews, 16, 547-563. https://doi.org/10.1016/S0277-3791(96)00081-9.

Gasse, F., Talling, F., Kilham, P., 1983. Diatom assemblages in East Africa: classification distribution and ecology. Revue d'Hydrobiologie Tropicale. 16, 3–34.

Gierlowski-Kordesch, E. 2010. Chapter 1 Lacustrine Carbonates, in: Developments in Sedimentology 61 http://doi:10.1016/S0070-4571(09)06101-9

Goldstein, J., 2003. Scanning electron microscopy and x-ray microanalysis. Kluwer Adacemic/Plenum Pulbishers, pp. 689.

Haliva-Cohen, A., Stein, M., Goldstein, S.L., Sandler, A., Starinsky, A., 2012. Sources and transport routes of fine detritus material to the Late Quaternary Dead Sea basin. Quaternary Science Reviews. 50, 55-70.

Hambrey, M.J., 2011. Earth's pre-Pleistocene glacial record. Cambridge University Press; 1st edition, pp. 1022.

Hegazi, F. 2016. Providing water for Syrian refugees in Jordan. Muftah 29, 2016 https://muftah.org/providing-water-syrian-refugees-jordan/#.WaRcWzth2wR

Ibrahim, K.M., 1996. The Regional Geology of Al-Azraq. Geological Mapping Division, Natural Resources Authority, Amman, Jordan, pp. 67.

Joeckel, R.M., Fielding, C.R., 2018. New Insights into Carboniferous Cyclothems. The Fourth Biennial Field Conference of the American Association of Petroleum Geologists

(AAPG) Midcontinent Section Fourth Biennial Field Conference Abstracts and Guidebook. Conservation and Survey Division. pp. 617. http://digitalcommons.unl.edu/conservationsurvey/617.

Jones, M.D., Richter, T., 2011. Paleoclimatic and archeological implications of Pleistocene and Holocene environments in Azraq, Jordan. Quaternary Research. 76, 363-372. https://doi.org/10.1016/j.yqres.2011.07.005

Julius, M.L., Theriot, E.C., 2010. The diatoms: a primer, in: Smol, J.P., Stoermer, E.F. (Eds.), The Diatoms: Applications for the Environmental and Earth Sciences, Cambridge University Press, pp. 8-22. doi: https://doi.org/10.1017/CBO9780511763175.003

Kaudse, T., 2014. Noble gases in groundwater of the Azraq Oasis, Jordan, and along the central Dead Sea Transform: Two case studies. Dissertation University of Heidelberg, Germany.

Kemp, A.E.S., 2003. Evidence for Abrupt Climate Changes in Annually Laminated Marine Sediments. Philosophical Transactions: Mathematical, Physical and Engineering Sciences, 361(1810), 1851-1870.

Kemp, A.E.S., 1996. Laminated sediments as palaeo-indicators. Geological Society, London, Special Publications, 116, vii-xii. https://doi.org/10.1144/GSL.SP.1996.116.01.01

Kilham, P., Kilham, S.S., 1971. Melosira granulata (Ehr.) Ralfs: morphology and ecology of a cosmopolitan freshwater diatom. Verhandlungen der Internationalen Vereinigung Limnologie. 19, 2716-2721.

Kirkland, D.W., 2003. An explanation for the varves of the Castile evaporates (Upper Permian), Texas and New Mexico, USA. Sedimentology. 50, 899-920.

Lamb, H.H., 1995. Climate, History and the Modern World. (2nd Edition). Routledge, 11 New Fetter Lane, London EC4P 4EE, pp. 433.

Lewin, J.C., 1961. The dissolution of silica from diatom walls. Geochimica et Cosmochimica Acta. 21, 182-198.

Lopez-Merino, L., Leroy, S.A.G., Eshel, A., Epshtein, V., Belmaker, R. Bookman, R., 2016. Using palynology to re-assess the Dead Sea laminated sediments – Indeed varves? Quaternary Science Review. 140, 49-66.

Margane, A., Hobler, M., Al-Momani, M., Subah, A., 2002. Contributions to the hydrogeology of northern and central Jordan. Geologisches Jahrbuch C. 68, 3–52.

Marks, L., Salem, A., Welc, F., Nitychoruk, J., Chen, Z., Blaauw, M., Zalat, A., Majecka, A., Szymanek, M., Chodyka, M., Toloczko-Pasek, A., Sun, Q., Zhao, X., Jiang, J., 2017. Holocene lake sediments from the Faiyum Oasis in Egypt: a record of environmental and climate change. Boreas. 47, 62-79.

Mastalerz, M., Kvale, E.P., Stankiewicz, B.A., Portle, K., 1999. Organic geochemistry in Pennsylvanian tidally influenced sediments from SW Indiana. Organic Geochemistry.

30, 57-73. https://doi.org/10.1016/S0146-6380(98)00196-X

McCave, I.N., Syvitski, J.P.M., 1991. Principles and methods of particle size analysis, in: Syvitski, J.P.M. (Ed.), Principles, Methods, and Applications of Particle Size Analysis, New York, Cambridge University Press, pp. 3-21.

McMullen, D., 2006. Scanning electron microscopy 1928-1965. Scanning. 17(3), 175-185.

Middleton, G.V. (ed.), 2003. Encyclopedia of sediments and sedimentary rocks. Second edition. Springer, pp. 928.

Migowski, C., Stein, M., Prasad, S., Negendank, J.F.W., Agnon, A., 2006. Holocene Climate Variability and Cultural Evolution in the Near East from the Dead Sea Sedimentary Record. Quaternary Research. 66, 421-431. https://doi.org/10.1016/j.yqres.2006.06.010.

Naeher, S., Gilli, A., North, R.P., Hamann, Y., Schubert, C.J., 2020. Tracing bottom water oxygenation with sedimentary Mn/Fe ratios in Lake Zurich, Switzerland. Chemical Geology. 352, 125-133.

Neev, D., Emery, K.O., 1967. The Dead Sea: depositional processes and environments of evaporites. Jerusalem, Geological Survey of Israel Bulletin. 41, pp. 147.

Neugebauer, I., Brauer, A., Schwab, M.J., Waldmann, N.D., Enzel, Y., Kitagawa, H., Torfstein, A., Frank, U., Dulski, P., Agnon, A., Ariztegui, D., 2014. Lithology of the long sediment record recovered by the ICDP Dead Sea deep drilling Project (DSDDP). Quaternary Science Reviews. 102, 149e165.

Ojala, A.E.K., Bigler, C., Weckstrom, J., 2014. Understanding varve formation processes from sediment trapping and limnological monitoring. PAGES Magazine. 22, 8-9.

Ojala, A.E.K., Francus, P., Zolitschka, B., Besonen, M., Lamoureux, S., 2012. Characteristics of sedimentary varve chronologies– a review. Quaternary Science Reviews. 43, 45–60. https://doi.org/10.1016/j.quascirev.2012.04.006

Ojala, A.E.K., Teija, Alenius.2005. 10, 000 Years of interannual sedimentation recorded in the Lake Nautajärvi (Finland) clastic-organic varves. Palaeogeography Palaeoclimatology Palaeoecology. 219, 285-302. 10.1016/j.palaeo.2005.01.002.

Poppe, L.J., Eliason, A.H., Fredericks, J.J., Rendigs, R.R., Blackwood, D., Polloni, C.F., 2013. US Geological Survey Open-File Report 00-358: Chapter L: Grain-Size Analysis of Marine Sediments: Methodology and Data Processing.

Poppe, L.J., Eliason, A.H., Hastings, M.E., 2003. A Visual Basic program to classify sediments based on gravel-sand-silt-clay ratios. Computers and Geosciences. 29(6), 805-809.

Rahman, K., Gorelick, S.M., Dennedy-Frank, P.J., Yoon, J., Rajaratnam, B., 2015. Declining rainfall and regional variability changes in Jordan. Water Resources Research. 51, 3828-3835. https://doi.org/10.1002/2015WR017153

Reeves, C.C., 2008. Chapter 5 Lacustrine Sediments: Chemical Precipitates, in: Reeves, C.C. (Ed.), Developments in Sedimentology, Elsevier, 11, 47-76, http://doi.org/10.1016/S0070-4571(08)70828-8.

Richter, T.O., van der Gaast, S., Koster, B., Vaars, A., Gieles, R., de Stigter, H.C., de Haas, H., van Weering, T.C.E., 2006. The Avaatech XRF core scanner: technical description and applications to NE Atlantic sediments, in: Rothwell, R.G. (Ed.), New Techniques in Sediment Core Analysis, Geological Society of London, London, pp. 39-50.

Schnurrenberger, D., Russell, J., Kelts, K., 2003. Classification of lacustrine sediments based on sedimentary components. Journal of Paleolimnology. 29, 141-154.

Shepard, F.P., 1954, Nomenclature based on sand-silt-clay ratios. Journal of Sedimentary Petrology. 24, 151-158.

Stockhecke, M., Anselmetti, F.S., Meydan, A.F, Odermatt, D., Sturm, M., 2012. The annual particle cycle in Lake Van (Turkey). Palaeogeography, Palaeoclimatology, Palaeoecology. 333-334, 148-159.

Stoermer, E.F., Smol, J. P., 1999. The Diatoms: Applications for the Environmental and Earth Sciences. Cambridge University Press.

Stoermer, E.F., Bowman, M., Kingston, J.C.V., Schaedel, A. L., 1975. Phytoplankton composition and abundance in Lake Ontario during IFYGL. U.S. Environmental Protection Agency. Report No. EPA-660/3-75-004. February 1975, Corvallis, Oregon.

Sturm, M., Lotter, A., 1995. Lake sediments as environmental archives. EAWAG News. 38, 6-9.

Theriot, E., Stoermer, E.F., 1981. Some aspects of morphological variation in *Stephanodiscus niagarae* (Bacillariophyceae) Journal of Phycology. 17, 64-72.

Turner, B., Makhlouf, I., 2005. Quaternary sandstones, northeast Jordan: age, depositional environments, and climatic implications: Paleogeography, Palaeoclimatology, Paleoecology. 229(3), 230-250.

van Geen, A., Zheng, Y., Bernhard, J. M., Cannariato, K. G., Carriquiry, J., Dean, W. E., Eakins, B. W., Ortiz, J. D., Pike, J., 2003. On the preservation of laminated sediments along the western margin of North America, Paleoceanography. 18, 1098. https://doi:10.1029/2003PA000911, 4.

Witter, R.C., Gelfenbaum, G., Corbett, R., Tam, A., La Selle, S.M., 2018. Radiocarbon, Cesium-137, Grain Size, and X-ray Fluorescence Data for Tsunami Geology Investigation, Driftwood Bay, Umnak Island, Alaska, U.S. Geological Survey data release. https://doi.org/10.5066/P9D7KLJV.

Zalat, A.A., Marks, L., Welc, F., Salem, A., Nitychoruk, J., Chen, Z., Majecka, A., Szymanek, M., Chodyka, M., Tołoczko-Pasek, A., Sun, Q., Zhao, X., Jiang, J., 2017. Diatom stratigraphy of FA-1 core, Qarun Lake, records of Holocene environmental and climatic change in Faiyum Oasis, Egypt. Studia Quaternaria. 34, 61–69 doi: 10.1515/squa-017-0005

Zolitschka, B., Francus, P., Ojala, A.E.K., Schimmelmann, A., 2015. Varves in lake sediments– a review. Quaternary Science Reviews. 117, 1-41. https://doi.org/10.1016/j.quascirev.2015.03.019

Zolitschka B., Enters D., 2009. Lacustrine Sediments, in: Gornitz V. (Ed.), Encyclopedia of Paleoclimatology and Ancient Environments, Encyclopedia of Earth Sciences Series. Springer, Dordrecht, https://doi.org/10.1007/978-1-4020-4411-3_120

Zuo, X., Li, C., Zhang, J., Ma, G., Chen, P. 2020. Geochemical characteristics and depositional environment of the Shahejie Formation in the Binnan Oilfield, China. Journal of Geophysics and Engineering. 17, 539–551.

VITA

Jessica J. Hirsch attended the University of Missouri – Kansas City and received her Bachelor of Science in Geography in 2012. She worked with Dr. Davies on the Al-Azraq core project for three years and presented her work at three national conferences, winning the national Best Paleoenvironmental poster and presentation in 2012. Ms. Hirsch entered the Master's program in the Geoscience department at the University of Missouri Kansas City, in December 2012. Ms. Hirsch hopes to complete her Master's in May, 2021. After which she plans to pursue her PhD. Ms. Hirsch has received numerous academic scholarships and awards during her studies at the UMKC. Ms. Hirsch is a member of numerous academic and professional organizations.